Design and elaboration of novel drug eluting stents to produce tailored releases aiming for the reduction of restenosis after implantation

Alberto Ponce Arrones

DOCTORAL THESIS

Title	Design and elaboration of novel drug eluting stents to produce tailored releases aiming for the reduction of restenosis after implantation.
Presented by	Alberto Ponce Arrones
Centre	School of Engineering IQS
Department	Bioengineering
Directed by	Dr. Salvador Borrós Gómez and Dr. Víctor Ramos Pèrez

This page intentionally left blank

“Quiero arrancar frutos silvestres de una senda virgen aún.”

Rafael Lechowski

This page intentionally left blank

Acknowledgments

En primer lugar me gustaría agradecer a mi director de tesis, el Dr. Salvador Borrós, y a mi codirector de tesis, el Dr. Víctor Ramos, por el apoyo y la oportunidad de realizar este trabajo. Gracias Chicho por saber guiarme durante esta tesis y conseguir redirigir mis momentos más caóticos y minimalistas. Ha sido un placer poder trabajar contigo durante estos años, a la vez que muy divertido. Sin tu confianza en mi esta tesis no hubiera empezado, gracias de corazón. También me gustaría agradecer a Víctor Ramos por la ayuda y los consejos ofrecidos durante la elaboración de este trabajo. Siempre encontró algún hueco para ayudarme y guiarme aunque fuera a distancia. Muchas gracias.

Estos años los recordaré siempre con gran cariño, ha sido una gran experiencia gracias a poder compartirla con todos mis compañeros. Me gustaría agradecer a todo el grupo GEMAT y Sagetis por su apoyo. Gracias Dr. Miguel Ángel Lázaro por compartir tu experiencia en el laboratorio, ha sido genial tenerte al lado. Dr. Núria Agulló y Marina Sarmiento, no solamente habéis aguantado mi paso por Mats Vells sino que además me habéis echado una mano incontables veces, muchas gracias por todo.

Hemos formado un grupo muy bueno tanto a nivel profesional como personal, gracias a todos los miembros del laboratorio. Germansito, Pere, Mario, Mire, Teresa, Pol, Anna, Alba, Laura, Robert, Joan, Cris, Patri, Toni... Me llevo muchísimos recuerdos vuestros tanto del laboratorio como de fuera. Rumanía, La Fira y las historias raras que le contaba el portero a Germán en la salida, la torreta y el gallego, Pere y yo en bici de madrugada, saltar la verja del laboratorio y Robert armado en una trinchera entre muchas otras. Nos vemos en breve, gracias por todos los momentos compartidos y os mando un beso enorme.

A mi familia que me ha apoyado siempre. A mis padres, gracias a su empeño, sacrificio y por todo lo que me han dado. Han tenido fe en mí en todo momento y se lo agradeceré siempre. Gracias Sofía por estar a mi lado y acompañarme en este viaje. Se cierra una etapa fantástica que recordaré con cariño toda la vida.

This page intentionally left blank

Abstract

Design and elaboration of novel drug eluting stents to produce tailored releases aiming for the reduction of restenosis after implantation

Coronary artery disease is the most typical type of heart disease, killing more than 385,000 people annually. Up to date, many different approaches have been tested in order to treat patients while trying to keep inflammatory responses to a minimum. Among these, the use of nanocarriers, multilayered coatings and gene therapy stand out as some of the most promising novel therapeutic strategies tested lately. Stents have been used throughout the years with different designs and coatings, achieving enhanced healing results with every new generation. Although their use is justified their results are not optimal, creating a need to develop better strategies to treat coronary artery diseases.

We understand that a total liberation control of the pharmacological drug load from a medical device can profoundly change a patient's outcome, therefore, becoming a priority of our work. Here, we present a way of producing in-lab and industrial scaled coatings for medical devices which are used to produce tailored multilayered coatings for drug eluting stents. Apart from this, an approach to treat coronary artery disease through gene therapy with nanocarriers is also introduced, opening new possibilities for localized treatments with drug eluting stents. Starting with the elaboration of methodologies and instrumentation required to produce tailored coatings, novel stent designs are created and studied in this work. This enables the production of new coatings and delivery systems which are tested *in-vitro* and *in-vivo* in order to prove their effectiveness.

In conclusion, this thesis demonstrated that a tailored drug release can be achieved through multilayered designs and nanoparticle liberations, which can be applied to drug eluting stents to obtain a reduction in restenosis rates with promising results.

This page intentionally left blank

Resumen

Design and elaboration of novel drug eluting stents to produce tailored releases aiming for the reduction of restenosis after implantation

Las enfermedades de arteria coronaria son el tipo más común de enfermedad cardíaca, matando a más de 385,000 personas anualmente. Hasta la fecha, se han probado muchos enfoques distintos a la hora de plantear tratamientos que mantengan las respuestas inflamatorias al mínimo. Entre estos, el uso de nanoparticulas, recubrimientos multicapa y terapia génica destacan como algunas de las estrategias terapéuticas novedosas más prometedoras. El uso de stents cardíacos se ha mantenido a lo largo de los años con diferentes diseños y recubrimientos, logrando mejores resultados con cada nueva generación. Aunque su uso está justificado, sus resultados no son óptimos, creando la necesidad de desarrollar mejores estrategias para tratar este tipo de enfermedades.

Entendemos que un control total de la liberación de la carga farmacológica de un dispositivo médico puede cambiar profundamente los resultados de un paciente, convirtiéndose así en una prioridad de nuestro trabajo. Presentamos una forma de producir recubrimientos, a escala industrial y de laboratorio, orientados para dispositivos médicos y que se utilizan para producir recubrimientos multicapa a medida para stents con liberación de fármaco. Además de esto, también se presenta un enfoque para tratar enfermedades de arteria coronaria a través de la terapia génica con nanoportadores, lo que abre nuevas posibilidades para tratamientos localizados empleando stents con liberación de fármaco. Comenzando con la elaboración de metodologías e instrumentos necesarios para producir recubrimientos a medida, se crean y estudian nuevos diseños de stent a lo largo de este trabajo. Esto permite la producción de nuevos recubrimientos y sistemas de liberación los cuales son probados *in-vitro* e *in-vivo* para demostrar su efectividad.

En conclusión, esta tesis demuestra que se puede lograr una liberación de fármacos a medida mediante diseños multicapa y liberación con nanoportadores, aplicable a stents con liberación de fármaco para obtener una reducción en las tasas de reestenosis con resultados prometedores.

This page intentionally left blank

Resum

Design and elaboration of novel drug eluting stents to produce tailored releases aiming for the reduction of restenosis after implantation

Les malalties d'artèria coronària són el tipus més comú de malaltia cardíaca, matant a més de 385,000 persones anualment. Fins a la data, s'han provat moltes estratègies diferents a l'hora de plantejar tractaments que mantinguin les respostes inflamatòries al mínim. Entre aquests, l'ús de nanopartícules, recobriments multicapa i teràpia gènica destaquen com algunes de les estratègies terapèutiques noves més prometedores. L'ús de stents cardíacs s'ha mantingut al llarg dels anys amb diferents dissenys i recobriments, aconseguint millors resultats amb cada nova generació. Encara que el seu ús està justificat, els seus resultats no són òptims, creant la necessitat de desenvolupar millors estratègies per tractar aquest tipus de malalties.

Entenem que un control total de l'alliberament de la càrrega farmacològica d'un dispositiu mèdic pot canviar profundament els resultats d'un pacient, convertint-se així en una prioritat del nostre treball. Presentem una forma de produir recobriments, a escala industrial i de laboratori, orientats per a dispositius mèdics i que s'utilitzen per produir recobriments multicapa a mida per stents amb alliberament de fàrmac. A més d'això, també es presenta un enfocament per tractar malalties d'artèria coronària a través de la teràpia gènica amb nanoportadors, el que obre noves possibilitats per a tractaments localitzats emprant stents amb alliberament de fàrmac. Començant amb l'elaboració de metodologies i instruments necessaris per a produir recobriments a mida, es creen i estudien nous dissenys de stent al llarg d'aquest treball. Això permet la producció de nous recobriments i sistemes d'alliberació els quals són provats *in-vitro* i *in-vivo* per demostrar la seva efectivitat.

En conclusió, aquesta tesi demostra que es pot aconseguir un alliberament de fàrmacs a mida mitjançant dissenys multicapa i alliberament amb nanoportadors, aplicable a stents amb alliberament de fàrmac per obtenir una reducció en les taxes de reestenosi amb resultats prometedors.

Table of Contents

This page intentionally left blank

Figure Index

Chapter I

Chapter II

Chapter III

Chapter IV

Table Index

Chapter II

Chapter III

Chapter IV

List of abbreviations

CAD	Coronary Artery Disease
DES	Drug eluting stents
CDCP	Centers for Disease Control and Prevention
MI	Myocardial infarction
LAD	the left anterior descending artery
ACS	Acute coronary syndrome
UAP	Acute coronary syndrome
AMI	Acute myocardial infarction
CABG	Coronary Artery Bypass Graft
PCI	Percutaneous Coronary Intervention
PTCA	Percutaneous Transluminal Coronary Angioplasty
BMS	Bare metal stent
BENESTENT	Belgium Netherlands Stent
STRESS	Study on Stent Restenosis
DAPT	dual antiplatelet therapy
DCM	dichloromethane
TGA	thermogravimetric analysis
ASTM	American Society for Testing and Materials
HPLC	High-performance liquid chromatography
UV	ultraviolet
PLGA	poly(lactic-co-glycolic acid)
PLA	Polylactic acid
pHPMA	poly(N-(2-hydroxypropyl) methacrylamide)
3-APTES	(3-Aminopropyl)triethoxysilane
SEM	Scanning electron microscopy
rpm	revolutions per minute
%wt.	weight percent
SMC	smooth muscle cells
ISR	in-stent restenosis
LAST	late stent thrombotic
VSMC	vascular smooth muscle cells
EES	everolimus eluting stents

PAP-1	5-(4-phenylbutoxy)psoralen
PLLA	Poly-L-lactic acid
PCL	poly-caprolactone
PGA	polyglycolic acid
PDLA	poly-D-lactic acid
PBAE	Poly(β-amino ester)
MiRNA	Micro RNA
SiRNA	Small interfering RNA
RNAi	Interfering RNA
PFM	Pentafluorophenyl methacrylate
GFP	Green fluorescent plasmid
PGFP	Green fluorescent protein vector
AFM	Atomic force microscopy
BSA	Bovine serum albumin
IR	Infrared
ATR	Attenuated Total Reflection
RF	Radiofrequency
DC	Duty cycles
DMEM	Dulbecco's modified Eagle medium
FBS	Fetal bovine serum
Ra	Roughness average
Rq	Root mean square roughness
Rmax	Maximum roughness
Rz	Mean roughness depth

Chapter I.

Introduction to coronary artery disease and therapeutic strategies for its treatment. Aims.

This page intentionally left blank

1. Introduction

Coronary artery disease (CAD)

As a way to start this thesis, a background is presented which aims to provide the reader with some knowledge on drug eluting stents (DES) and medical terminology which go hand in hand with these medical devices. As the main issue being confronted in this work is CAD, this introduction will start off focusing on describing it and showing the most frequently used treatments.

CAD is the most typical type of heart disease, killing more than 385,000 people annually **(Centers for Disease Control and Prevention (CDC)** [1][2]). It is a serious and common ailment that can profoundly influence a patient's prognosis and quality of life, caused by myocardial tissue ischemia. The mechanism through which coronary ischemia happens is the development of coronary atherosclerotic plaque. It starts with the deposition of fatty substances (cholesterol, fatty acids, etc.) in arteries, resulting in a narrowed blood vessel lumen and thus reduced myocardial oxygen supply. This type of ischemia can result in the following clinical syndromes: Coronary Artery Disease (CAD), angina pectoris and myocardial infarction (MI) [3]-[5]. Throughout this thesis, the focus will be drawn towards CAD and its treatment using tailored polymeric coated stents.

There are different therapeutic strategies to treat CAD, these include pharmacological treatments and myocardial reperfusion or revascularization. In addition to appropriate hygienic and dietary regimen (to reduce risk factors), administration of pharmacological agents is systematic and is done prior to any cardiovascular intervention, and may include [6][7] anti-thrombotic drugs, anti-ischemic drugs and prophylactic or symptomatic lipid lowering drugs.

Myocardial revascularization has been an established mainstay in the treatment of CAD for almost half a century. In the recent years, invasive cardiology has gained a pivotal role in the management of acute and stable heart disease by improving outcomes and/ or quality of life. The interventional strategies include:

- Coronary Artery Bypass Graft (CABG): First performed in 1962, CABG is a surgical procedure which has been used in multivessel and left main stem disease for almost 40 years. In CABG, bypass grafts are placed to the mid-coronary vessel beyond the culprit lesion(s), providing extra sources of nutrient blood flow to the myocardium and offering protection against the consequences of further proximal obstructive disease. The procedure is usually performed by stopping the heart, needing a cardiopulmonary bypass. Indications for CABG are: Chronic and unstable angina, acute MI, Failure of PTCA and severe CAD [8][9].

- Percutaneous Coronary Intervention (PCI): A non-surgical procedure that uses a catheter to place a stent to open up blood vessels in the heart that have been narrowed by plaque build-up. Although initially limited to Percutaneous Transluminal Coronary Angioplasty (PTCA), Percutaneous Coronary Intervention (PCI) now associates PTCA and several new techniques, such as stent implantation (bare-metal, BMS; and drug-eluting, DES), atherectomy, distal protection during saphenous vein graft, thrombectomy, vascular brachytherapy, laser angioplasty and balloon angioplasty [10]. Coronary stent implantation is a procedure used for the permanent dilation of coronary artery stenosis in order to improve the myocardial perfusion and extensively for the coronary artery disease (CAD).

As PCI is an interesting conceptual part of stent deployment, it feels necessary to present some more information about these techniques and how they were developed.

The birth of interventionist cardiology and BMS

In 1964, Charles Theodore Dotter and Melvin P. Judkins described the first angioplasty after using a balloon attached to the tip of a catheter for the treatment of the atherosclerotic vascular disease in the superficial femoral artery of the left leg [11][12]. In the mid-1970s, Andreas Gruentzing performed the first coronary balloon angioplasty, which marked the beginnings of interventionist cardiology and a major change in the treatment of patients with obstructive diseases of the coronary artery [12].

Once access into the femoral, radial or brachial artery is gained, the tip of a long, flexible, soft plastic guiding catheter is seated within the opening of the coronary artery and x-ray movie pictures are recorded during the injection of radiopaque agents into the coronary artery. This is done so that the disease state and location can be readily assessed using real time x-ray visualization. After evaluating the x-ray movie pictures, the cardiologist estimates the size of the coronary artery and selects the type of balloon catheter and wire that will be used. The coronary guidewire, which is an extremely thin wire with a radio-opaque flexible tip, is inserted through the guiding catheter and into the coronary artery. After doing this, the tip of the wire is then passed across the stenosis. The guidewire now acts as a pathway for the balloon catheter leading it to the stenosis. The folded balloon is inserted into the site of the lesion, where it is inflated at an established pressure, reducing the obstructing plaques. Once the blood flow passage is open, it is deflated and removed (Figure 1).

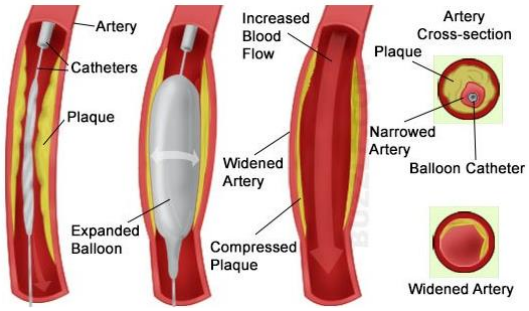

Figure 1: Balloon angioplasty process [13]. *At the left of this figure, a catheter is used to place a balloon on the area were the plaque has built up. A second image starting from the left shows how a balloon expands and compresses the plaque onto the artery wall. A third image starting from the left depicts a catheter extraction after plaque compression. At the right of the figure, two cross-sections are shown. One displays an artery cross-section before the treatment (top), while the other shows the resulting lumen after the procedure has been done (bottom).*

Since the beginning, a great number of medical advances have been made which have allowed percutaneous coronary interventions (PCI) to become an effective alternative treatment to coronary artery bypass surgery (CABG). Currently, PCI has become one of the most frequently performed invasive medical procedures in clinical practice [14].

In the end, PTCA procedures gave way to other PCI techniques such as bare metal stent implantation. Next, these two are described giving a general background of their development. PTCA causes plaque compression, but the major change in lumen geometry is caused by fracturing and fissuring of the atheroma, extending into the vessel wall at variable depths and lengths. This injury accounts for the three major limitations of PTCA - coronary artery dissection, abrupt vessel closure, and restenosis. Although balloon angioplasty progressed and was promptly adopted as a technique, rising from a success rate of 78% obtained in the first international register in 1977-1981 to a success rate of 90% in 1991-1994, it did not provide long-term solutions. It was often necessary to repeat the procedure due to problems of acute vascular occlusion (2-4%) and restenosis (30-50%), mainly in the first 6 months [12].

In 1969, Dotter began studies on the implantation of coil wires, the stent precursor, in animals [15]. As no satisfactory results were obtained, this device was abandoned until the early 1980s when it was taken up again by Dotter and Cragg through the use of nitinol wires [12][15]. Late in the same decade, Sigwart and Puel performed the first implantation in humans. It was a self-expandable stent known as a “Wall” stent [16]. At the same time, the Palmaz-Schatz balloon-expandable intracoronary stent was developed [12][17][18]. This first generation comprised three closed cell segments connected by two spiral-shaped segments commonly known as Palmaz-Schatz balloon expandable stents (Figure 2). Today, balloon-expandable stents are much more widely used than self-expandable stents(Figure 3).

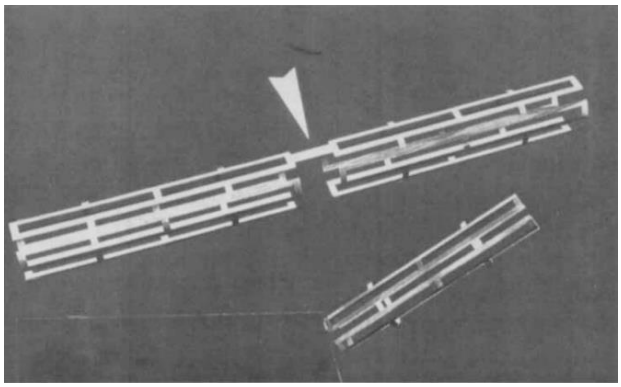

Figure 2: Palmaz-Schatz balloon-expandable stent [19]*. This figure shows the metallic cell structure of the first balloon expandable stents.*

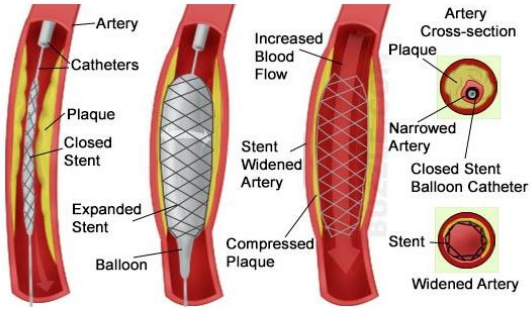

Figure 3: Implantation of a balloon-expandable stent [20]*. At the left of this figure, a catheter is used to place a balloon on the area were the plaque has built up. A second image starting from the left shows how a balloon expands a stent which compresses the plaque onto the artery wall. A third image starting from the left depicts a catheter extraction after plaque compression while a stent remains on the affected area. At the right of the figure, two cross-sections are shown. One displays an artery cross-section before the treatment with a closed stent deployed on the affected area (top), while the other shows the resulting lumen after the procedure has been done (bottom). An expanded stent structure can be seen in this last image.*

Initially, the metal stent was used only in cases of restenosis of the native vessel or of the aortocoronary venous bypass graft and in acute occlusions caused during balloon angioplasty. The main danger of stents was the risk of subacute thrombotic occlusion of the coronary artery that could reach up to 18% of cases in the initial weeks of implantation. This led to the use of complex anticoagulation regimens with the attendant increase in bleeding events and prolonged hospital stays [16]**.**

The publication of the results of the randomized studies on balloon vs. stent, BENESTENT I and II (Belgium Netherlands Stent) [12][21][22] and STRESS (Study on Stent Restenosis) [12][23] obtained results which indicated a lower restenosis rate and better long-term results with the stent. They also showed the advance in the study of anticoagulant-antiplatelet regimens. This work evidenced that stent implantation was a safe technique without anticoagulant treatment and with the administration of dual antiplatelet therapy [24]. This marked the turning point in the establishment of stent implantation as a treatment for coronary artery disease. In 1999 they accounted for 84.2% of PCI procedures [25].

Inflammation and the era of drug-eluting stents

After stent implantation, smooth muscle cells (SMC) can undergo a rapid adhesion and proliferation also known as in-stent restenosis (ISR). This process causes a narrowing of the vessel in an average of 15-20% of patients, being a phenomenon of concern [26]-[28]. DES have proven to reduce stenosis, but the risk of late local endothelium regeneration events and late stent thrombotic (LAST) events are still present and can affect clinical long-term implantation [29]-[31]. Previous studies have demonstrated that the migration and proliferation of SMCs induced by injury and the delay of re-endothelialization comprise the major events which lead to neointima formation. Endothelium has an important role maintaining the integrity of the vessel by preventing thrombosis and hyperplasia during regeneration. Rapid re-endothelization has proven to contribute with a correct healing of the tissue avoiding ISR and LAST [32]-[34].

At early stages of restenosis, platelet activation and thrombosis take place at the affected area accompanied by the recruitment of monocytes, neutrophils and lymphocytes. The main problem derived from this is the hyperplastic response of medial vascular smooth muscle cells (VSMC) caused by the chemotactic and mitogenic factors produced by neointimal cells. These VSMC migrate to the growing neointima and exhibit a high proliferative activity as seen in Figure 4. VSMC are normally fusiform and show a differentiated contractile phenotype which is characterized by a reduced proliferative activity. On the other hand, activated VSMC found on injured vessels have an undifferentiated phenotype which shows broader and flatter shapes. They are characterized by the expression of embryonic isoforms of contractile proteins, high proliferation and responsiveness to growth and chemotactic stimuli. After these initial stages, inflammation starts to recede as a sign of the restoration of the contractile phenotype of neointimal VSMC. This leads to normalization of the composition of the extracellular matrix leading to a final stage where the vessel wall is restored [35].

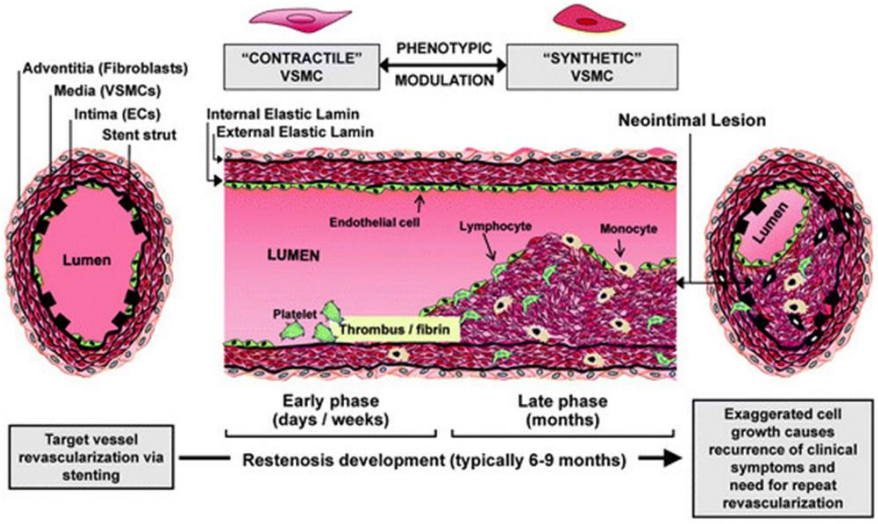

Figure 4:Diagram illustrating restenosis development in a vessel after stenting. Left part of the image shows a vertical section of a target vessel right after stenting. Center of the image shows a horizontal section of the vessel with the representation of early and late phases of restenosis development with the different cell types involved. Right part shows late phase restenosis on a vertical section of a vessel. Changes in VSMC phenotype are depicted with a clear lumen reduction process seen from left to right. Adapted from [36].

Together with the risk of subacute thrombosis, the main problem of metal stents was late intra-stent restenosis linked to multiple factors. A stent acts as a platform preventing acute vascular occlusion, removing the elastic recoil and reducing late remodeling. These are some of the main factors causing post-balloon restenosis, but proliferation and hyperplasia of the neointima persist after implantation and are even stimulated by the stent itself. By the end of the 90s, the incidence of stent restenosis ranged from 15 to 30%, and these percentages were greater in the groups of higher risk patients. These are specifically those with lesions in small vessels, long and/or bifurcation lesions, patients with diabetes mellitus, etc.

The attempt to minimize hyperplasia of the neointima caused by stent implantation and thus reduce repetitive revascularization led to the development of another revolutionary treatment concept: The drug-eluting stent or DES [16]. These types of stents contain antiproliferative drugs which are released from a polymer carrier, regulating the pharmacological release rate. The mechanism of action of the drug released focuses on the inhibition of smooth muscle cell growth, the main component of intimal hyperplasia. The first DES to be developed were the Taxus and Cypher stents, incorporating paclitaxel and sirolimus, respectively. Both stents demonstrated a marked reduction in restenosis compared to BMS stents, without inhibiting it (TAXUS I, II, II and IV, SIRIUS, E- SIRIUS and C-SIRIUS studies) [37]-[40].

The observed reduction in the restenosis rates, as compared to BMS, was the driving force which provided the greatest exponential growth of PCI as a treatment for patients with coronary artery disease (CAD). However, in 2006, serious doubts were raised on the safety profile of these stents, as results of studies reporting a slight increase in late thrombosis and late mortality associated with the use of drug-eluting stents were published [41][42]. Late stent thrombosis is a multifactorial process, but it is clearly related to the presence of polymer in the vascular wall which causes a healing delay favoring the formation of a thrombus with fatal consequences.

Although the increase in late stent thrombosis was not statistically significant and the results published in subsequent years indicated contradictory data, these concerns were a vital stimulus in guiding the investigation and have ultimately led to the development of second generations stents. These are loaded with new drugs such as everolimus, biolimus or zotarolimus, and new platforms: CoCr, PtCr, and more biocompatible and reabsorbable polymers or polymer-free platforms [16]. As the risk of thrombosis is minimized with the prolongation of dual antiplatelet therapy for one year, its use started to be recommended in the 2011 ACCF/AHA/SCAI PCI Guideline for Percutaneous Coronary Intervention [24].

The latest advances in DES use reabsorbable polymers or even polymer-free platforms that directly release the drug, with the aim of improving their integration into the vascular wall and thereby reducing the incidence of late thrombosis. Furthermore, fully reabsorbable stents have been developed. The favorable results obtained with DES, when applying the recommended antiplatelet regime, has led to the predominance of their use in PCI and is now an accepted treatment for patients with a high risk of developing restenosis. This patients usually suffer from diseases such as diabetes, myocardial infarction and complex CAD, as well as risk lesions, such as vessels of small diameter, lesions in bifurcation, arteries with restenosis, saphenous vein graft (bypass, CAGB), left coronary trunk, etc. [24][43]–[47]

Up to this point a main issue has been described which will lead to the main objective of this thesis. In order to treat CAD, DES are commonly used, although their designs are not optimum and can be improved in order to reduce restenosis. Being so, the main objective of this thesis becomes the design and development of new types of stents which, through tailored drug release, aim to minimize the actual inflammatory response derived from medical device implantations.

The next section will focus on some key points which will be discussed throughout this thesis. In order to do so, some questions should be put forward: Why is the design of a stent so important? Do the polymers used influence their performance? Is there a unique optimum design for stents? Following next, these issues are addressed in order to narrow the focus of this introduction and to present the next chapters.

Importance of the design and materials which compose a stent

The stent is a mechanical device that keeps the vascular lumen open via a vessel scaffold. The shape, thickness, coating and selection of the material are some of the factors that need to be considered in the design of the device, since subtle differences can lead to completely different medical results. In an ideal design of a stent and its carrier matrix, all the following aspects need to be considered:

- Ease of use
- Wide range of sizes
- Low profile with ability to cross severe stenosis
- Firm adherence to the balloon
- High expandability with no length changes
- Uniform scaffold of the vessel without obstruction of the lateral branches, with good conformability to vessel angulations, which must also be recrossable, with a good cell opening capacity.

The material must be biocompatible, resistant to corrosion, migration and extrinsic compression (radial force), must not show permanent deformability or degradation over time and must show radiopacity to be viewed by fluoroscopy. In particular, corrosion is a critical parameter. High concentration of cell chloride creates a particularly corrosive environment, which is known to be the principal cause of stent fracture [48].

The design of the stent is defined by the pattern, if any, which has been cut off from the cylindrical strut. Strategies used vary from a tubular shape obtained by laser cut to the obtention of different patterns derived from one or several wires with a sinusoid and joined crowns (Figure 5). Most coronary stents used at the moment develop their design from the first strategy, a tube shaped by laser cut. Closed designs provide a better coverage to the luminal surface and greater scaffold to the vessel due to a higher radial force. This structure is also less flexible and makes it difficult to access winding and calcified lesions. Open designs provide a greater stent flexibility and easier access to winding, calcified lesions and lateral branches. On the other hand, the radial force is lower as well as the coverage of the luminal opening.

To improve flexibility in the new designs, the number of crowns has been increased as this is associated with a reduction in the length and thickness of the strut (wire). Currently, the geometry of the strut section has been largely improved compared with initial models. Many have a circular or round section rather than a rectangular one with more acute edges. This shape modification was done to minimize lesions in the vascular wall during implantation [16].

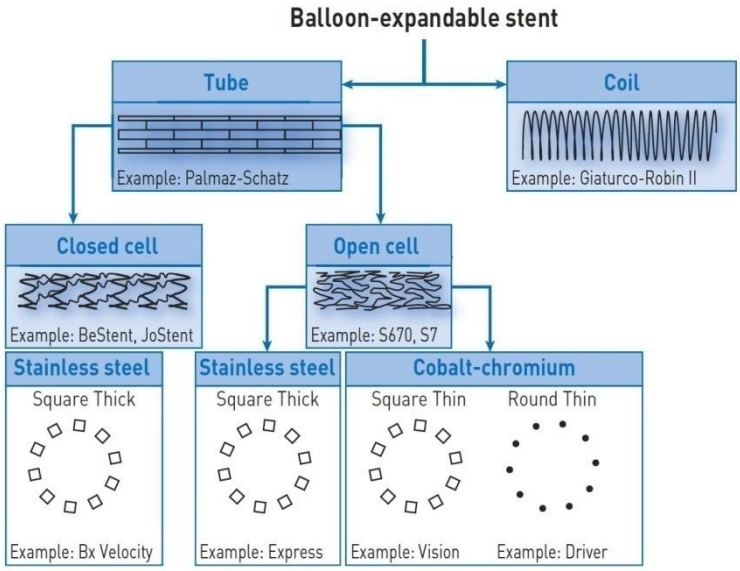

Figure 5: Design of coronary stents. This flow chart shows the main structure designs used to elaborate stents. Starting with Tubular and coil structures, the first one is commonly used with closed or open structures. Some examples of commercial stents are presented under each cell structure.

Results from studies performed *in vitro* and *in vivo* with animals have shown that the lower the thickness of the wire, the better the endothelialization and the lower the restenosis due to reduced trauma in the vascular wall [49][50]. These findings are confirmed in the ISAR-STEREO clinical trial, which show that a lower strut thickness induces less restenosis [51].

Research also shows that the strut thickness is related to the susceptibility of thrombi formation and risk of stent thrombosis [52]. New generation stents have focused on the reduction of the cross profile, reduction of strut thickness and improved flexibility.

The alloys most commonly used in coronary stents are made either of stainless steel, which were the first available stents, or cobalt chrome (CoCr). The first stents were made of stainless Steel, widely used, but more and more these alloys have been replaced by CoCr (2nd generation bare metal coronary stents, and new DES), the most widely used up to date [16]. The CoCr alloy is 45% stronger than stainless steel, allowing reduction of the strut thickness maintaining the radial force, increasing stent flexibility and navigability. In addition, it is more resistant to fatigue and corrosion and due to the higher material density, it is more radiopaque. The first CoCr stents placed on the market with a high relevance in their clinical use are the Multilink Vision stent from Abbott Laboratories, made of CoCr L605, and the Driver stent from Medtronic, made of CoCr F562. Both have a similar wire thickness and comparable clinical results showing no inferiority when compared to stainless steel stents [53][54].

On the other hand, it is also of high importance to use a biocompatible material for stent production. Lower biocompatibility of the stent strut is related to thrombogenesis and the inflammatory reaction, which in turn favors thrombogenesis and neointimal proliferation (restenosis). On the other hand, a greater biocompatibility promotes endothelization and healing of the arterial wall.

In addition, new stent designs with novel alloys, other than stainless steel, allow an area reduction (thin strut) in contact with the body after implantation. Different coatings and surface treatments (inertization) have also been developed with the intention to minimize ion release from the platform. These approaches have led to biocompatibility improvement and increased resistance of the struts. Some examples are stents based on silicon carbide, turbostatic carbon/diamond-like carbon (DLC, Chrono stent (Sorin)), titanium nitride (Titan BAS stent (Hexacat)), silicon carbide (Pro-kinetic stent (Biotronik)) or ion implantation (ICROS stent (amg)).

So far, a type of strut as well as a combination of biocompatible polymers will have to be selected to produce the new stent designs in this thesis. To produce our tailored designs, it is necessary to develop suitable coating techniques and analytical methodology which allow the elaboration and characterization of designed stents. To address this issue, Chapter II will focus on the development of the required techniques and methodologies. This will enable the proposal of new types of coatings and will produce the first DES which will be elaborated in this thesis.

Following, clinical use of drug eluting stents will be discussed to understand why there is no single unique solution for DES.

Clinical use of coronary stents and the search for an optimum design

The use of DES is recommended both in simple and complex lesions and in low and high-risk patients, but in general the difference in efficacy between DES and BMS appears to be higher in complex lesions and in patients at risk.

However, it must be considered that the greatest inconvenience of DES is the need for prolonged antiplatelet therapy of at least 1 year, to prevent the risk of late stent thrombosis, as well as its cost, which is significantly higher than that of BMS stents. On the other hand, the designs of the new BMS stents have allowed a significant reduction in the strut thickness (thin-strut), a critical factor in the development of restenosis, the use of more biocompatible materials and, in some cases have included surface treatments that improve biocompatibility (inertization). These innovations have been translated into an improvement of vascular response compared with the original stents [51][55].

The 2011 ACCF-AHA-SCAI Guideline for Percutaneous Coronary Intervention [24] has established the recommendations for use of coronary stents based on the level of evidence of the benefit-risk for the patient, established in the multiple randomized, controlled trials (RTC) performed with BMS and DES stents, which are as follows:

- Before implanting a DES, it must be ensured that the patient will be able to tolerate the prolonged antiplatelet treatment (dual antiplatelet therapy, DAPT) for at least 12 months.

- DES are useful as an alternative to BMS stents to reduce the risk of restenosis in cases where the risk of restenosis is increased, and it is likely that the patients can tolerate and comply with the prolonged DAPT treatment.

- The use of BMS stents should occur in patients with a high risk of bleeding, who are unable to comply with the DAPT treatment for at least 12 months, or who have scheduled an invasive and/or surgical procedure for the following 12 months that would require discontinuing DAPT treatment.

- DES coronary stents should not be used in patients where it is likely that they will not tolerate and comply with prolonged DAPT treatment for at least 12 months or where this cannot be established before implantation.

Therefore, it can be concluded that considering the variety of designs, characteristics and types of stents, BMS and DES, and in particular the clinical results obtained in the studies performed with different stents, the experts consider that there is no single stent design, type of polymer or adequate drug for all patients and types of lesions. As a result, a more individualized selection of the stent considering the characteristics of the patient will be translated into an improvement in clinical safety and efficacy in the long term.

If there is no unique solution for DES designs, then the problem should be addressed slightly different. In order to produce a desired drug release profile, a complete understanding and tailoring of the elution phenomenon from a designed polymeric matrix is needed. To address this, Chapter III will focus on the selection of various biodegradable polymers and antiproliferative drugs to produce a set of experiments which will enable complete control of drug elution. The sublimation of this work will produce a novel tailored multilayered DES ready to be used.

Next, a brief background is given on how the development of new concept/formulations for DES will be carried out in a research laboratory.

Development of new concept/formulations for DES elaborated in research laboratories

As seen, a key factor to take in account in order to reduce proliferation and hyperplasia of the neointima has proven to be the polymeric matrix in which the drug is embedded, which will affect the recovery of the patient. This leads to the development of new coating strategies and new polymers which will not cause, or will at least diminish, these negative effects when they are in contact with intima and neointima [56]–[58].This has led to the development and testing of biodegradable and multicoated stent, [56][58][59] among other types, to achieve an improved healing behavior seen in clinical trials such as ABSORB [60]. As previously discussed, new DES designs need to balance the amount of antiproliferative drug released so the endothelization and cicatrization are not affected. Some DES have applied an interesting approach based on the coating of their abluminal part enabling the drug to be released directly on the arterial wall, while the part in contact with the blood stream is only bare metal [61][62]. Polymer matrix, drug elution and stent design are key factors which have to be taken in account while developing new stents.

On the other hand, these types of DES are usually fabricated with industrial sprayers or through dipping techniques, which must be tailored to assure good coating results. These stents also must be characterized to compare them with other gold standards and to detail their complex composition.

The promising results achieved up to date on clinical trials and the need to develop better solutions for these current problems have encouraged the elaboration of this thesis. Having all this in mind, a new type of stent coating is going to be designed in order to reduce the inflammatory response seen in common DES. This thesis will start with the characterization of market standard stents to help build a background which will enable useful coating designs. Knowing which compositions are going to be pursued, the next chapter will focus on the elaboration of the necessary equipment and techniques to create novel coatings. From this point on, the next two chapters focus on the study of the releases obtained from the different layer designs elaborated in our laboratory. As the reader may notice through this last part of the thesis, a wide variety of profiles and various eluting phenomenon are described, opening new possibilities for tailored drug delivery.

Gene therapy and its role in the treatment of restenosis after stent implantation.

Over the last decade gene therapy has emerged as a novel, viable and promising approach to prevent restenosis. Based on local delivery of therapeutic agents to a target site, gene therapy proposes a biological solution to growth of intimal mass or vascular wall remodelling [63]. Gene therapeutic strategies offer novel treatment methods to promote re-endothelialization, and inhibit inflammation, neointimal hyperplasia and late stent thrombosis [64]-[67].

The translation of gene therapy into clinical application must be safe and requires an effective, site-specific delivery system as well as the ability to provide sustained transgene expression. Some examples of the application of this strategy can be seen in the development of treatments with an antibody to the platelet fibrinogen receptor (glycoprotein IIb/IIIa or integrin αIIb/βIII) [68], platelet-derived growth factor (PDGF) antagonist tradipil [69] or the anti-oxidant probucol [70] which reduced restenosis rate to 15 - 20%. In both the Stent Restenosis Study (STRESS) and Belgian Netherlands Stent Study (BENESTENT) trials, intracoronary stent placement reduced restenosis rates to 15% [71][72].

As discussed throughout this chapter, the development of new technologies/strategies and the use of novel drugs can improve stenting, but they leave room for complimentary therapies that could further decrease restenosis or eliminate it entirely. This achievement would make coronary interventions become a cure for symptomatic stenoses rather than merely a temporizing procedure. Against this background, gene therapy has emerged as a promising approach aimed at modification of cellular processes that give rise to restenosis [73].

This thesis was designed to take one last step, aiming to produce on more type of novel coating. As addressed in this introduction, gene therapy is a parallel line of work which can lead to the reduction or elimination of restenosis. Most important, this strategy can also be used to produce a tailored release. Aiming for a richer approach for restenosis treatment throughout this thesis, Chapter IV will tackle a novel stent design which will use a polymeric coating to adhere nanocarriers.

2. Aims

This thesis has focused on treating CAD, which remains the leading cause of death in many countries. The main challenge discussed, is improving CAD treatment through restenosis reduction. This is achieved by the elaboration of tailored pharmacological releases and the design of mechanisms which enable gene therapies and antirestenotic agents to be deployed in a controlled manner.

A work plan is performed to achieve this goal, which starts with the development of coating techniques and analytical methodologies. These will render the possibility of producing our own tailored coatings and the chance of experimenting with them, charting the influence of several parameters which directly influence drug deployment. Next, this work presents two different paths which can be followed to achieve restenosis reduction in stent implantation.

First, experimentation is focused on producing a novel multilayered stent which aims to reduce restenosis through tailored drug release. After, a second and final approach is presented, through the elaboration of a coating which immobilizes loaded nanoparticles aimed for gene therapy. After completing this workplan, a final chapter closes this thesis with the conclusions drawn from all the experimentation.

Following, the aims of each chapter are presented.

The main objective of this thesis is to design and develop new types of stents which, through tailored drug release, aim to minimize the actual inflammatory response derived from medical device implantations.

The goals of the present thesis can be summarized in the following points:

- Development of suitable coating techniques and an analytical methodology that allows the elaboration and characterization of designed stents. This will enable the proposal of new types of coatings and will produce the first DES which will be elaborated in this thesis (chapter II).

- Using the techniques tuned in the previous chapter, a variety of DES will be produced, and their release will be characterized to achieve different profiles. The main goal of this chapter is to achieve complete control of drug release in order to produce a target type of stent which will be designed to perform with a designed release profile. This stent will be tested in an *in-vivo* trial to check its efficacy (chapter III).

- After achieving the desired release control through the creation of tailored polymeric layers, this thesis was planned to make one last step towards novel coatings for DES. Inspired by nanoparticle coatings used recently in DES, a new proposal is made. To achieve a new design, a novel polymer for DES is used and an original way to adhere nanocarriers is tailored. The goal of this chapter is to develop a strategy to coat stents with nanocarriers which can show a good adhesion and avoid the washing away of the nanoparticles when deployed (Chapter IV).

3. References

[1] CDC, “Division for Heart Disease and Stroke Prevention,” 2018. [Online]. Available: https://www.cdc.gov/dhdsp/.

[2] CDC, “National Center for Chronic Disease Prevention and Health Promotion,” 2018. [Online]. Available: https://www.cdc.gov/chronicdisease/index.htm.

[3] H. GK., “Inflammation, atherosclerosis, and coronary artery disease,” *N. Engl. J. Med.*, pp. 1685–1695, 2005.

[4] American Heart Society, “Angina (Chest Pain).” 2020. [Online]. Available: https://www.heart.org/en/health-topics/heart-attack/angina-chest-pain

[5] MedlinePlus, “Angina de pecho.” 2020. [Online]. Available: https://medlineplus.gov/spanish/angina.html.

[6] J. I. Weitz, J. W. Eikelboom, and M. M. Samama, “New antithrombotic drugs - Antithrombotic therapy and prevention of thrombosis, 9th ed: American College of Chest Physicians evidence-based clinical practice guidelines,” *Chest*, vol. 141, no. 2 SUPPL., 2012.

[7] P. F. Cohn, “Pharmacological treatment of ischaemic heart disease Monotherapy vs combination therapy,” *Eur. Heart J.*, vol. 18 Suppl B, no. July, pp. B27-34, 1997.

[8] UCSF, “Coronary Artery Bypass Grafting (CABG),” 2020. [Online]. Available: https://cardiacsurgery.ucsf.edu/conditions--procedures/coronary-artery-bypass-grafting-(cabg).aspx.

[9] Ter Woorst, J., Sjatskig, J., Soliman-Hamad, M., Akca, F., Haanschoten, M., & van Straten, A. (2020). Evolution of perioperative blood transfusion practice after coronary artery bypass grafting in the past two decades. Journal of Cardiac Surgery.

[10] Heart&Stroke, “Percutaneous coronary intervention (PCI or angioplasty with stent),” 2020. [Online]. Available: http://www.heartandstroke.ca/heart/treatments/surgery-and-other-procedures/percutaneous-coronary-intervention.

[11] C. T. Dotter and M. P. Judkins, “Percutaneous Transluminal Treatment of Arteriosclerotic Obstruction.,” *Radiology*, vol. 84, no. November, pp. 631–643, 1965.

[12] W. S. Garg S, R.L., Serruys PW, “Coronary artery stents.,” in *The PCR-EAPCI Textbook Percutaneous interventional cardiovascular medicine.*, 2012.

[13] isic, “The indonesian society of interventional cardiology.” 2020. [Online]. Available: http://www.isic.or.id/patient_education_and_collaboration/2014/11/mengenal_lebih_dekat_stent_jantung_1.

[14] C. Casey, “Multi-vessel coronary disease and percutaneous coronary intervention,” *Heart*, vol. 90, no. 3, pp. 341–346, 2004.

[15] C. T. Dotter, R. W. Buschmann, M. K. McKinney, and J. Rösch, “Transluminal expandable nitinol coil stent grafting: preliminary report.,” *Radiology*, vol. 147, no. 1, pp. 259–260, 1983.

[16] V. A. P. Mª Pilar Guillén Goberna, Purifiación Mogollón Cardero, Inés Lago Celada, “Procedimientos Intervencionistas,” *Man. Enfermería en Cardiol. Interv. y Hemodinámica. Protoc. unificados*, pp. 188–238, 2014.

[17] J. C. Palmaz, R. R. Sibbitt, S. R. Reuter, F. O. Tio, and W. J. Rice, “Expandable intraluminal graft: a preliminary study. Work in progress.,” *Radiology*, vol. 156, no. 1, pp. 73–77, 1985.

[18] R. A. Schatz, J. C. Palmaz, F. O. Tio, F. Garcia, O. Garcia, and S. R. Reuter, “Balloon-expandable intracoronary stents in the adult dog,” *Circulation*, vol. 76, no. 2, pp. 450–457, 1987.

[19] A. Colombo, P. Hall, J. Thomas, Y. Almagor, and L. Finci, “Initial Experience With the Disart icu lated (One-Half) Palmaz-Schatz Stent : A Technical Report,” vol. 308, pp. 15–19, 1992.

[20] Scgvs, “P.A.D / Cath Lab,” 2020. [Online]. Available: https://www.scgvs.com/contents/patient-resources/pad-cath-lab.

[21] P. W. Serruys *et al.*, “Randomised comparison of implantation of heparin-coated stents with balloon angioplasty in selected patients with coronary artery disease (Benestent II)[erratum appears in Lancet 1998 Oct 31;352(9138):1478],” *Lancet*, vol. 352, no. Benestent II, pp. 673–681, 1998.

[22] Piccolo, R., & Windecker, S. (2018). Stent Technology. In The Interventional Cardiology Training Manual (pp. 137-159). Springer, Cham.

[23] Fischman, D. L., Leon, M. B., Baim, D. S., Schatz, R. A., Savage, M. P., Penn, I., ... & Cleman, M. (1994). A randomized comparison of coronary-stent placement and balloon angioplasty in the treatment of coronary artery disease. New England Journal of Medicine, 331(8), 496-501.

[24] G. N. Levine *et al.*, “2011 ACCF/AHA/SCAI guideline for percutaneous coronary intervention,” *J. Am. Coll. Cardiol.*, vol. 58, no. 24, pp. e44–e122, 2011.

[25] D. R. Holmes *et al.*, “Results of prevention of REStenosis with tranilast and its outcomes (PRESTO) trial,” *Circulation*, vol. 106, no. 10, pp. 1243–1250, 2002.

[26] C. A. Kavanagh, Y. A. Rochev, W. M. Gallagher, K. A. Dawson, and A. K. Keenan, “Local drug delivery in restenosis injury: Thermoresponsive co-polymers as potential drug delivery systems,” *Pharmacol. Ther.*, vol. 102, no. 1, pp. 1–15, 2004.

[27] Katsanos, K., Kitrou, P., Spiliopoulos, S., Diamantopoulos, A., & Karnabatidis, D. (2016). Comparative effectiveness of plain balloon angioplasty, bare metal stents, drug-coated balloons, and drug-eluting stents for the treatment of infrapopliteal artery disease: systematic review and Bayesian network meta-analysis of randomized controlled trials. Journal of Endovascular Therapy, 23(6), 851-863.

[28] T. C. Woods and A. R. Marks, “Drug-Eluting Stents,” *Annu. Rev. Med.*, vol. 55, no. 1, pp. 169–178, 2004.

[29] G. Acharya and K. Park, “Mechanisms of controlled drug release from drug-eluting stents,” *Adv. Drug Deliv. Rev.*, vol. 58, no. 3, pp. 387–401, 2006.

[30] Kang, S. H., Chae, I. H., Park, J. J., Lee, H. S., Kang, D. Y., Hwang, S. S., ... & Kim, H. S. (2016). Stent thrombosis with drug-eluting stents and bioresorbable scaffolds: evidence from a network meta-analysis of 147 trials. JACC: Cardiovascular Interventions, 9(12), 1203-1212.

[31] S. Venkatraman, F. Boey, and L. L. Lao, “Implanted cardiovascular polymers: Natural, synthetic and bio-inspired,” *Prog. Polym. Sci.*, vol. 33, no. 9, pp. 853–874, 2008.

[32] A. de Mel, G. Jell, M. M. Stevens, and A. M. Seifalian, “Biofunctionalization of biomaterials for accelerated in situ endothelialization: A review,” *Biomacromolecules*, vol. 9, no. 11, pp. 2969–2979, 2008.

[33] S. Meng *et al.*, “The effect of a layer-by-layer chitosan-heparin coating on the endothelialization and coagulation properties of a coronary stent system,” *Biomaterials*, vol. 30, no. 12, pp. 2276–2283, 2009.

[34] Q. Lin, X. Ding, F. Qiu, X. Song, G. Fu, and J. Ji, “In situ endothelialization of intravascular stents coated with an anti-CD34 antibody functionalized heparin-collagen multilayer,” *Biomaterials*, vol. 31, no. 14, pp. 4017–4025, 2010.

[35] M. A. Costa and D. I. Simon, “Molecular basis of restenosis and drug-eluting stents,” *Circulation*, vol. 111, no. 17, pp. 2257–2273, 2005.

[36] A. V., “Modulating the proliferative response to treat restenosis after vascular injury, in Molecular and Translational Vascular Medicine.,” in *Modulating the proliferative response to treat restenosis after vascular injury, in Molecular and Translational Vascular Medicine.*, Springer, 2012, pp. 228–248.

[37] E. Schampaert *et al.*, “The Canadian study of the sirolimus-eluting stent in the treatment of patients with long de novo lesions in small native coronary arteries (C-SIRIUS),” *J. Am. Coll. Cardiol.*, vol. 43, no. 6, pp. 1110–1115, 2004.

[38] J. Schofer *et al.*, “Sirolimus-eluting stents for treatment of patients with long atherosclerotic lesions in small coronary arteries: Double-blind, randomised controlled trial (E-SIRIUS),” *Lancet*, vol. 362, no. 9390, pp. 1093–1099, 2003.

[39] D. R. Holmes *et al.*, “Analysis of 1-Year Clinical Outcomes in the SIRIUS Trial: A Randomized Trial of a Sirolimus-Eluting Stent Versus a Standard Stent in Patients at High Risk for Coronary Restenosis,” *Circulation*, vol. 109, no. 5, pp. 634–640, 2004.

[40] A. Halkin and G. W. Stone, “Polymer-based paclitaxel-eluting stents in percutaneous coronary intervention: A review of the TAXUS trials,” *J. Interv. Cardiol.*, vol. 17, no. 5, pp. 271–282, 2004.

[41] D. Stents, G. M. Sangiorgi, and G. Stankovic, “Incidence, Predictors, and Outcome of Thrombosis After Successful Implantation of Drug-Eluting Stents,” vol. 293, no. 17, 2005.

[42] R. Moreno *et al.*, “Drug-eluting stent thrombosis: Results from a pooled analysis including 10 randomized studies,” *J. Am. Coll. Cardiol.*, vol. 45, no. 6, pp. 954–959, 2005.

[43] H. V. Anderson and T. D. Henry, “Drug-Eluting or Bare-Metal Stents for Acute Myocardial Infarction,” vol. 49, no. 19, pp. 7–9, 2007.

[44] J. Mehilli *et al.*, “Drug-eluting versus bare-metal stents in saphenous vein graft lesions (ISAR-CABG): A randomised controlled superiority trial,” *Lancet*, vol. 378, no. 9796, pp. 1071–1078, 2011.

[45] G. W. Stone *et al.*, “Paclitaxel-eluting stents versus bare-metal stents in acute myocardial infarction,” *N.Engl.J.Med.*, vol. 360, no. 1533-4406 (Electronic), pp. 1946–1959, 2009.

[46] P. W. Serruys, P. A. Lemos, and B. A. Van Hout, “Sirolimus eluting stent implantation for patients with multivessel disease: Rationale for the arterial revascularisation therapies study part II (ARTS II),” *Heart*, vol. 90, no. 9, pp. 995–998, 2004.

[47] A. T. L. Ong *et al.*, “The unrestricted use of paclitaxel- versus sirolimus-eluting stents for coronary artery disease in an unselected population: One-year results of the Taxus-Stent Evaluated at Rotterdam Cardiology Hospital (T-SEARCH) registry,” *J. Am. Coll. Cardiol.*, vol. 45, no. 7, pp. 1135–1141, 2005.

[48] D. R. Whittaker and M. F. Fillinger, “Vascular and Endovascular Surgery The Engineering of Endovascular Stent Technology : A Review,” vol. 40, no. 2, pp. 85–94, 2006.

[49] R. Jabara *et al.*, “A third generation ultra-thin strut cobalt chromium stent: Histopathological evaluation in porcine coronary arteries,” *EuroIntervention*, vol. 5, no. 5, pp. 619–626, 2009.

[50] C. Rogers and E. R. Edelman, “Endovascular stent design dictates experimental restenosis and thrombosis.,” *Circ. J.*, vol. 91, no. 12, pp. 2995–3001, 1995.

[51] J. Pache *et al.*, “Intracoronary stenting and angiographic results: Strut thickness effect on restenosis outcome (ISAR-STEREO-2) trial,” *J. Am. Coll. Cardiol.*, vol. 41, no. 8, pp. 1283–1288, 2003.

[52] A. Manuscript and T. Structures, “NIH Public Access,” vol. 6, no. 13, pp. 247–253, 2009.

[53] D. J. Kereiakes *et al.*, “Usefulness of a cobalt chromium coronary stent alloy,” *Am. J. Cardiol.*, vol. 92, no. 4, pp. 463–466, 2003.

[54] M. H. Sketch, M. Ball, B. Rutherford, J. J. Popma, C. Russell, and D. J. Kereiakes, “Evaluation of the Medtronic (Driver) cobalt-chromium alloy coronary stent system,” *Am. J. Cardiol.*, vol. 95, no. 1, pp. 8–12, 2005.

[55] CX charing cross, “Multilayer stent not a breakthrough, say 56% of CX audience.”

[56] S. Youssefian and N. Rahbar, “Nano-scale adhesion in multilayered drug eluting stents,” *J. Mech. Behav. Biomed. Mater.*, vol. 18, pp. 1–11, 2013.

[57] S. (CN) Yi Zhang, Shanghai (CN); Qiyi Luo, Shanghai (CN); Zhirong Tang, Shanghai (CA); Junfei Li, “DRUG-ELUTING STENT WITH MULTI-LAYER COATINGS,” US 2005/0033414A1, 2005.

[58] L. C. Su, Y. H. Chen, and M. C. Chen, “Dual drug-eluting stents coated with multilayers of hydrophobic heparin and sirolimus,” *ACS Appl. Mater. Interfaces*, vol. 5, no. 24, pp. 12944–12953, 2013.

[59] X. Wang, S. S. Venkatraman, F. Y. C. Boey, J. S. C. Loo, and L. P. Tan, “Controlled release of sirolimus from a multilayered PLGA stent matrix,” *Biomaterials*, vol. 27, no. 32, pp. 5588–5595, 2006.

[60] A. Colombo and A. S. Sharp, “The bioabsorbable stent as a virtual prosthesis,” *Lancet*, vol. 373, no. 9667, pp. 869–870, 2009.

[61] A. Abizaid and J. R. Costa, “New drug-eluting stents an overview on biodegradable and polymer-free next-generation stent systems,” *Circ. Cardiovasc. Interv.*, vol. 3, no. 4, pp. 384–393, 2010.

[62] S. Garg and P. W. Serruys, “Coronary stents: Current status,” *J. Am. Coll. Cardiol.*, vol. 56, no. 10 SUPPL., pp. S1–S42, 2010.

[63] P. Holvoet, R. Quarck, and P. Holvoet, “Restenosis and gene therapy,” *Ashley Publ.*, no. February, 2001.

[64] K. Yin and D. K. Agrawal, “Gene therapy for in-stent restenosis : Targets and delivery system,” vol. 1, no. 2, pp. 93–101, 2014.

[65] P. Jarkko, “Local adventitial anti-angiogenic gene therapy reduces growth of vasa-vasorum and in-stent restenosis in WHHL rabbits,” 2018.

[66] S. Ylä-Herttuala and A. H. Baker, “Cardiovascular Gene Therapy: Past, Present, and Future,” *Mol. Ther.*, vol. 25, no. 5, pp. 1095–1106, 2017.

[67] W. Ye *et al.*, “Reduction-Responsive Nucleic Acid Delivery Systems To Prevent In-Stent Restenosis in Rabbits,” *ACS Appl. Mater. Interfaces*, vol. 11, pp. 28307–28316, 2019.

[68] S. Francisco and I. D. State-of-the-art, “Randomised trial of coronary intervention with antibody against platelet IIb / IIIa iritegrin for reduction of clinical restenosis : results at six months *,” pp. 881–886, 1993.

[69] A. Maresta *et al.*, “Trapidil (Triazolopyrimidine), a Platelet-Derived Growth Factor Antagonist , Reduces Restenosis After Percutaneous Transluminal Coronary Angioplast Results of the Randomized , Double-Blind STARC Study,” no. April 1990, pp. 2710–2715, 1992.

[70] M. D. JEAN-CLAUDE TARDIF, M.D., GILLES CÔTÉ, M.D., JACQUES LESPÉRANCE, M.D., MARTIAL BOURASSA, M. D. JEAN LAMBERT, PH.D., SERGE DOUCET, M.D., LUC BILODEAU, M.D., STANLEY NATTEL, M.D., AND PIERRE DE GUISE, and F. T. M. A. P. S. GROUP, “Probucol and multivitamins in the prevention of restenosis after coronary angioplasty,” *N. Engl. J. Med.*, vol. 337, no. 6, pp. 365–372, 1997.

[71] Fischman, D. L., Leon, M. B., Baim, D. S., Schatz, R. A., Savage, M. P., Penn, I., ... & Cleman, M. (1994). A randomized comparison of coronary-stent placement and balloon angioplasty in the treatment of coronary artery disease. New England Journal of Medicine, 331(8), 496-501.

[72] Serruys, P. W., De Jaegere, P., Kiemeneij, F., Macaya, C., Rutsch, W., Heyndrickx, G., ... & Belardi, J. (1994). A comparison of balloon-expandable-stent implantation with balloon angioplasty in patients with coronary artery disease. New England Journal of Medicine, 331(8), 489-495.

[73] R. Kishore and D. W. Losordo, “Gene therapy for restenosis : Biological solution to a biological problem,” *J. Mol. Cell. Cardiol.*, vol. 42, pp. 461–468, 2007.

Chapter II.

Design and production of multi-layered stents

This page intentionally left blank

2.1 Introduction

This first experimental chapter is based on the elaboration of the first stent models obtained at our laboratory. A brief description of the common industrial methods used to produce DES will be followed by the characterization techniques and production methods developed throughout the initial part of this work. This will help to understand the main issues encountered when producing polymeric coatings. At the end of this chapter the first stents obtained are shown, opening a whole range of possibilities for the design and creation of new DES. As discussed on chapter I, the whole purpose of creating new designs for DES is based on the need to reduce the side effects related to their implantation. To achieve effective coating designs, it is necessary to achieve a good understanding relative to the composition of the golden standard stents present in the market. This is one of the main reasons, apart from characterizing the new stents produced, why the development of analytical and characterization methods is so important.

Currently, the most used techniques to produce DES in the industry are spraying and dipping. Both systems can be appropriate for the elaboration of the new coatings pursued in this thesis, so they will be adjusted and applied as to obtain the desired results. To understand these processes better they are briefly described next, including the main issues encountered when applying these techniques to DES coatings. The two most important techniques used to produce these types of films are dipping and spraying.

Stents are generally coated by dipping or spray coating with polymer and a pharmaceutical agent. ***Dipping*** consists in the immersion of the stent strut on a mix composed of polymer, drug and solvent. Concentration and timings differ with the dipping process used. Some may depend mostly on an ultraviolet (UV) curing done afterwards and others may require to be left drying at room temperature [1][2]. After a certain period, the stent is slowly pulled out and dried/cured to finish the process. To avoid agglomerates or irregular surfaces, relatively low concentration mixes are used [3][4].

One of the most common issues encountered while using high concentration mixes is the formation of film structures across the open spaces between the filaments of the device. This phenomenon is called webbing, and it's particularly concerning when working with modern stents which are designed with less open structures. An incident such as this may interfere with the performance of the stent, as entire films may detach. This can be specially dangerous while performing a balloon expansion at stent deployment [5]. Films may rupture and provide sites that activate platelet deposition or pieces of the bridging film may break off and cause further complications such as obstructions in the vessel. In general, dipping techniques are used to coat single layers or to create multilayers using different fixing methods such as UV curing [6].

Applying a process to coat a medical device using a ***spray*** technique usually involves the implementation of a polymeric carrier. DES coatings should have a composition which includes a solvent, a dissolved polymer, and a therapeutic substance dispersed or dissolved in the mix. After applying the mixture to the stent, the solvent is allowed to evaporate. When dry, this process will produce a thin layer of polymer mixed with the therapeutic substance over the stent strut [4][7]. Depending upon the final coating thickness desired on the stent, a multi-step coating may be applied to achieve a multi-layered stent.

Determined by the solvent used and its volatility, a resting period is required after the spraying process. This time may be reduced by applying heat or a gas current to facilitate the evaporation of the solvent [8]. An important concept to take in account when spraying an optimal layer is that all parameters have to be optimized and fixed. These include distance from the sprayer tip to the stent, rotational speed of the stent, horizontal speed of the sprayer, solvent and air flow and polymer and drug concentration in the sprayed solution.

These techniques can prove to be adequate for multiple types of coatings, but in both cases, the surface treated is usually activated in some way to enhance adhesion. If the union between coating and strut is not good enough, the whole system may detach during stent implementation causing serious complications. Next, two of the most well-known methods used to improve adhesion between two surfaces are going to be described.

Applying a polymeric matrix may seem the most important part of producing DES, but this will render useless if the adhesion between the polymer and the strut is weak. To assure good adhesion between them, two methods can prove useful. These are plasma and silanization.

When applying ***plasma*** to modify a selected surface, there are different processes that can be considered to achieve satisfactory results. One of these is known as physical sputtering of materials, which takes place with a non-reactive gas in the plasma phase. During this process, the atoms which compose this gas are turned into ions and accelerated towards the materials surface when achieving a plasma phase. When this happens, these ions transfer the energy they store through the collision with atoms located on the surface of the material. These atoms will also dissipate this energy to their neighbors, and the process will go on until an atom is expelled into the vapor phase [9][10]. This sputtering process is used frequently as a cleaning process and is commonly put to practice in the glass and ceramic industry.

A second method, called chemical etching, involves a chemical reaction of the exited species with the elements in the substrate surface. During this process both chemical and physical reactions usually take place. These generate superficial modifications which lead to further cross-linking on polymers or changes on the hydrophobicity of the recently chemically modified surface [11]–[13]. Chemical etching is also largely used as a cleaning process for a wide range of materials. These two methods are used throughout Chapter II and III, as they can prepare the stent struts to show a good adhesion and hydrophilic behavior.

A third type of plasma process, called plasma deposition, is of particular interest. It may be used to produce plasma polymerizations, commonly described as “the formation of polymeric materials under the influence of plasma” [14]. This involves the dissociation of starting materials and reorganization of the resulting neutral and charged molecular fragments into macromolecular structures on the surface of the substrate. During this plasma polymerization, a precursor is added into the system in order to be activated by plasma to bombard the surface which will lead to the dissociation of bonds at the interface, etching and chemical reactions between the active sites in the material’s surface and the activated monomer [15]. This method can be used to deposit polymeric films over the stent strut and will be studied on Chapter IV.

Silanes are commonly known for their use as coupling agents which enhance adhesion between inorganic and polymeric materials. After activating the surface through the creation of hydroxyl groups, these agents can chemically bond to it and improve adhesion with polymeric coatings [16]. Usually, these agents share a common structure R'-Si-X3 where X is a hydrolyzable group which will react with the substrate, and R' a reactive group which bonds to the polymer [17].

Hydrolysis occurs stepwise to form alkoxysilanols and silane triols. Silanol groups are extremely reactive and condensation reactions occur easily with silanols on the mineral substrate or with other alkoxysilanols [18]. Silanization processes take place through hydrogen bonding when the silane solution is applied to the substrate and by further covalent M-O-Si oxane bond formation when drying [19][20]. This method can provide a quick and easy way to adhere polymeric coatings with no specialized instrumentation required. This can be a good method to produce good adhesion for stents and will be used throughout Chapter II.

Now that the processes of activation and coating have been described, the next logical step is to comprehend better the composition and design of these films. Following, this introduction will lead to how stents are pharmacologically loaded and how can multilayers be achieved. Some main issues such as which drug loads should be targeted, or which combinations can produce satisfactory results will be tackled.

In commercial stents, high concentration coatings are one of the preferred means to achieve high ***drug loadings*** which usually go up to 50% in spraying mixes. These drug loads, once the mix is applied and dry on the stent, are usually measured by calculating the µg of drug / surface area coated in mm^2. Target values are usually over 1 µg/ mm^2 [21]–[25]. Depending on the concentration of drug or polymer used to spray, the density of the formulation may vary, and the sprayed material may produce undesired morphologies over the strut. Multiple dip-coating has been used as a method to build thicker coatings on a stent although this has not always been achieved. The application of multiple dip coats from low concentration solutions often reach a limiting loading level as equilibrium is reached between the solution concentration and the amount of coating deposited [26]. Having this in mind it is important to know if the concentrations which are going to be used are suitable for a multi-layered application.

Various polymers were selected to elaborate the different matrices adhered on the stent struts throughout this thesis. PLGA and PLA were the first selected as their release profile was sufficiently different and both were well studied and used in commercial stents [27]–[32]. Apart from these two polymers, poly(N-(2-hydroxypropyl) methacrylamide) (pHPMA) with a 5% of cholesterol was also selected as it had already been elaborated and tested by our group, showing promising results. PHPMA is an amphiphilic copolymer that can be used in film-forming compositions. The amphiphilic copolymer is characterized by having a defined structure with a hydrophilic polymer backbone and pendant hydrophobic groups. When applied to the skin, the copolymer rearranges in contact with the lipid-rich domains of the outermost layer of the skin, resulting in stable film formation [33]. Due to its characteristics, it may adhere to the artery wall to achieve a control liberation if it has been pharmacologically loaded previously. Having these three polymers available, they were used in this work to elaborate the different stent coatings.

These coating systems are usually preceded by surface treatments which enable a good adhesion to the stent strut. Using activation procedures previously described in our group and others prepared throughout this thesis, an optimal solution will be achieved to enhance adhesion during the preparation of the designed stents. In terms of elaborating the different coatings for DES, an optimization of spraying and dipping techniques will be done in order to achieve optimum quality layers over the stent struts. As described further on throughout this chapter, all methods are going to be prepared in order to be used in a laboratory, and later, scaled for industrial use. The main reason to build all this methodology and machinery is to have a functional system which allows the production of designed stents. As the main objective of this thesis, throughout the elaboration of coatings with different mixes of polymers and drugs and the study of their performance, combinations which aim for a reduction of restenosis through the design of novel DES are sought. Following, Chapter II will focus on the first aim of this thesis as previously described in Chapter I:

- Development of suitable coating techniques and an analytical methodology that allows the elaboration and characterization of designed stents. This will enable the proposal of new types of coatings and will produce the first DES which will be elaborated in this thesis.

2.2 Materials and methods

Figure 1 presents a diagram of the plasma reactor used in this chapter. An analogical Pirani type vacuum meter (MKS, USA) was connected near the middle of the reactor chamber to monitor the pressure. In a home-built system, the pulse generator controlled the pulsing of the radio frequency signal, which was then treated with a 100W amplifier and passed via an analogue wattmeter and a matching network to a 10 cm long coil located around the exterior of the reactor. The typical base pressure prior to all experiments was $2x10^{-2}$ mbar. A 50/50 mix of O_2 and Ar was used with a final working pressure of $8x10^{-1}$ mbar. The reactor's inner volume is approximately 3 L. Stents activated in this reactor were mounted on a metallic filament which suspends the struts in the middle of the tubular reactor. Apart from applying 100W, activation was also performed at 120 and 150W. Adhesion tests and contact angle results were practically identical for the three methods so an activation with 100W was used throughout the thesis to avoid modifying excessively the stent surface.

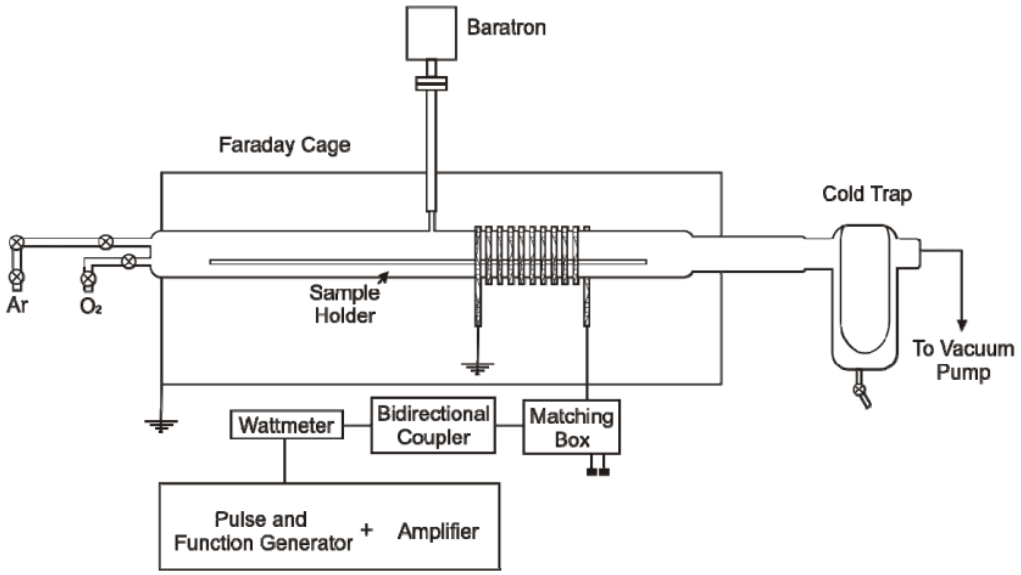

Figure 1: Home-built 70 cm long cylindrical Pyrex reactor and its electrical components. Ar and O_2 flow is regulated and added into the reactor chamber through the left entries. Samples are places on top of the crystal sample holder and in the interior of the copper coil. A cold trap is situated at the exit to avoid damaging the vacuum pump and to prevent venting the gases outside of the system. In the reduction between the faraday cage and the cold trap there is a threaded connection which enables the opening/closing of the system in order to introduce or remove samples. System pressure is measured with a baratron locates in the reaction chamber and the plasma conditions are fixed with the rest of instrumentation depicted at the bottom of the image.

Silanization

There are various ways to achieve an adequate coating adhesion to a stent strut. An interesting and accessible method can be a silanization process performed after the activation of the metallic surface. Testing of different activation methods was carried out with different metallic samples, with the same composition as the stents used, placed on different vials. A selection of methods listed next were tried out on each sample and evaluated through contact angle and surface inspection using a DM2500 microscope from Leica. Some of these techniques are a selection of various well-known methods used in our group. Others are a recompilation of different strategies found throughout literature [34]–[41]. Next, a list of the techniques used is shown:

- Immersion of the sample in acetone and sonication during 5 min.
- Immersion of the sample in an EtOH/H_2O (1:1) mix for 5 min. Posterior wash with ultrapure H_2O.
- Immersion of the sample in H_2SO_4 5% for 5 min. Posterior wash with ultrapure H_2O.
- Immersion of the sample in HNO_3 5% for 5 min followed by an immersion in H_2SO_4 5% for 1 min. Final wash with ultrapure H_2O.
- Immersion of the sample in H_2SO_4 20% for 10 min. Posterior wash with ultrapure H_2O.
- Immersion of the sample in H_2SO_4 20% for 3h. Posterior wash with ultrapure H_2O.
- Immersion of the sample in H_2SO_4 5% for 10 min followed by an immersion in HNO_3 5% for 5 min. Posterior wash with ultrapure H_2O.

Through the different activation methods, a slight oxidation of the surface followed by the presence of water will create rugosities and generate hydroxyl groups attached to the surface. These two surface modifications are desirable, as they will enhance adhesion. Hydroxyl groups will react with the (3-Aminopropyl)triethoxysilane (3-APTES) as shown in Figure 2, leaving the sample with a silanization which will enhance the adhesion of the polymer coating applied over it. This is possible due to the bonding with its amine groups which will react with the acid groups found on the polymers applied later. Once each sample is activated, the coating process is carried out through a dipping process with 3-APTES at 0.2% during 1 min as described by Chovelon et al [19]. After the samples are dry, these are ready to be coated.

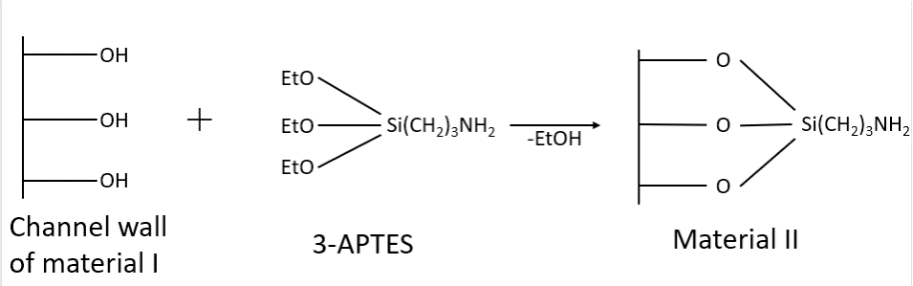

Figure 2: Process carried out to obtain a silanized surface with 3-APTES. After the activation process, hydroxyl groups are attached to the surface as seen on the left. 3-APTES bonds to the hydroxyl groups through 3 different sites, releasing EtOH during the reaction.

Spray technique

An important part of having a reliable coating technique is the obtention of reproducible and repeatable results. To produce good quality coatings that comply with these requirements, a functional laboratory spraying machine was built. Starting with the sprayer design, a basic concept was drawn to show how it would work. This draft, shown in Figure 3, is used to build a first version which became useful to optimize various parameters. A new model is drawn with Solidworks, showing a final design which is 3D printed to obtain a final version. This last version was obtained using an industrial HP Multi Jet Fusion 4210 3D printer provided by Barel SA. Motors, potentiometers, spray nozzle, compressor and power supplies are attached to the final version and the wiring is passed through the drilled holes and stored at the bottom of this structure.

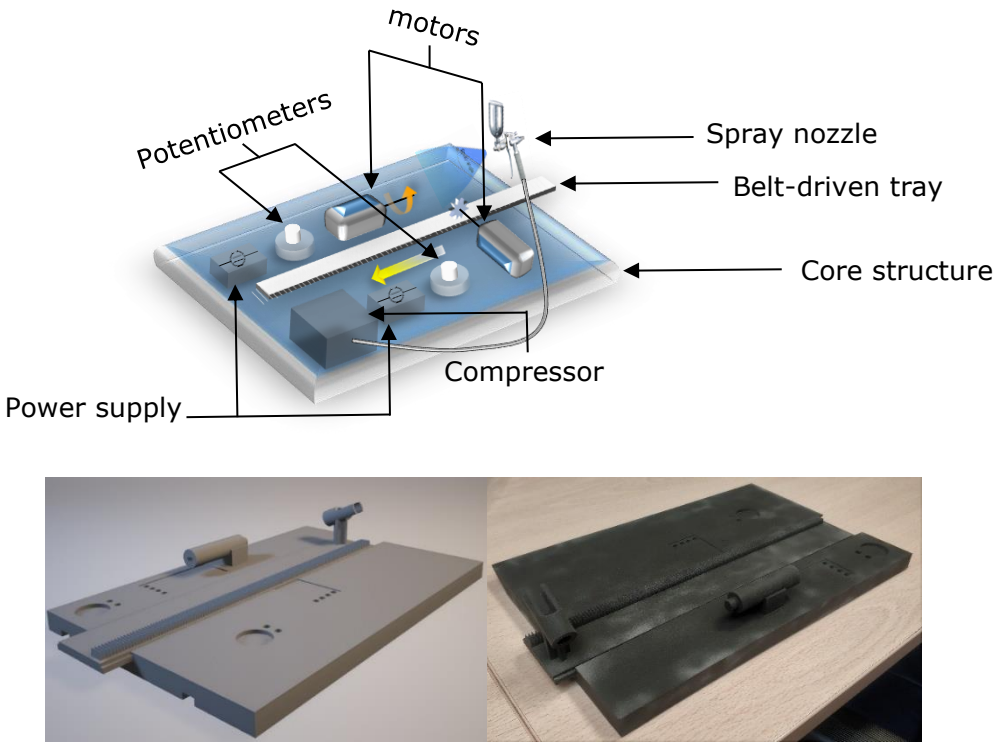

Figure 3:Elaboration of a lab scale sprayer model. Starting with the image located at the top, a basic concept of a laboratory sprayer is depicted. At the upper part of the core structure, a small motor rotates the stents while a resistance is used to control the rotation speed. At the bottom, another motor rotates with a gear attached to its end which is used to slide the sprayer's nozzle side-ways following the direction shown by the yellow arrow. Under this first image, a dimetric view of the core structure shows indentations made to place the motors, circular indentations for the resistances and perforations used to pass all the cables under the surface. A tray is designed to slide on one axis through a step design which prevents all other movements. Mounted on the tray, a holder is designed to fix the sprayer's nozzle. On a semicircular mount, a cylindrical piece is placed to enable the transmission of the rotation from the motor to a different type of outlet used to hold the stents. A last image located at the bottom shows a 3D model printed and ready to be customized.

Some basic parameters had to be adjusted, such as the distance from the nozzle to the stent, the speed of the motors or the flow sprayed through the nozzle. A fan was added to the design later on to assure the complete drying of each layer. Following some guidance from different sources [42], [43] parameter intervals are tested until optimal values are achieved. Coating results are checked through a DM2500 microscope and SEM imaging. Taking all this into account and after optimizing the parameters, the rotation of the upper motor is set to 120 revolutions per minute (rpm) (30-200 rpm recommended interval [42]) and the bottom motor is set to 24 rpm which creates a linear movement of 8 mm/sec (1-30 mm/sec recommended interval [42]). The solid composition in the sprayed mixture varies between 1.3 weight percent (%wt.) and 3 %wt. Distance between the nozzle and the stent is 2.3 cm and there are 7.5 cm between the stent and the fan. Every stent sprayed later,

with a different parameter, was visually inspected through a microscope. Inspection of samples was done to compare the quality of the coatings.

On the core structure of the sprayer, the rest of components are added as following. Two 100:1 gear compact motors 1.5 to 3 V DC from Cebekit were attached to the small rectangular slots, each connected to a variable resistance. These are connected to a charger and these to a switch to close the circuits. Each one was assembled as shown in Figure 3. An extra piece is machined for the top motor to separate it from the spraying zone and to change the shape of the rotating output, so it would match the mounting support for the stents.

Spraying mixes were prepared at different concentrations as detailed further on, but the combination of solvents and polymers was fixed throughout the thesis. PLA and PLGA were sprayed in our lab by mixing them with acetone, while pHPMA was mixed with ethanol. This selection of solvents is due to the bad solubility of each polymer with their other respective solvent, thus preventing the elimination or fusion with previous sprayed layers when proceeding through a multi-layer spraying process. These solvents were selected to elaborate the spraying mixes, discarding others such as DCM, for safety reasons and due to its easy scale up and industrialization.

Dipping

In this thesis, a basic dipping method is set up consisting in the slow immersion of a stent in a vial which contains the coating mixture prepared at a concentration of 1% w/v. This stent is attached to a thin thread at one of its ends, providing a grip for the user while holding the other end of the filament. When immersed in the mixture, the stent is left for 10 seconds before being slowly extracted. After a dip, the stent is left hanging from a support during 5 minutes until the layer is dry due to the evaporation of the solvent. A schematic example of the process is shown next in Figure 4.

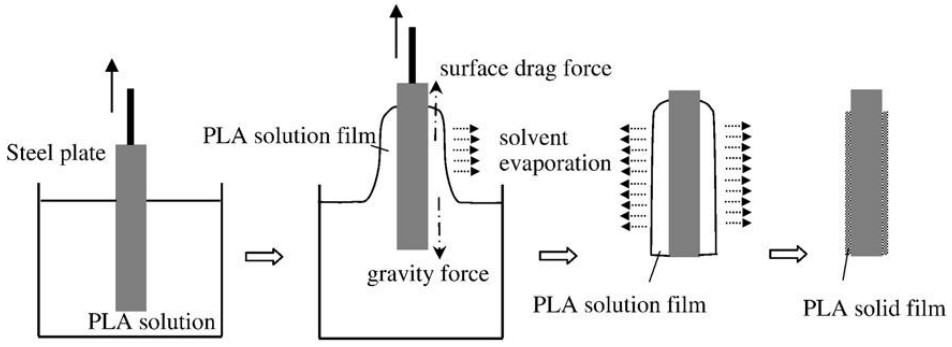

Figure 4: Dipping process. From left to right, the stent is dipped slowly into the solution and later extracted to let dry at room temperature.

This method has principally a main drawback called webbing, or bridging. To avoid this, some modifications are done enabling better results. A modified version of the dip process is carried out in this work by making the filament pass through its entire lumen and holding both ends by the user. After the dip is done, the user can gently spin the filament by rotating both ends so the excess of mixture in the stent will be expelled outwards. When this is done, the stent is dried with a gentle air flow to accelerate the process.

Scratch test

As coating thickness was not going to be the same through the different samples, method A was selected from the American Society for Testing and Materials (ASTM) adhesion test D3359 [44]. After the coating is dry and ready to be characterized, an x shaped cut is done to the coating with a scalpel and the aid of a cutting guide. After doing this, the surface was photographed with a DM2500 microscope from Leica to obtain an image of the x cut before the adhesion test was done. Next, a semitransparent pressure sensitive tape from Scotch ™ was applied over the coating using a rubber eraser on the end of a pencil. Adhesive tape was left for 90 seconds with a free end to simplify posterior removal. This tape was pulled by its free end in a quick manner at 180º.

Another image is taken from the surface of the sample to compare the condition of the coating around the x cut area. A rating was assigned to the quality of the coating based on visual inspection following the ASTM criteria shown next:

- 5A No peeling or removal
- 4A Trace peeling or removal along incisions or at their intersection
- 3A Jagged removal along incisions up to 1.6 mm on either side
- 2A Jagged removal along most of incisions up to 3.2 mm on either side
- 1A Removal from most of the area of the X under the tape
- 0A Removal beyond the area of the X
- Each test is repeated three times to ensure repeatability.

Extraction and analysis setup for stents.

Extraction of the different drugs found on stents was performed using 30 ml flasks. A stent is placed inside, and 5 ml of dichloromethane (DCM) are added to dissolve its coating (flask 1). The container is placed in an ultrasonic bath for 1 minute and the solvent is later separated in a different flask (flask 2). This process is repeated 2 more times, separating the solvent into the same flask (flask 2) and storing the total of 15 ml. To avoid the hydrolyzation that may occur during the last step of evaporation, flask 2 is placed in an acetone bath cooled with dry ice. Next, liquid DCM (flask 2) is separated into another flask (flask 3) from ice remaining on the previous one. This ice remaining in flask 2 is broken down with a spatula and washed with 5 ml of DCM. Flask 2 is placed in the cool bath and liquid DCM is separated into flask 3. This process is repeated 2 more times rendering flask 3 with an approximate volume of 25 ml.

At this moment, flask 3 contains the stent coating dissolved in DCM with no water. A current of N_2 is used to completely dry the solvent without heating the container. When the container is almost dry, the liquid is passed to a smaller 3ml flask which is easier to store. Flask 3 is washed and sonicated with DCM 2 extra times to avoid losing any amount of drug in the process. Evaporation with N_2 is continued with the small container. Once this flask is dry, a cap is placed and sealed by wrapping the exterior with parafilm. From now on, the product is dry and sealed in N_2, ready to be stored at 4ºC.

All samples are refrigerated until they are analyzed through High-performance liquid chromatography (HPLC). Preparation of the samples starts with the addition of 0.25 ml of methanol. Next, they are sonicated for 1 minute and left in an orbital shaker at 100 rpms for 10 minutes to ensure dissolving the drug remains attached to the vial walls. The resulting solution is filtered before adding it to a micro-insert to avoid residues of insoluble polymers.

HPLC

The following HPLC system was used through all the work: ELITE LaChrom from Hitachi composed of the following modulus. Organizer, Diode array detector L-2455, column oven L-2300, autosampler L-2200 and pump L-2130. A Kromasil 100 C18 15x0,4 cm column with a particle size of 5µm from Teknokroma was used to analyze the sirolimus releases. Samples obtained from the stents were extracted with DCM, dried and rediluted in 0.25 ml of methanol. To analyze the concentrated samples, micro-inserts were used in 1.5 ml vials (0.1 ml micro-inserts, 31 x 6mm, clear glass, 1st hydrolytic class, 15mm top). HPLC conditions were the following: Methanol as eluent, at a flow of 1 ml/min. Oven temperature is set to 30ºC and the detection wavelength to 278nm.

Chromatograms are done up to a final time of 5 minutes per sample with a characteristic peak of sirolimus appearing at 2.3 min. A linearity check is done through a calibration line which has minimum and maximum values obtained from initial tests, plus a security margin. This calibration is seen in Figure 5, were a clear linear tendency can be seen in the working concentration range. Different methods were originally tried out which included different eluents, retention times, flows, temperatures and working volumes [45]–[49], but modifications were introduced until the quickest reliable way was found. Everolimus was also analyzed following the same process described with sirolimus, as the group had commercial stents which were also loaded with this drug.

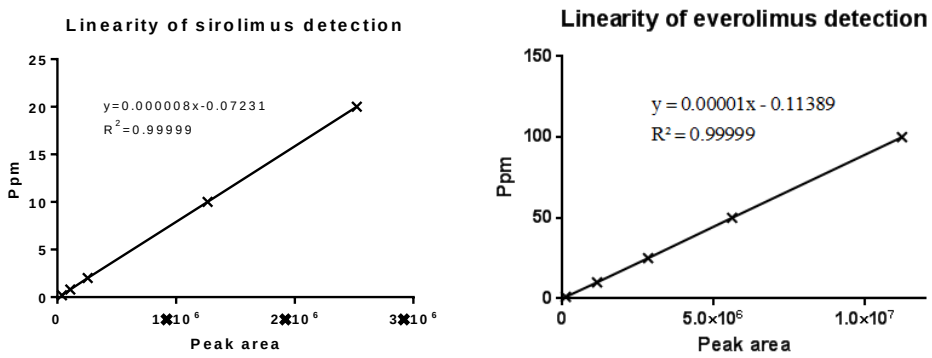

Figure 5: Linearity curves for sirolimus and everolimus detection. Image at the left shows a calibration curve obtained with sirolimus samples prepared from 0.2 to 20 ppm. On the right, a calibration curve obtained with everolimus with samples that range from 0.2 to 100 ppm. Both graphs have been plotted as ppm vs peak area, showing their respective linear equation at the center.

2.3 Results and Discussion

Setting up a characterization methodology

In order to develop a new stent design, a validation process which allows the characterization of the coating was prepared. To fulfil this need, a methodology was set up by selecting the tests which rendered the most interesting data through the analysis of commercial stents. When characterizing stent coatings, an important data to search for is the amount of drug and polymer loaded on the stent. Various methods were proposed to quantify this. First, the stents were weighted with an analytical balance (Sartorius XS105 DualRange) to know their total mass and, right after, their coating was removed. The stent was weighted once more, so the difference in mass was equivalent to the weight of the coating. This process was performed on 4 different commercial stents as shown in Table 1. Separating polymer and drug from the strut was done by solvent extraction with the aid of an ultrasound treatment as described previously, presenting a solid and simple method which proved to work better than Soxhlet extractions.

Table 1: Results obtained from a solvent extraction methodology used to quantify coating mass of different stents. Four different stents were weighed in order to obtain their coating mass. Dimensions of the stents are listed on the first column (exterior diameter x length). On the second column, the total mass in mg of each stent is shown. Strut mass is shown in the third column, which is obtained by weighing a stent after its coating has been removed. Weights obtained by the subtraction of the strut mass from the total mass are listed in the fourth column. This mass is equivalent to the coating mass.

Stent dimensions / mm	*Total mass / mg*	*Strut mass / mg*	*Coating mass / mg*
4 x 18	33.185	32.625	0.560
4 x 14	20.569	20.125	0.444
2.5 x 18	22.484	21.919	0.565
3 x 33	39.529	38.480	1.049

Other 4 stents were analyzed by thermogravimetric analysis (TGA) in order to find out their drug load. These commercial stents were supplied with their composition data, so the results obtained could be easily compared with the ones provided by their suppliers. Results obtained are shown in Table 2, were the data presented shows that the drug load was about 51.8%, very similar to the 50% claimed by the supplier.

Table 2: Drug quantification obtained by TGA. Dimensions of the stents are listed on the first column (exterior diameter x length). On the second column, the total mass in mg of each stent is shown. The amount of polymer expressed as % is shown in the third column. Polymer mass obtained is listed in the fourth column. Results obtained are coherent with the ones provided by the suppliers.

Stent dimensions / mm	*Coating mass / mg*	*Polymer by TGA / %*	*Polymer / mg*
4 x 18	0.560	48.571	0.272
4 x 14	0.251	48.185	0.121
2.5 x 18	0.444	48.198	0.214
3 x 33	0.565	48.142	0.272

Next, the composition of the polymer had to be fully detailed. To achieve this, several characterization techniques such as ToF-SIMS and HPLC were carried out on commercial stents. ToF-SIMS was initially selected, as it could be a useful method to determine the layer thickness of each coating. After several attempts, stent geometry presented complications which made this method unviable. If a stent is analyzed without modifying its geometry, no result is obtained, and if the stent strut is flattened, the coating cracks and peels off. In the end, initial results could only be used to characterize coating composition. As seen in Figure 6, characteristic peaks were found through ToF-SIMS which identified the polymer as PLA.

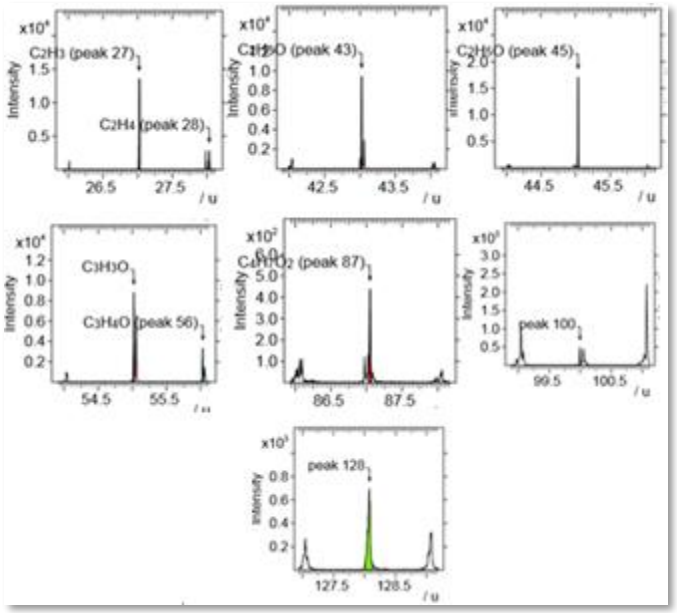

Figure 6: ToF-SIMS obtained from commercial stent. Peaks obtained match the characteristic peaks found when analyzing PLA. This methodology can be used to check the polymeric nature of the coating.

These stents were also successfully characterized by HRMN as seen in Figure 7, showing valuable information. The coating was identified as PLA and the structure of the lactides were obtained. A characteristic shift at 5.1-5.3 ppm confirmed the mixture of D, L-lactide in these PLA coatings.

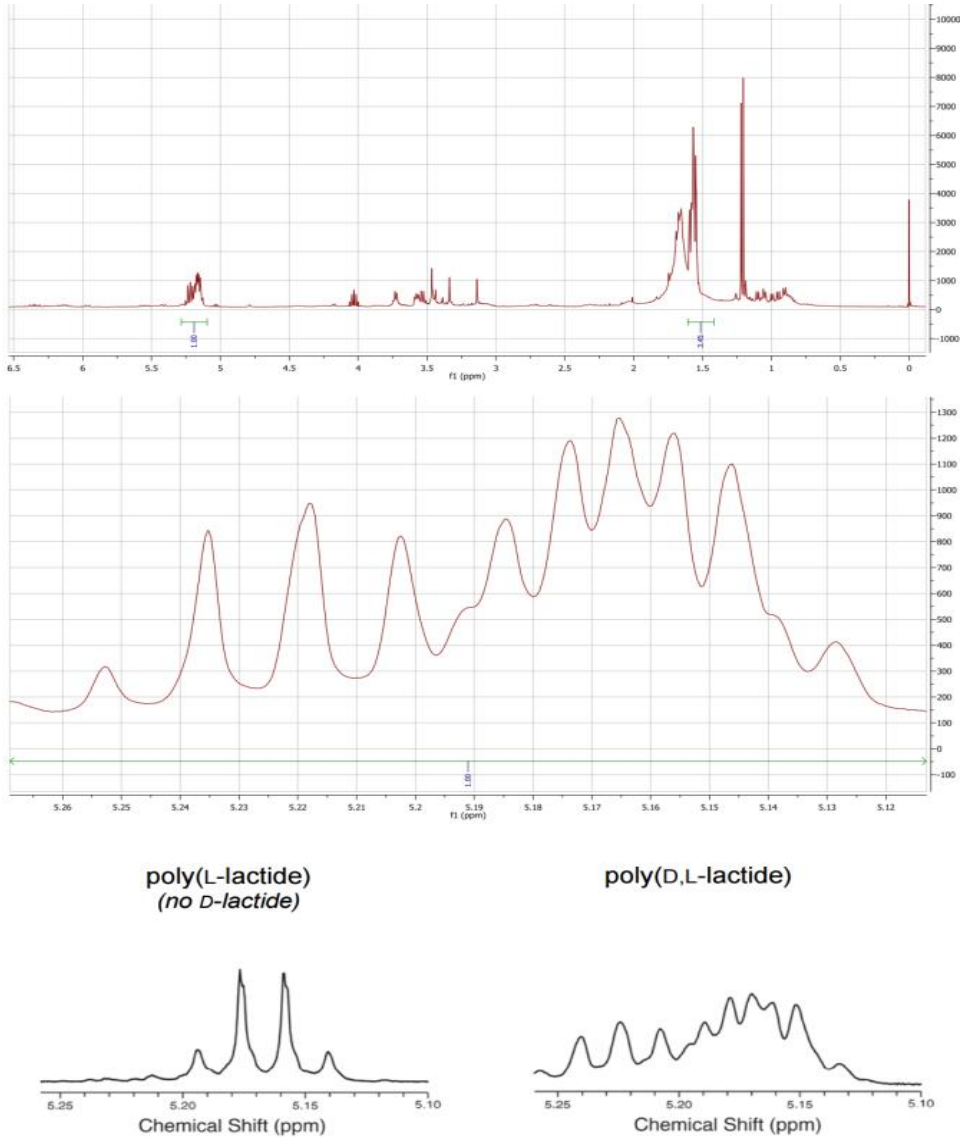

Figure 7: HRMN obtained from a PLA coated stent. Image at the top shows the spectrum obtained from the coating. The image located at the middle shows an amplified area of the first spectrum, which is useful to identify the PLA structure. Images at the bottom display standard HRMN spectra used to identify lactide structures [50]. *HRMN spectrum obtained is identified as poly (D,L-lactide).*

After obtaining the chemical composition and polymer/drug ratio of the coatings, it is important to analyze their morphology in detail. To accomplish this, the most effective way is to examine the stents with a SEM. Before surface examination takes place, various cuts and torsions were performed to separate the coating from the strut. This facilitated the obtention of coating thickness measures. When performing this surface aggression, coatings react in a similar way as when undergoing a balloon expansion. Images obtained can also offer a general idea of coating cohesion and adhesion to the stent strut. Figure 8 shows how after manipulating these stents, film thickness was measured, and the condition of the PLA coatings was checked.

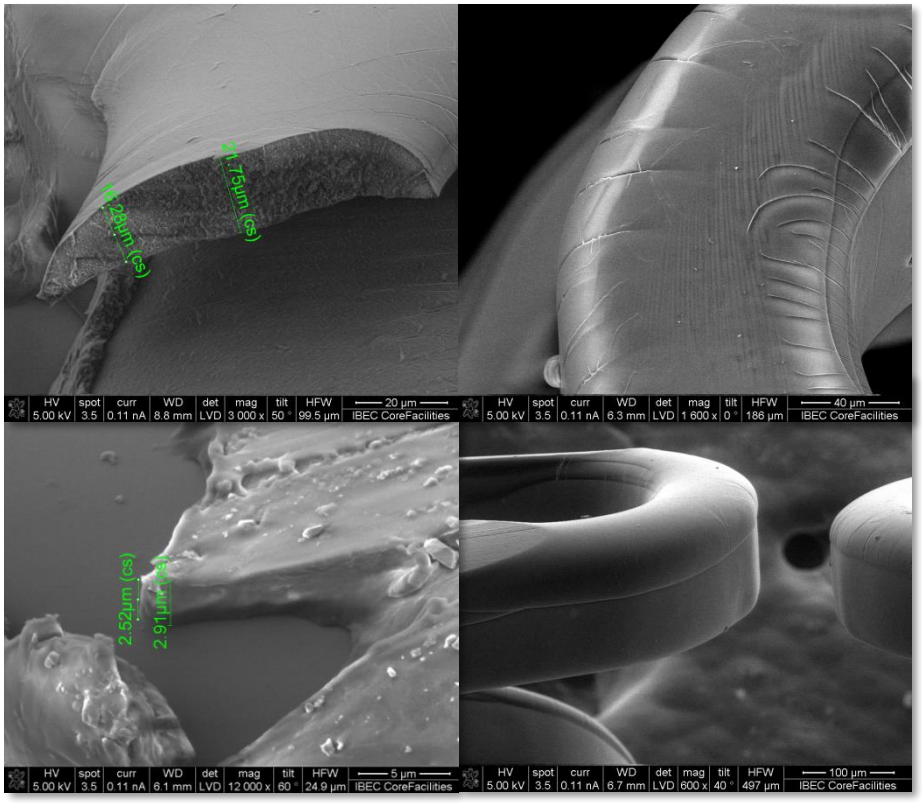

Figure 8: SEM images taken from commercial stents. On the first column, thickness is obtained by measuring the distance with the integrated software from the SEM. Images located at the second column show surface cracking with general good adhesion of the coating.

Once having a solid methodology tested, which enabled a good characterization of the coatings, the elaboration process of stents was initiated. Although new stent coatings could be designed at this point, a way to adhere the polymer to the strut should be optimized before continuing. Following, two of the most useful activation methods were tried out to find the most suitable one for our developing process.

Surface treatments for optimal coating adhesion

Surface activation is carried out in different ways to ensure a correct adhesion on the surface of the stents. Prior to a silanization process, the different methods described previously on “materials and methods” are tested on stainless steel samples. Surface modification was checked by contact angle as shown in Figure 9. Before silanization took place, surface treatments were applied to obtain modified surfaces presenting etching and the formation of hydroxyl groups associated to a reduction of the surface contact angle. Once silanization took place, as hydrophilic amine groups were going to be exposed, a reduction of the contact angle was also expected. Granting method “A” modified the contact angle much more when compared to others, methods which use acids are usually preferred. This is due to the stronger surface etching produced, which could increase the adhesion of the silane. Although method “G” produced a more hydrophilic result, this process was too aggressive and modified its surface in a manner which could affect its mechanical properties. A change in color due to heavy oxidation was seen in processes such as “F” and “G”. After seeing this data, method “D” was selected as optimal for the silanization process. Each sample was measured three times and triplicates were done for each process.

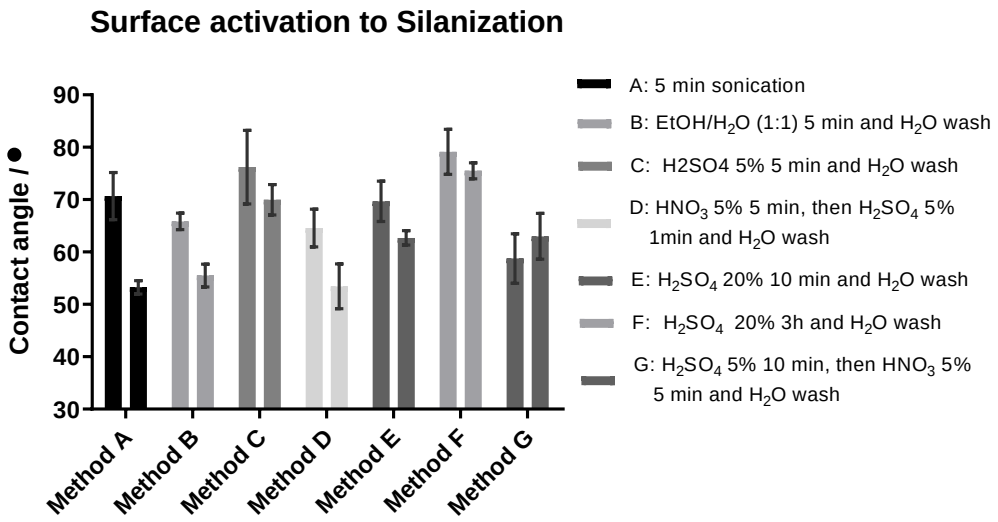

Figure 9: Contact angle on samples activated before and after silanization. Columns at the left of each method represent results pre-treatment. Columns at the right of each method show results post-treatment. Contact angles under 90º on the left columns show surface modification through etching and hydroxyl formation. A low contact angle in the right columns indicates the formation of a silane coating. Untreated samples present a contact angle of 90º.

Plasma activation was carried out as an alternative method for silanization. When testing plasma activation, an interesting idea found in scientific literature led to the addition of some extra experimentation. As seen in Choi's et al research [51], the chemical bonds formed with PLA onto a substrate can induce a better adhesion with the surface while entangling with the next layer of polymer added. Continuing with this idea, plasma activation was done on three samples followed by soaking them in melted PLA. This was done without any solvents to assure the maximum amount of bonds forming between the substrate and the polymer. Samples were left to cool down at room temperature for 1 hour, and later on, the bulk was physically removed with a scalpel. What remains attached to the metal was slightly rinsed with acetone and air dried to remove polymer chains which had not bonded. Once dry, samples were stored 24 h, and after, contact angle was measured on each. A diagram of this process is described in Figure 10.

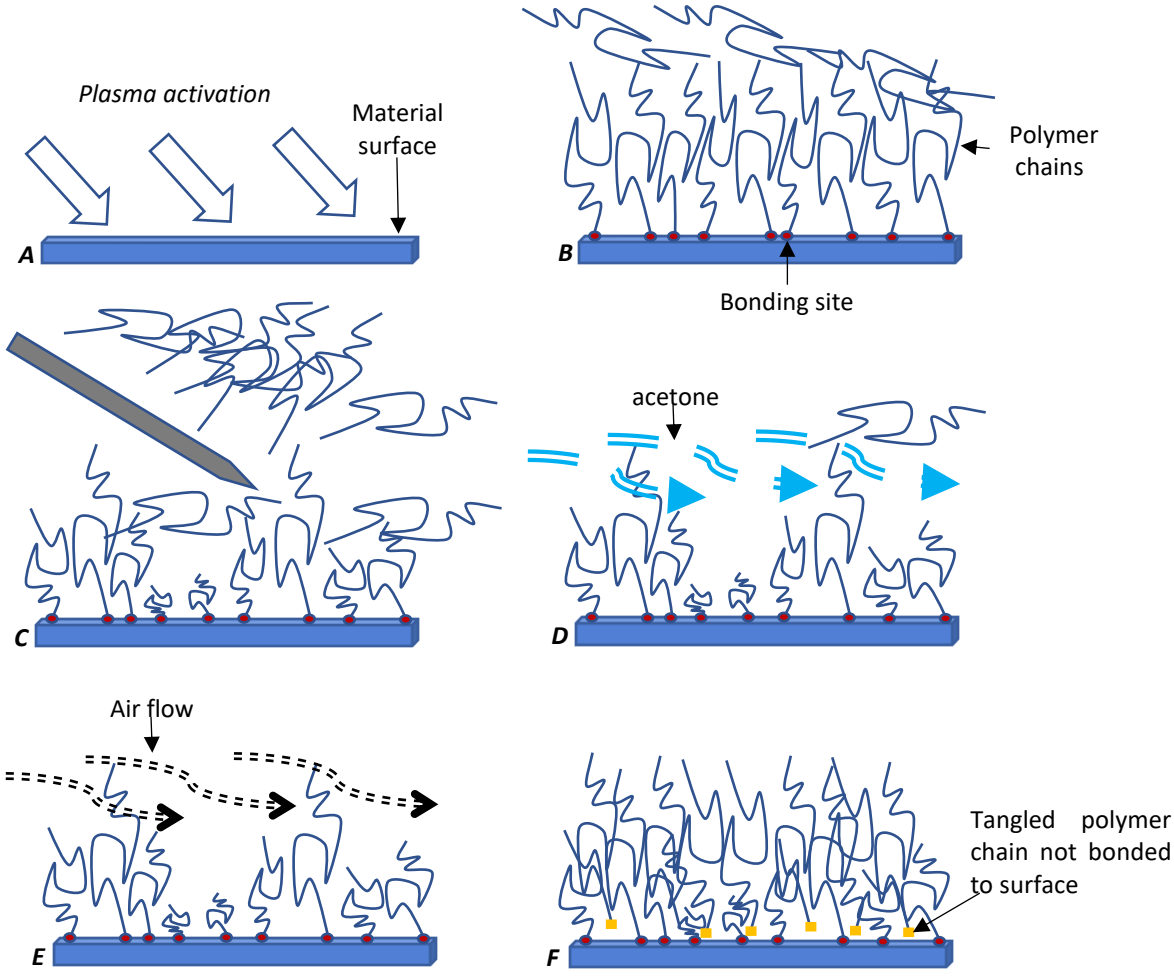

Figure 10: Illustrated process underwent to produce tangled polymer chains of PLA on a metal surface. Image "A" shows plasma activation done to prepare the surface before adding the polymer. Image "B" depicts how after activating and adding fused PLA, some polymer chains bonded to the surface. As seen in image "C", the bulk of material was physically peeled, removing most of the polymer not bonded to the substrate. In image "D", a slight rinse of acetone was used to take away the rest of polymer chains which were not bonded to the substrate located in the most interior layer next to the material surface. After this last step the material was air dried as seen in image "E", right before the polymer was added again. Last image, "F", shows how after the polymer solution was added, the polymer chains were entangled with the already bonded ones.

Results achieved from plasma activation and from the entangled PLA chain experiments are presented in Figure 11. Method A showed a very low contact angle after plasma activation. This provided good wettability for the polymeric coating and the possibility of producing chemical bonding. Method B, C and D showed how, after their respective treatments, the contact angle matched the expected value derived from having a PLA coating. On the other hand, method D showed how results varied after removing the melted PLA from the plasma activated sample by physically peeling and rinsing with acetone. In this case, contact angles showed big variations depending on the analyzed area and samples due to the heterogeneity of the surface.

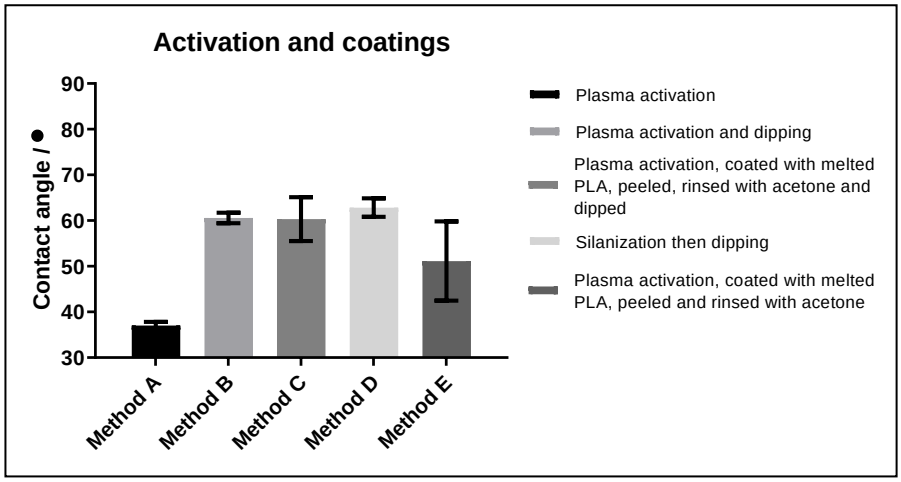

Figure 11: Contact angle on samples activated and treated with different coating methods. Starting from left to right, the first column shows contact angles obtained after the metallic samples were treated with plasma activation. Samples which had also undergone a plasma activation were dipped and their contact angle was later measured and presented in the second column. In the third column, samples had been treated with a plasma activation, coated with melted PLA, peeled, rinsed with acetone and then dipped. The fourth column shows samples which had undergone a silanization process and posteriorly dipped. In the last column, samples had been treated with plasma activation, coated with melted PLA, peeled and rinsed with acetone. Method A showed an excellent activation resulting in a very hydrophilic surface. Method B, C and D showed contact angles corresponding to a PLA surface adhered to the substrate. These samples were ready to be used in an adhesion test. Method E showed a high dispersion due to certain areas which had been completely cleaned and no PLA was adhered. Each sample was measured three times and triplicates were done for each process.

If plasma activation showed good adhesion properties it could be a promising method due to its low industrialization cost. Four differently treated samples were coated with PLA and a scratch test was performed on each to evaluate adhesion. Each test was done in triplicate. Figure 12 shows how these four different treatments modified the adhesion of a PLA film on stainless steel. A control group was tested by depositing a film of PLA on stainless-steel samples and reproducing the ASTM adhesion test (sample A). Films obtained in this test were reproduced by applying a dipping technique onto the metallic parts. Dipping was also applied to silanized (B) and plasma treated parts (C). One last sample was activated by a plasma treatment and coated with melted PLA. Then, the polymer was peeled, rinsed with acetone and dipped in a PLA solution (sample D). 24h later, the adhesion tests were performed.

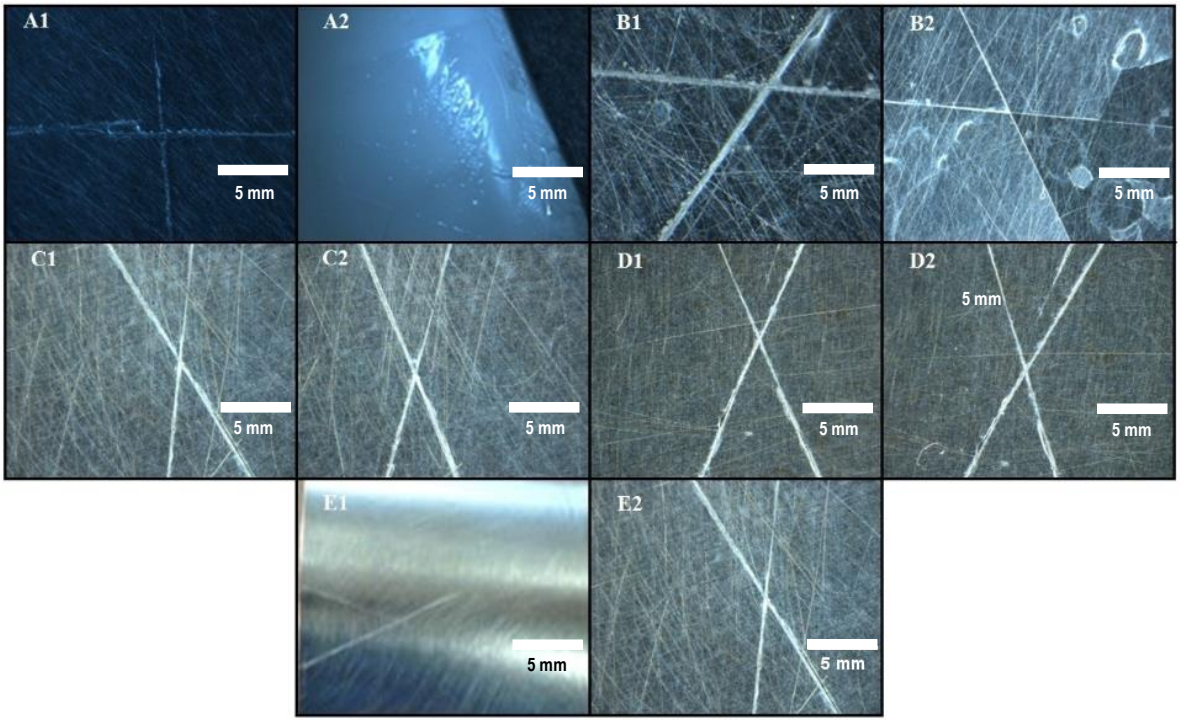

Figure 12: Adhesion test on differently activated surfaces. Samples are indexed with a letter in order to identify them and a number which clarifies if the image was taken prior reproducing the adhesion test (1) or right after finishing it (2). Images from the control samples are labeled as "A". Label "B" depicts silanized samples while label C shows the plasma activated samples. Images labeled as "D" show the samples activated by plasma, coated with melted PLA, peeled, rinsed with acetone and dipped in a PLA solution. Label "E" shows samples treated as the ones labeled as "C", but which had undergone a last flexing step in order to evaluate cracking. Controls show no adhesion and silanized samples show a 2A ASTM adhesion. In the other hand, the rest of samples show an excellent 5A ASTM adhesion result. Images were obtained by using a DM2500 microscope from Leica.

In Figure 12, images labeled as “A” showed how a control was totally peeled off leaving the PLA film attached to the adhesive tape. These tests rendered a 0A adhesion in the ASTM adhesion scale. Images labeled as “B” showed a 2A adhesion result in which an entire section of the cross was removed as well as part of an adjacent portion. Images labeled as “C” showed the plasma treated and PLA coated samples which were rated as 5A. Labeled “C” and “D” images showed a 5A adhesion result. These last samples were also flexed, in order to see if cracks appeared, and the images obtained were labeled as “E”. These presented a good behavior and no surface defects were seen. Silanized parts presented better results than the control group, but were clearly not as good as the plasma activated samples. Seeing that plasma activations showed promising results, an adhesion test was carried out on samples activated with atmospheric plasma. As atmospheric plasma is easier to implement in an industrial environment, an analogous experiment was carried out with this method to check if the results rendered were similar. Images obtained from the scratch test done to each sample are presented on the next figure.

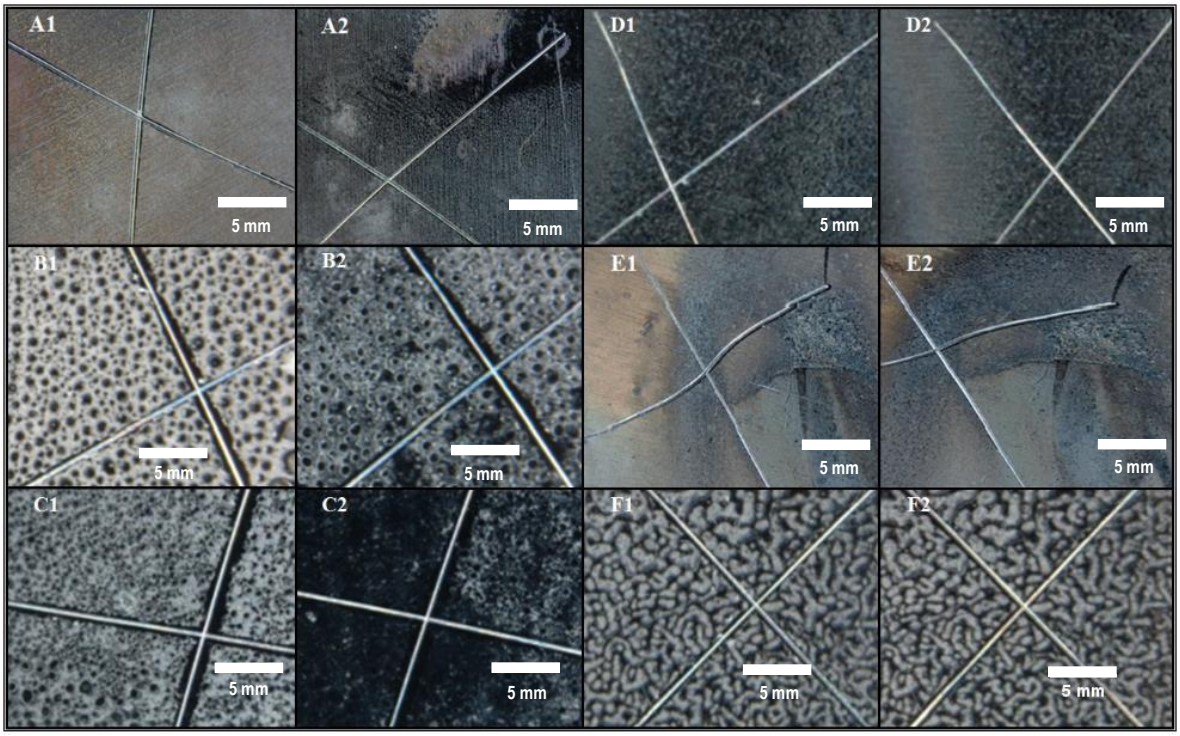

Figure 13: Adhesion tests performed on surfaces treated with atmospherical plasma. Samples were indexed with a letter to identify them and assigned a number which clarified if the image was taken prior reproducing the adhesion test (1) or right after finishing it (2). Images labeled as “A” represented the control group which had a PLA solution deposited on top of the metal samples and were left to evaporate. Images labeled as “B” depict samples which had undergone the same experiment as “A”, but with a PLA solution twice as concentrated. “C” samples were submitted to the same experiment as “B”, but with a PLA solution twice as concentrated. “D”, “E” and “F” were treated as “A”, “B” and “C” with a single difference, they had previously been activated with atmospheric plasma. Worm-like and circular patterns appeared due to thick and high concentrated coatings. Samples with no activation treatment had the thick PLA layer removed. The rest of samples showed an excellent 5A adhesion. Images were obtained by using a DM2500 microscope from Leica.

Figure 13 presents the results obtained from the adhesion tests with atmospheric plasma treated samples. Images tagged as “A” show how portions from the upper right section were removed completely. “B” and “C” images show how samples lost a considerable amount of their PLA coating although the quantity deposited was so high that some polymer still remained in adjacent areas. Detailed exploration confirmed that images A, B and C showed a bad behavior when scratched even before the adhesion test was carried out. Images labeled as D, E and F showed a perfect result with a 5A adhesion behavior and no polymer removed. A granulated pattern could be seen on the samples as the PLA solution was added on top of the surfaces and dried afterwards, producing a thick and irregular layer. Atmospheric plasma was an interesting option to take in account due to its easy adaptation to an industrial process. Although this method also rendered good results, vacuum plasma was selected as the optimal method to activate stents. Due to its excellent results and disponibility in our lab, it was the most suitable activation method to achieve the objectives pursued.

Coatings elaborated with dipping techniques

Traditional dipping was performed on stents through immersion in a PLA or a PLGA solution as described previously on the “materials and methods” section. This technique was useful and produced acceptable results, although webbing occurred randomly on some stents. Irregular coatings could also be an issue as they occur when these films break, leaving uncoated areas on the strut. During experimentation, this occasional phenomenon was documented as seen in Figure 14.

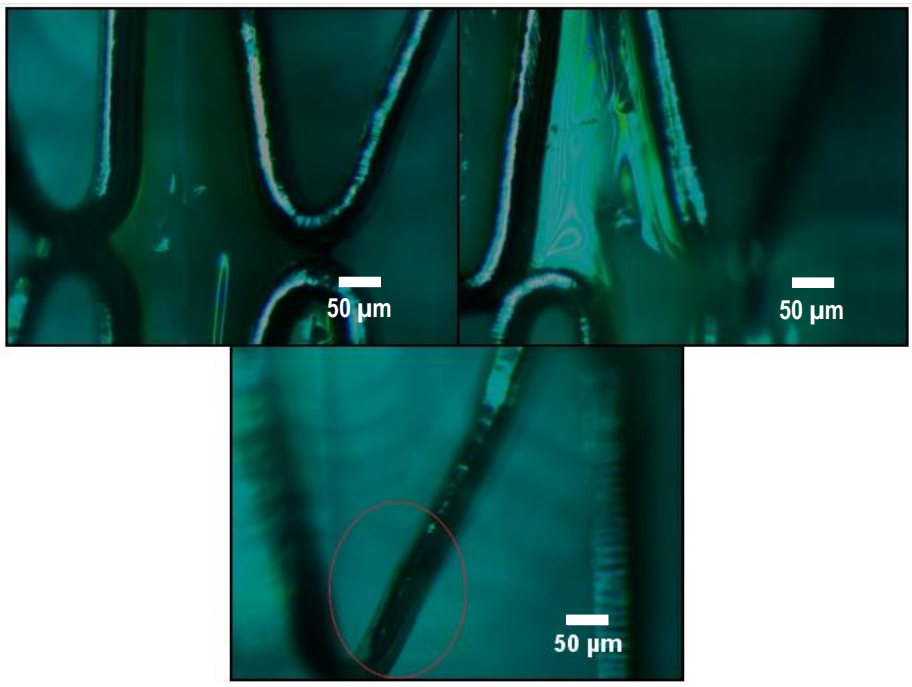

Figure 14: Webbing and delamination phenomena registered from dipped stents. First row of images show webbing obtained in stents coated through a traditional dipping process. In the second row, an image displays delamination derived from physical removal of the PLA bulk caused by webbing. Images were obtained by using a DM2500 microscope from Leica.

A modified dipping protocol was applied to avoid surface defects and achieve better results. This technique was used to coat stents with PLGA and pHPMA as seen in Figure 15, guaranteeing smoother coatings. In these images no webbing or delaminations could be seen, although at some areas irregular morphologies were observed. While this may not be the optimal method used to obtain quality coatings, results proved to be acceptable to produce layered stents.

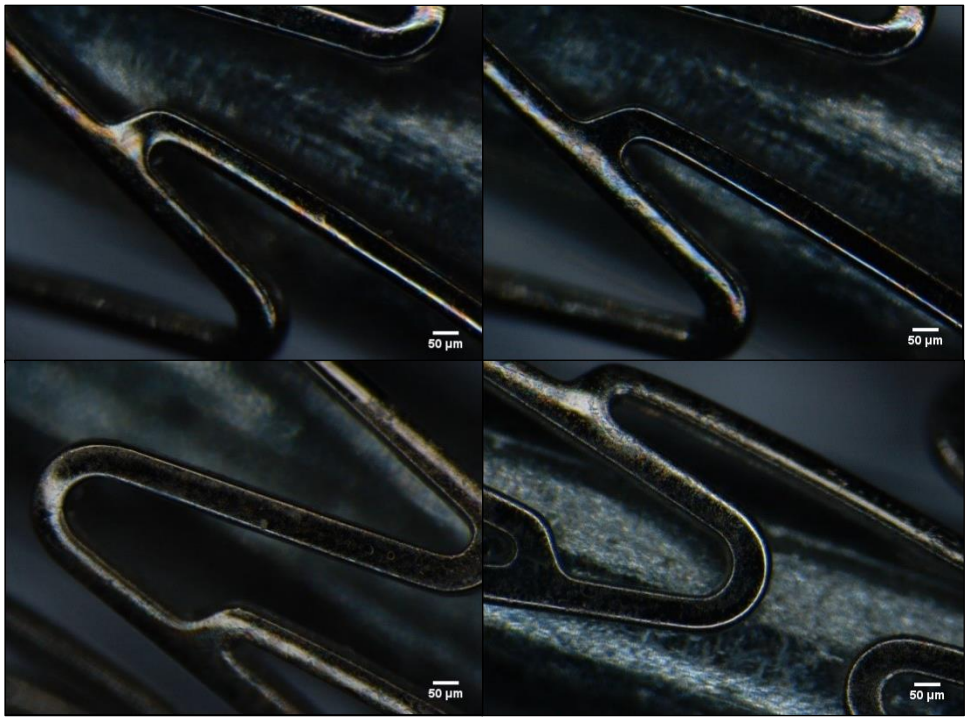

Figure 15: Images from a stent coated with a modified dipping method obtained by using a DM2500 microscope from Leica. First row of images displays pHPMA coated stents while the second row shows PLGA coated stents. No webbing or delaminations were observed in these stents.

As the results obtained with both polymers were satisfactory, some experimentation was done to check if they could be produced in a multilayer structure. Three stents were coated with PLGA by modified dipping technique with different number of iterating dips. A first stent was dipped once and left to dry at room temperature (group 1). Two more stents were coated following the same procedure, but one was dipped three consecutive times (group 2) while the other one was dipped nine times (group 3). This experiment was done with triplicates and all stents were weighted before and after each dip was carried out, in order to evaluate the amount of polymer deposited. Stents from the first group rendered a % of polymer/Strut (w/w) of 0.0823 ± 0.0294, the second group of 0.0905 ± 0.0272 and the third group of 0.0346 ± 0.0203.

These results indicated that the amount attached to the stents did not increase in a linear manner as desired. Although dipping times were short, this experiment was tried out once more with the shortest dipping times possible, but in the end, these rendered the same results. If a single layered coating was going to be tailored for a new stent design this technique could be useful, but it was not suitable for a multilayered proposal. With the purpose of validating our spraying technique to produce multilayered coatings, this same experiment was carried out once more by spraying stents instead of using a dipping method.

Coatings elaborated with a laboratory sprayer

As the ability to stack layers was key to achieve correct multilayered coatings, a similar experiment as the one described with dipping was performed with sprayed stents. Three stents were sprayed a different number of layers and weighted before and after the process was completed to quantify the amount of polymer deposited on each. Not all parameters were optimized in this first experiment, as this only evaluated the capability of stacking layers without considering surface quality.

Results obtained from these tests are shown on Figure 16, comparing them with the dipping results obtained previously. As depicted before, dipping methods show how the quantity deposited after one or three consecutive dips were very similar. After nine consecutive dips, the quantity of polymer on the stent reduced drastically. This reduction was associated to the dissolution of previous coats in the dipping mixture. As the layers were not fixed in any manner which protected the polymer from the solvent, further dips did not contribute to an increase in coating thickness. Three other stents were sprayed two, four and eight times to build different layer thicknesses. These stents were weighted before and after the process was finished. Each condition was tested in triplicate with different stents.

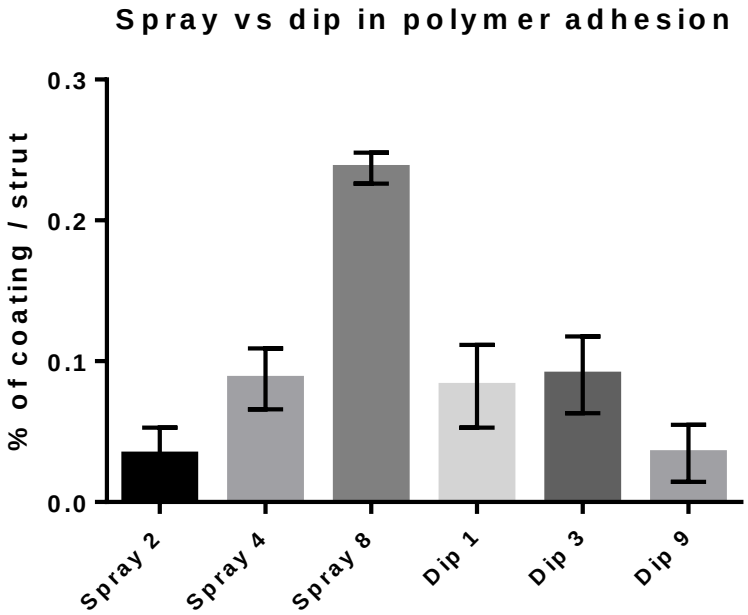

Figure 16: Spray vs dip methodology for multilayers coatings. Triplicates of each type of stent are shown with different number of layers pursued by spraying or dipping. Labels in the x axis show the coating technique applied followed by the number of repetitions/layers. Spraying technique showed accumulative results (first three columns) which validated this procedure as adequate to produce multilayered stents. The last three columns (dipping) displayed non accumulative results due to the dissolution of previous coats in the dipping mixture, thus not presenting satisfactory results for multilayered coatings.

This spraying technique proved to be a reproducible and repeatable method to elaborate different thickness layered coatings. In this case, the modified dipping method did not offer this possibility while working with the selected polymers. Considering these outcomes, a spraying method was chosen to achieve the multilayered coatings pursued. As described in the materials and methods section, to obtain quality coatings through spraying all parameters had to be optimized. These parameters were fixed as different stents were sprayed and checked through a DM2500 microscope from Leica. A first optimization was done using pHPMA with mixes prepared at 0.2% w/v.

To evaluate the quality of the layers, 50 mg of fluorescein were added to the 10 ml of spraying solution to check the uniformity of the layer. Images obtained by this system provided a better visualization of the coating homogeneity. A stent was sprayed with five layers of this mixture and checked on an optical fluorescent microscope (Nikon eclipse TE 2000-U) as seen in Figure 17. This image provides a general idea of the layer's morphology in which no patches or large uncoated areas are seen, thus encouraging a deeper inspection by SEM.

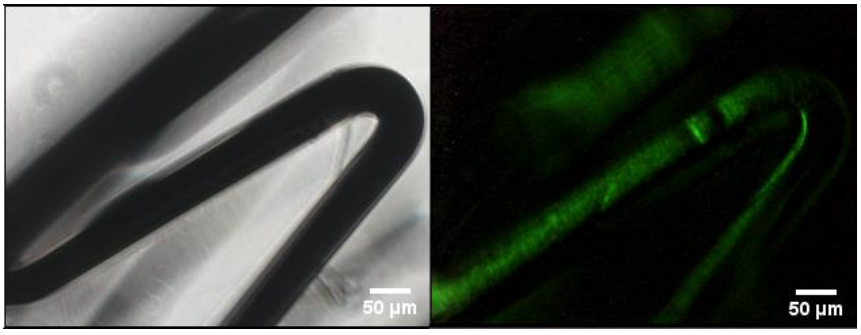

Figure 17: PLGA sprayed stent with fluorescein. At the left, a brightfield image of the stent is displayed. At the right, its corresponding darkfield image was obtained to check for fluorescence corresponding to the presence of a polymer layer. This images show a homogeneous coating with no patches or large uncoated areas. Images were obtained with a Nikon eclipse TE 2000-U microscope.

Stents were sprayed with ten pHPMA layers right after undergoing a plasma activation. SEM images were taken to check surface morphology, as seen in Figure 18, showing a very smooth and homogeneous coating. Spraying conditions fixed at this moment rendered quality layers with pHPMA and were suitable for multi-layered configurations. As this method produced quality pHPMA coatings, the same method was replicated with PLA and PLGA. In Figure 19, experimentation was repeated with PLA, but results showed poor-quality coatings in the form of small drops scattered through the strut. Willing to maintain a low concentration spraying mix to keep the layers as thin as possible, the concentration was raised until acceptable results were obtained.

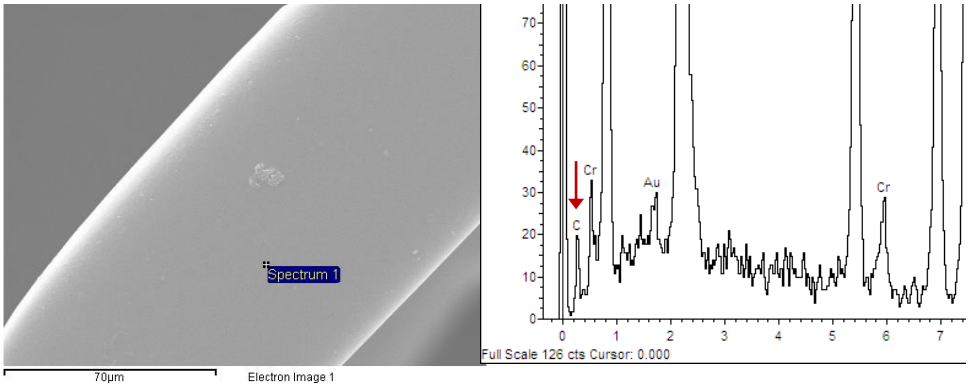

Figure 18: Ten layered pHPMA stent sprayed at 0.2% w/v. In the SEM image shown at the left, a smooth pHPMA coating obtained by a spraying technique can be observed. At the right, an EDX spectrum confirms the presence of pHPMA through a C peak.

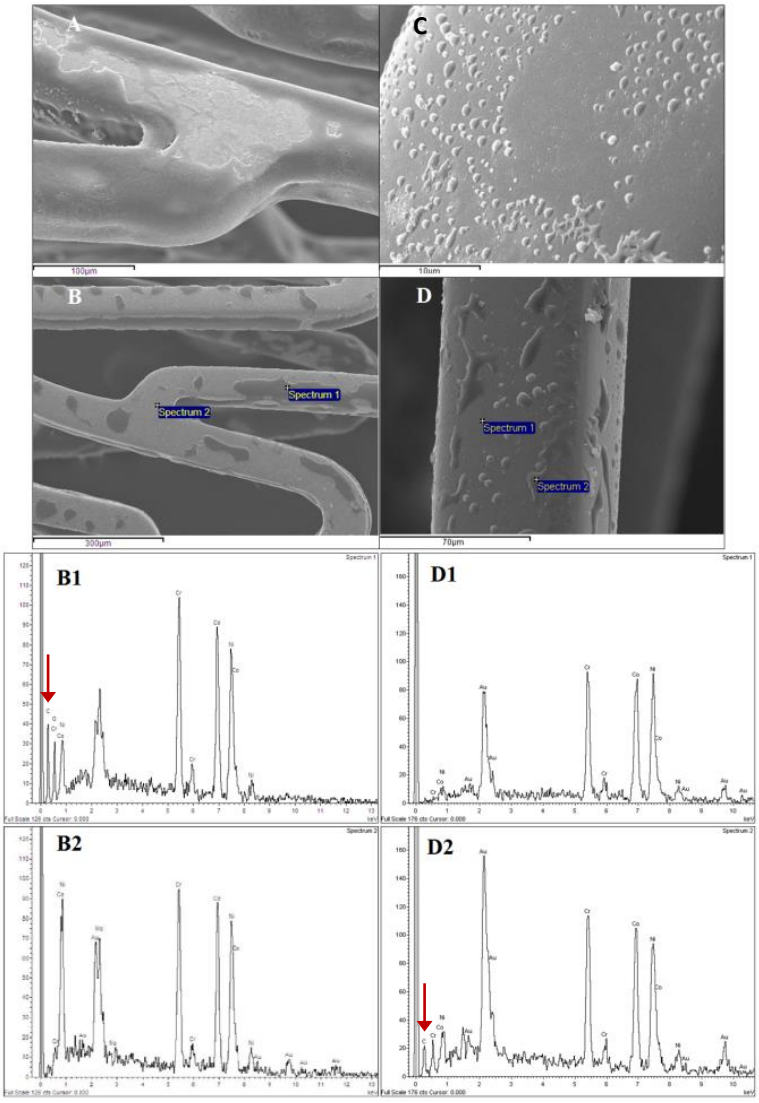

Figure 19: Ten PLA layered stent sprayed at 0.2% w/v. Images labeled A-D show bad quality coatings obtained with PLA, further optimization had to be done. EDX spectra obtained from the areas surrounding the drop-like structures (D1 and B2) showed absence of C peak. On the other hand, B1 and D2 showed a clear C peak due to the polymeric coating. EDX was useful to validate the presence of PLA in the drop-like structures and to prove PLA absence in the rest of the strut.

Mixes prepared with a 1% w/v showed better results with pHPMA, PLA and PLGA. PHPMA layers exhibited smooth morphologies, independently of the mixing concentration variations at these low ratios. Figure 20 depicts struts sprayed with different number of pHPMA layers with a 1% w/v mixture. Quality of these coatings was excellent for multi-layered applications. Determination of polymer presence at the surface of the strut was checked through EDX analysis. A quick verification test was also prepared to visually assure that the smooth coating observed was pHPMA. Activation and pHPMA spraying processes were repeated with stents which had been partially masked with PTFE tape. As seen in Figure 21, a clear interphase is observed through SEM imaging after removing the tape, separating the coated area from the metallic uncoated surface and providing a fast visual confirmation of the polymeric layer.

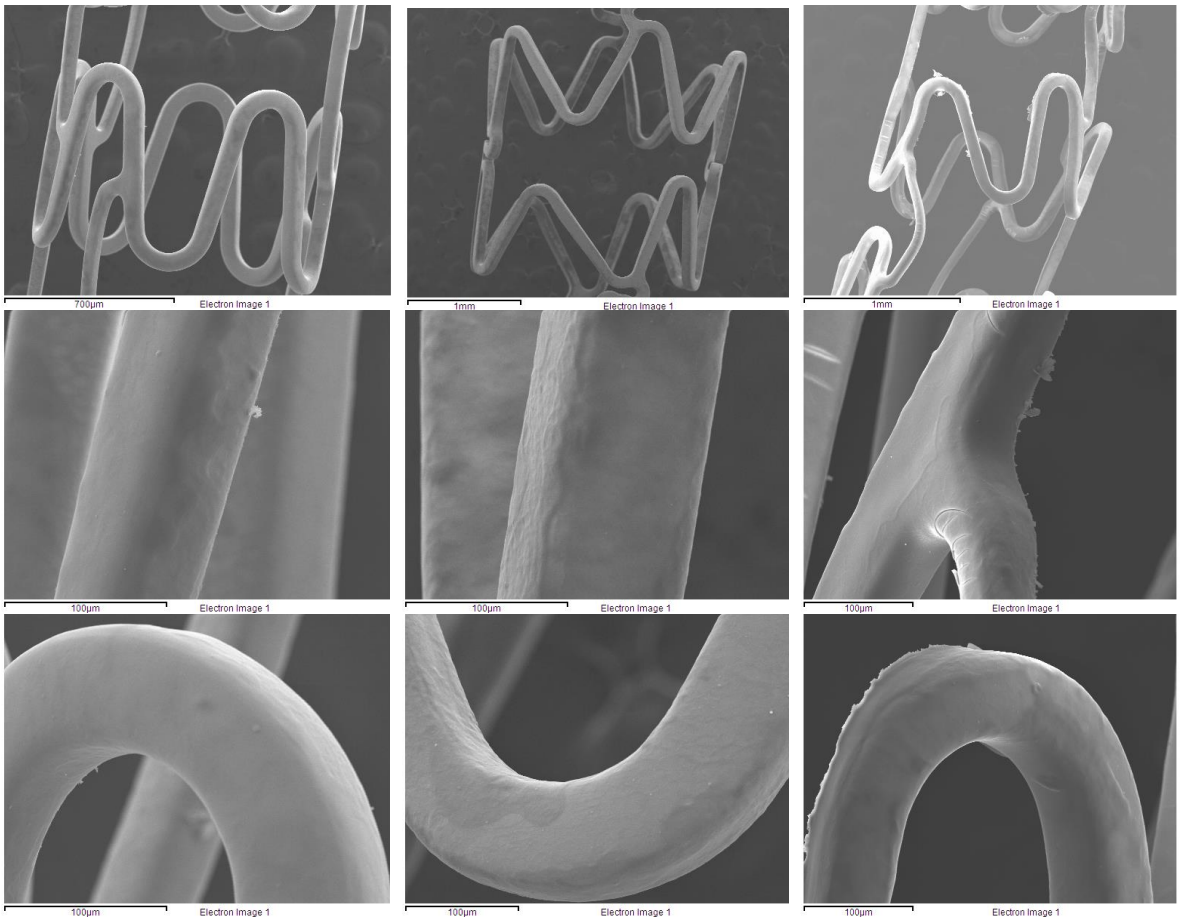

Figure 20: SEM images of optimized pHPMA coatings sprayed on activated stent struts. Images at the left column illustrated five layered coatings obtained after spraying with pHPMA. On the middle column, images presented ten pHPMA layered stents. Images at the right column showed a thick and smooth pHPMA coating composed of twenty layers. Samples had been sprayed with a 1% w/v mixture rendering smooth coatings with five, ten and twenty layers.

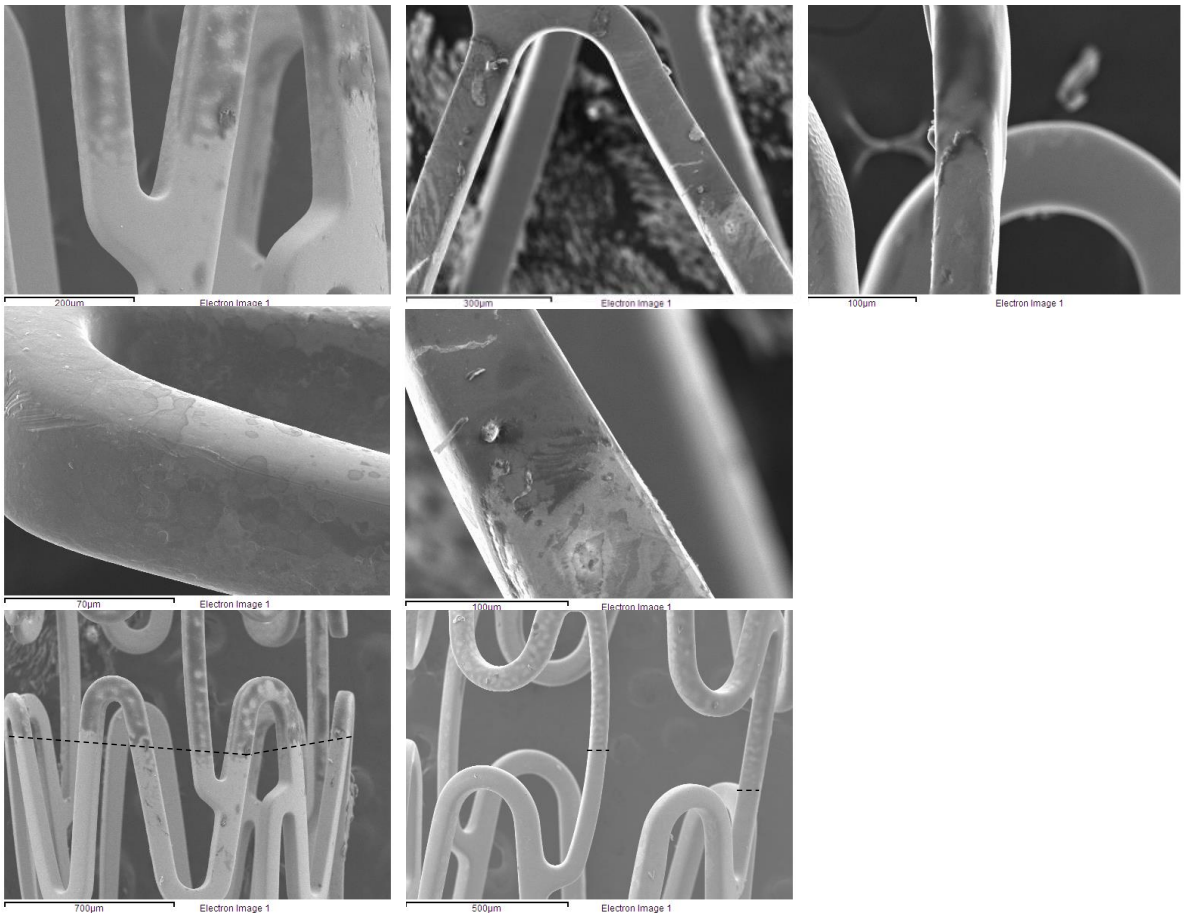

Figure 21: SEM images obtained from pHPMA coated stents with an uncoated interphase. Images at the left column showed a five layered stent interphase. At the middle column, images displayed were obtained from a ten layered stent. The image at the right was acquired from a twenty layered stent. Images showed interfaces separating the polymeric coating from the masked metallic strut. This test was used as a quick presence verification for polymeric coating.

PLA coatings obtained with these same spraying conditions exhibited more homogeneous coatings. Although results obtained with PLA showed stent struts completely coated, these were not perfect. The whole stent struts revealed PLA presence through EDX analysis, but some sections show occasional reduced thicknesses with well-like structures. This micro-phenomenon was observed at random spots and its reduction was associated with an increase in the number of layers. Results are detailed next in Figure 22.

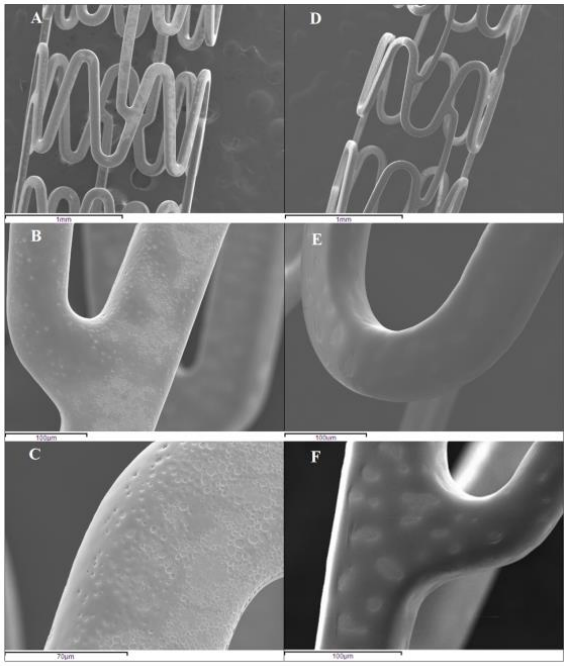

Figure 22: SEM images of optimized PLA coatings sprayed on activated stent struts. Images at the left column (A, B and C) showed five layered PLA coatings sprayed with 1% w/v mixtures. At the right column, images (D, E and F) showed results obtained after applying ten layers of PLA. A reduction of this well-like structures was observed as the number of PLA layers increased.

This process was tried one last time with PLGA to check the morphology obtained, rendering the excellent results shown on Figure 23. At this point, all conditions were optimized to achieve quality coatings on struts by a lab scale spraying technique applied after plasma activation. A next step to focus on was to achieve mixed multi-layered stents with these polymers.

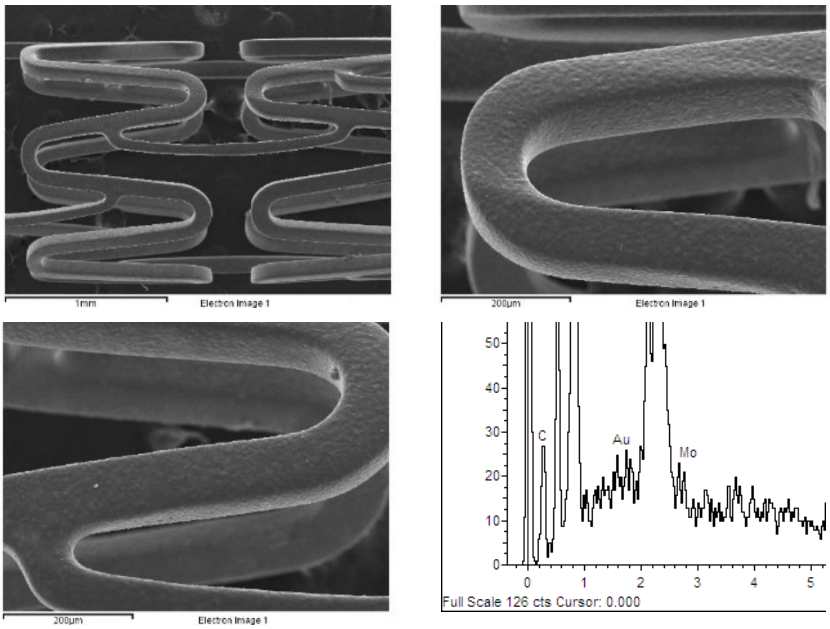

Figure 23: SEM imaging and EDX analysis of ten layered PLGA coated stents sprayed with a 1% w/v mixture. Coating were confirmed by the presence of a C peak at EDX spectrum. Homogeneous smooth results were obtained with PLGA coatings.

Design of first pHPMA/PLGA multi-layered stents

Data obtained up to this point was used to design a first model for a multi-layered stent. This basic prototype was going to be composed of different layers of pHPMA and PLGA/PLA to achieve controlled pharmacological liberation. Activation of the metallic strut was performed through vacuum plasma with an O_2/Ar flow and the coating was sprayed on top with a 1 % w/v concentration. Target drug loads of 50% were achieved using sirolimus, a golden standard in the market. A metallic comb-like structure was used to place up to four stents in the plasma reactor to activate their surface simultaneously. Once the activation process was completed, these struts were removed from the reactor to undergo an immediate spray coating process.

A first stent design was proposed, which had a thick interior core composed of pHPMA in contact with the stent strut. This initial pharmacological reservoir was elaborated by the addition of eighteen pHPMA layers over the stent strut right after the activation process was completed. As mentioned before, this polymer had already been used in our group and tested *in-vivo*, showing an excellent behavior when placed in contact with live tissue. As the drug release obtained from a pHPMA matrix could be excessively fast, a second layer of PLGA/PLA placed on top of the pHPMA coating was thought to help reduce this liberation. PLGA or PLA could reduce this release with only a few layers so, having in mind previous discussed recommendations (minimum of two-three layers to have a solid coating), a minimum of three layers was fixed. To assure this, three stents were sprayed with this combination of polymers. Complete coatings were obtained through eighteen layers of pHPMA (first coating) and three layers of PLGA/PLA (second coating). As a last third coating, a thin pHPMA film was placed on top to enhance adhesion with the artery wall in future designs. This was thought to be sufficient with the same three layers as with the PLGA/PLA coatings.

The testing of this initial design was used to clarify if the multi-layered elaboration idea with different polymers such as pHPMA, PLA and PLGA was functional with the set up developed at this laboratory. Execution of this idea was carried out starting from the plasma activation of three stents. Immediate after, they are sprayed to create the first pHPMA layers. A small fan was placed close to the stents to generate a light air current which enabled a thorough drying of the spraying mix. Completion of this process was assumed after two minutes, and it was repeated after ending each coating. Finished stents were analyzed through SEM imaging to check their morphology. Some examples are shown in Figure 24.

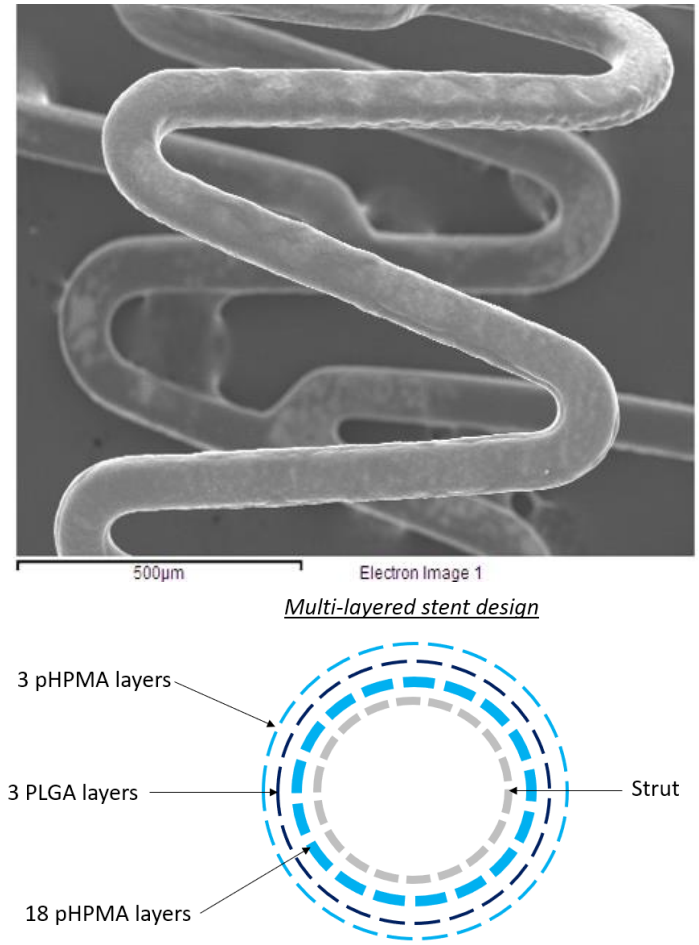

Figure 24: Composition and SEM imaging of first multi-layered stent design. At the top part, SEM images displayed the morphology of a multi-layered stent composed of eighteen layers of pHPMA, three layers of PLGA and three layers of pHPMA. These SEM images showed an expected morphology for the selected layer distribution. A characteristic morphology was displayed, showing a mix of both polymers slightly smoothed by the last layer of pHPMA. The Image located at the bottom showed a sketch clarifying the polymer layer distribution for the stents elaborated in this last section of the chapter.

The stent shown on the previous figure presented a mix of the morphology seen previously with PLGA coatings and pHPMA throughout the surface. Image displayed in Figure 24 showed a difference in coloring attributed to a change in thickness. To assure a more homogeneous result, configurations elaborated with five to eighteen layers are recommended in order to render the same smooth layers obtained previously. Now that stents sprayed with this methodology and instrumentation showed adequate morphologies and tailored distributions, new designs could be pharmacologically loaded and studied as seen throughout the next chapter.

2.4 Concluding Remarks

This chapter presents an in-lab procedure to analyze, characterize and elaborate multi-layered stents. A deeper knowledge obtained by studying the composition of various market golden standards has proven useful to design coherent polymer coatings to use on next chapters with reasonable drug loadings. Viability of silanization and various types of plasma activation techniques have been tested for stent use, being vacuum plasma, the method selected as optimal for our laboratory. Adhesion of the polymers to the metallic surface was validated through ASTM scratch test with excellent results for samples activated through plasma processes. Dipping and spraying methodologies have been used to elaborate stent coatings, creating variations for traditional dipping techniques to obtain better quality results. Both systems, dipping and spraying, proved useful to obtain polymeric coatings on stent struts, although only spraying was adequate for the obtention of more than one layer on a same stent.

A first multi-layer design has been proposed and elaborated using the apparels and methods designed for this purpose as described through the chapter. Stents obtained have shown excellent quality coatings which enable the study of controlled release with different variations on polymer and drug combinations. On the next chapter, new designs will be tested with different pharmacological contents to achieve a novel stent which performs as desired.

2.5 References

[1] Ding, N., & Helmus, M. N. (2002). U.S. Patent No. 6,358,556. Washington, DC: U.S. Patent and Trademark Office.

[2] Kangas, S. (2009). U.S. Patent No. 7,544,381. Washington, DC: U.S. Patent and Trademark Office.

[3] Tartaglia, J. M., Loeffler, J. P., & Turnlund, T. H. (1997). U.S. Patent No. 5,700,286. Washington, DC: U.S. Patent and Trademark Office.

[4] Acharya, G., & Park, K. (2006). Mechanisms of controlled drug release from drug-eluting stents. Advanced drug delivery reviews, 58(3), 387-401.

[5] Thornton, R., & Dolan, F. (2012). U.S. Patent No. 8,227,016. Washington, DC: U.S. Patent and Trademark Office.

[6] Labrecque, R., Moodie, G., Ferraro, J., Rogers, L., Martakos, P., Karwoski, T., & Herweck, S. A. (2012). U.S. Patent No. 8,263,102. Washington, DC: U.S. Patent and Trademark Office.

[7] Villareal, P. K. (2003). U.S. Patent No. 6,605,154. Washington, DC: U.S. Patent and Trademark Office.

[8] Ding, N. (1999). U.S. Patent No. 5,980,972. Washington, DC: U.S. Patent and Trademark Office.

[9] Yasuda, H. (2004). Luminous chemical vapor deposition and interface engineering. CRC Press.

[10] Chu, P. K. (2018, July). Modification of Biomaterials by Plasma and Related Techniques. In 9th International Conference on Technological Advances of Thin Films and Surface Coatings (ThinFilms2018).

[11] Vandenbossche, M., Dorst, J., Amberg, M., Schütz, U., Rupper, P., Heuberger, M., & Hegemann, D. (2018). Functionality and chemical stability of plasma polymer films exhibiting a vertical cross-linking gradient in their subsurface. Polymer degradation and stability, 156, 259-268.

[12] Hegemann, D., Michlíček, M., Blanchard, N. E., Schütz, U., Lohmann, D., Vandenbossche, M., ... & Drábik, M. (2016). Deposition of functional plasma polymers influenced by reactor geometry in capacitively coupled discharges. Plasma Processes and Polymers, 13(2), 279-286.

[13] More, S. E., Dave, J. R., Makar, P. K., Bhoraskar, S. V., Premkumar, S., Tomar, G. B., & Mathe, V. L. (2020). Surface modification of UHMWPE using ECR plasma for osteoblast and osteoclast differentiation. Applied Surface Science, 506, 144665.

[14] Yasuda, H., & Wang, C. R. (1985). Plasma polymerization investigated by the substrate temperature dependence. Journal of Polymer Science: Polymer Chemistry Edition, 23(1), 87-106.

[15] Jangid, N. K., Jadoun, S., & Kaur, N. (2020). A Review on high-throughput Synthesis, Deposition of Thin Films and properties of Polyaniline. European Polymer Journal, 109485.

[16] Kathi, J., & Rhee, K. Y. (2008). Surface modification of multi-walled carbon nanotubes using 3-aminopropyltriethoxysilane. Journal of Materials Science, 43(1), 33-37.

[17] Gener, M., Chico, B., Simancas, J., de la Fuente, D., & Morcillo, M. (2005). Caracterización superficial de nuevos pre-tratamientos a base de silanos aplicados sobre aluminio. Revista de metalurgia, 41(Extra), 428-432.

[18] Tesoro, G., & Wu, Y. (1991). Silane coupling agents: the role of the organofunctional group. Journal of adhesion science and technology, 5(10), 771-784.

[19] Chovelon, J. M., Aarch, L. E., Charbonnier, M., & Romand, M. (1995). Silanization of stainless steel surfaces: influence of application parameters. The Journal of Adhesion, 50(1), 43-58.

[20] Xu, Z., Liu, Q., & Finch, J. A. (1997). Silanation and stability of 3-aminopropyl triethoxy silane on nanosized superparamagnetic particles: I. Direct silanation. Applied Surface Science, 120(3-4), 269-278.

[21] Schmidt, W., Lanzer, P., Behrens, P., Brandt-Wunderlich, C., Öner, A., Ince, H., ... & Grabow, N. (2018). Direct comparison of coronary bare metal vs. drug-eluting stents: same platform, different mechanics?. European journal of medical research, 23(1), 2.

[22] Mikkonen, J., Uurto, I., Isotalo, T., Kotsar, A., Tammela, T. L. J., Talja, M., ... & Kellomäki, M. (2009). Drug-eluting bioabsorbable stents–An in vitro study. Acta biomaterialia, 5(8), 2894-2900.

[23] Bozsak, F., Gonzalez-Rodriguez, D., Sternberger, Z., Belitz, P., Bewley, T., Chomaz, J. M., & Barakat, A. I. (2015). Optimization of drug delivery by drug-eluting stents. PloS one, 10(6), e0130182.

[24] Joner, M., Nakazawa, G., Finn, A. V., Quee, S. C., Coleman, L., Acampado, E., ... & Gold, H. K. (2008). Endothelial cell recovery between comparator polymer-based drug-eluting stents. Journal of the American College of Cardiology, 52(5), 333-342.

[25] Chin-Quee, S. L., Hsu, S. H., Nguyen-Ehrenreich, K. L., Tai, J. T., Abraham, G. M., Pacetti, S. D., ... & Ding, N. N. (2010). Endothelial cell recovery, acute thrombogenicity, and monocyte adhesion and activation on fluorinated copolymer and phosphorylcholine polymer stent coatings. Biomaterials, 31(4), 648-657.

[26] Hossainy, S. F., Roller, M. B., Llanos, G. H., & Kopia, G. A. (2000). U.S. Patent No. 6,153,252. Washington, DC: U.S. Patent and Trademark Office.

[27] Garg, S., & Serruys, P. W. (2010). Coronary stents: current status. Journal of the American College of Cardiology, 56(10 Supplement), S1-S42.

[28] Abizaid, A., & Costa Jr, J. R. (2010). New drug-eluting stents: an overview on biodegradable and polymer-free next-generation stent systems. Circulation: Cardiovascular Interventions, 3(4), 384-393.

[29] Alexy, R. D., & Levi, D. S. (2013). Materials and manufacturing technologies available for production of a pediatric bioabsorbable stent. BioMed research international, 2013.

[30] Nogic, J., McCormick, L. M., Francis, R., Nerlekar, N., Jaworski, C., West, N. E., & Brown, A. J. (2018). Novel bioabsorbable polymer and polymer-free metallic drug-eluting stents. Journal of cardiology, 71(5), 435-443.

[31] Song, L., Li, J., Guan, C., Jing, Q., Lu, S., Yang, L., ... & I-LOVE-IT 2 Investigators. (2018). Randomized comparison of novel biodegradable polymer and durable polymer-coated cobalt-chromium sirolimus-eluting stents: Three-Year Outcomes of the I-LOVE-IT 2 Trial. Catheterization and Cardiovascular Interventions, 91(S1), 608-616.

[32] Xu, W., Yagoshi, K., Koga, Y., Sasaki, M., & Niidome, T. (2018). Optimized polymer coating for magnesium alloy-based bioresorbable scaffolds for long-lasting drug release and corrosion resistance. Colloids and Surfaces B: Biointerfaces, 163, 100-106.

[33] Ramos, V., Borrós, S., Fisher, K.D. (2012). European Patent Application EP 2 438 908 A1. European patent office.

[34] Tuthill, A. H. (1994). Stainless steel: surface cleanliness. Pharmaceutical engineering, 14, 34-34.

[35] Groshart, E. C. (1995). Preparation of basis metals for plating. Metal Finishing, 93(1), 185-195.

[36] Mahla, E. M., & Nielsen, N. A. (1946). Passivation of stainless steel. Transactions of The Electrochemical Society, 89(1), 167-194.

[37] Maller, R. R. (1998). Passivation of stainless steel. Trends in food science & technology, 9(1), 28-32.

[38] Noh, J. S., Laycock, N. J., Gao, W., & Wells, D. B. (2000). Effects of nitric acid passivation on the pitting resistance of 316 stainless steel. Corrosion science, 42(12), 2069-2084.

[39] Shi, J., Ming, J., & Wu, M. (2020). Passivation and corrosion behavior of 2304 duplex stainless steel in alkali-activated slag materials. Cement and Concrete Composites, 108, 103532.

[40] Debold, T. A., & Martin, J. W. (2003). How to Passivate Stainless Steel Parts. Caprenter Technical Articles (Oct. 2003).

[41] Davis, J. R. (Ed.). (1994). Stainless steels. ASM international.

[42] Rego, D., Kilchenmann, K., Park, S. J., Haight, M., Andreacchi, A. S., Chen, Y. M., ... & Glenn, B. D. (2011). U.S. Patent No. 7,897,195. Washington, DC: U.S. Patent and Trademark Office.

[43] Kramer, P. A. (2007). U.S. Patent No. 7,163,715. Washington, DC: U.S. Patent and Trademark Office.

[44] ASTM int, "Standard Test Methods for Measuring Adhesion by Tape Test D3359-09," *Astm*, no. December 2007, pp. 1–7, 2013.

[45] Holt, D. W., Lee, T., Jones, K., & Johnston, A. (2000). Validation of an assay for routine monitoring of sirolimus using HPLC with mass spectrometric detection. Clinical chemistry, 46(8), 1179-1183.

[46] Streit, F., Christians, U., Schiebel, H. M., Napoli, K. L., Ernst, L., Linck, A., ... & Sewing, K. F. (1996). Sensitive and specific quantification of sirolimus (rapamycin) and its metabolites in blood of kidney graft recipients by HPLC/electrospray-mass spectrometry. Clinical chemistry, 42(9), 1417-1425.

[47] Napoli, K. L., & Kahan, B. D. (1996). Routine clinical monitoring of sirolimus (rapamycin) whole-blood concentrations by HPLC with ultraviolet detection. Clinical chemistry, 42(12), 1943-1948.

[48] Taylor, P. J., Salm, P., Lynch, S. V., & Pillans, P. I. (2000). Simultaneous quantification of tacrolimus and sirolimus, in human blood, by high-performance liquid chromatography–tandem mass spectrometry. Therapeutic drug monitoring, 22(5), 608-612.

[49] Di Marco, G. S., de Andrade, M. C. C., Felipe, C. R., Alfieri, F., Gooding, A., Júnior, H. T. S., ... & Casarini, D. E. (2003). Determination of sirolimus blood concentration using high-performance liquid chromatography with ultraviolet detection. Therapeutic drug monitoring, 25(5), 558-564.

[50] Singla, P., Mehta, R., Berek, D., & Upadhyay, S. N. (2012). Microwave assisted synthesis of poly (lactic acid) and its characterization using size exclusion chromatography. Journal of Macromolecular Science, Part A, 49(11), 963-970.

[51] Choi, J., Cho, S. B., Lee, B. S., Joung, Y. K., Park, K., & Han, D. K. (2011). Improvement of interfacial adhesion of biodegradable polymers coated on metal surface by nanocoupling. Langmuir, 27(23), 14232-14239.

Chapter III.

Controlled drug release in DES through tailored coating

Accepted:

Joaqium Bobi, Manel Garabito, Núria Solanes, Pilar Cidad, Víctor Ramos, Alberto Ponce…, "Kv1.3 blockade Inhibits Proliferation of Vascular Smooth Muscle Cells In Vitro and Intimal Hyperplasia In Vivo", Translational Research, June 2020.

This page intentionally left blank

3.1 Introduction

During this third chapter, a variety of DES designs are going to be studied through their drug release. Results obtained guide the research in order to learn how different ways of elaborating multi-layered coatings affect the pharmacological liberation. Through this process a complete control of the release is sought, enabling the elaboration of tailored coatings which can liberate pharmacological treatment at a desired rate and time. At the end of this chapter, a new DES prepared for *in-vivo* testing is produced. To start the chapter, a brief introduction sets the importance of antiproliferative drugs in DES. Through this section, basic concepts such as how is the drug released to the injured area or how is their effect tested, are explained. Following, an experimental section will be focused in the obtention and analysis of release profiles. This process will be accumulative, meaning that each experiment adds knowledge on how to control drug release in specific situations and influences the next designs tested. As mentioned, this will add up to enable a DES design which will bring best results with the polymers and drugs used. Following, a brief introduction focused on the effect of antiproliferative drugs and polymers used for stent coatings will present this chapter and will identify the main issues which will be encountered when developing novel DES designs.

As described in previous chapters, 2nd-generation DES have dramatically improved the safety and efficacy of PCI [1]–[3]. In the Limus family, everolimus eluting stents (EES) have demonstrated their superiority when compared to bare metal stents and 1st-generation DES, in terms of rates of target lesion revascularization and stent thrombosis [4][5]. These stents have been the bench mark for emerging DES for several years and even though many competitors have emerged on the market, new DES are mostly equivalent to EES except for the carrier matrix [6][7]. A clear tendency to reduce the size of the stent strut has also been observed as this reduces the inflammatory response. This progression can be seen through different stent generations in Figure 1.

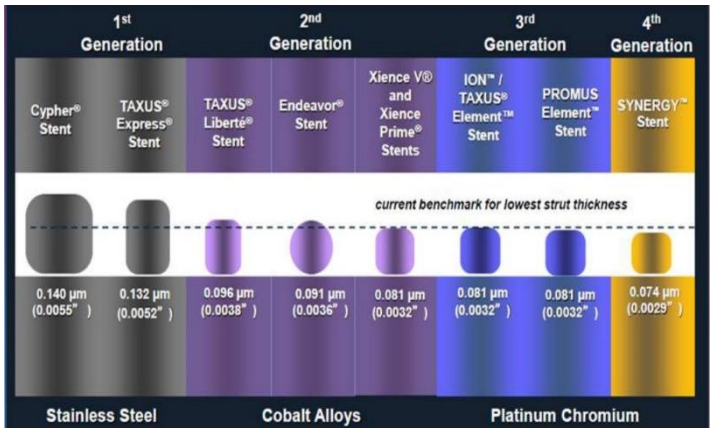

Figure 1: Progression of strut thickness through generations. From left to right, thickness and material changes performed to the stent struts in order to reduce inflammatory response during stent implantation. Adapted from [8].

Although drugs used in DES are mostly from the Limus family, except for paclitaxel, the search for new antiproliferative drugs is not over. This is due to the need of finding a solution for delayed healing of the stented lesion [9]. Antiproliferative drugs inhibit proliferation of endothelial cells, as well as smooth muscle cells, being of vital importance to achieve a controlled release which is reduced at the final stages of DES liberation.

To search for a suitable and innovative drug for DES, this must be capable of inhibiting the well-known cascade of restenosis, including platelet aggregation, inflammation, smooth muscle cell proliferation and migration, as well as extracellular matrix formation [10]. As to promote appropriate healing these drugs should have a selective mode of action, several drugs should be used, treatment should be complemented with anti-platelet therapy or the amount of drug released should be controlled. This last strategy needs a mix of varied polymers or the careful tailoring of different burst layers and barrier layers to be successful. Burst layers, as treated in this work, are designed as quick drug eluting coatings which are used to inhibit SMC proliferation at early stages, and which should not be used at final phases. On the other hand, barrier layers are used to slow down drug release at a given stage or to avoid external layers to lose pharmacological load during stent deploy.

Apart from the Limus drug family and paclitaxel, other drugs could be used to fulfil their task in a more fitting way. An example of this is 5-(4-phenylbutoxy) psoralen (PAP-1), an antiproliferative drug which acts blocking the voltage-dependent Kv1.3 channel. Up to date, a decrease of ion channels expression on proliferative switch is observed, except for Kv1.3 channel and Kv1.2 auxiliary subunit. As the Kv1.3 increases, the dominant channel in the contractile state, Kv1.5, decreases. The importance of Kv1.3 channel is recognized because its functional expression is associated with the proliferative phenotype. This is supported by the fact that channel blocking induces a significant inhibition of cell proliferation. The relevant role of Kv1.3 channels in VSMC proliferation has also been shown in a human model of neointimal hyperplasia, which supports previous statements [11]. Furthermore, association between Kv1.3 expression and cell proliferation has been studied in many cell types such as several cancer lines [12][13], endothelial cells [14], lymphocytes [15] and macrophages [16] among others. Apart from its interesting properties, PAP-1 has been used in our group with positive *in-vivo* results by deploying it in a pHPMA matrix, making this drug a good option for DES [17]. Due to these results, pHPMA is one of the polymers selected to produce tailored coatings. During this chapter, initial release screenings are performed using sirolimus due to the high difference in cost compared with PAP-1.

Bioresorbable stents depend much on the polymers used as they are the ones which will mostly affect the drug release and the inflammatory response caused during a stent implantation. Some of the most commonly used in order to fulfil this duty are Poly-L-lactic acid (PLLA), poly-D,L-lactic acid (PLA), poly-caprolactone (PCL) and polyglycolic acid (PGA), aliphatic polyesters and different blends of these [18][19]. PLLA and poly-D-lactic acid (PDLA) have a high tensile strength which permits robust designs but, at the same time, exhibit long degradation times. On the other hand, PGA and PCL show less tensile strength but much faster degradation times.

As mentioned before, combinations and blends of these different polymers help achieve controlled releases with their diverse degradation rates. This phenomenon is mostly dominated by simple hydrolysis of the ester bond in the polymer backbone, and although it is not the only parameter affecting it, it is considered the predominant one. When partial chain scission occurs, the polymer breaks down to 10-40 μm sized particles which are then phagocytosed and metabolized into carbon dioxide and water in order to be resorbed [20].

Degradation rates are highly influenced by the chemical structure of polymers and their molecular weights. A practical example of this can be seen with PGA, which typically degrades over a time period of 6-12 months while PLLA takes over months to years. Table 1 shows degradation rates of common polymers used to create stent coatings [21]–[35] .

Table 1: Properties of biodegradable polymers used for drug elution. This table shows molar mass, tensile strength, glass transition temperature, tensile or flexural modulus and degradation times of different biodegradable polymers. Information provided in this table can be particularly useful as a quick reference for pharmacological elution times depending on the carrier matrix. Adapted from [51].

Polymer	M_n (g/mol)	Tensile Strength (MPa)	Glass Transition Temperature (°C)	Modulus (GPa)	Degradation Time[b] (Months)
PLLA	~100 K	55 - 80	60 - 65	2.8 - 4.2	>24
PDLLA	~20 K	25 - 40	55 - 60	1.4 - 2.8	12 - 16
PCL	50 - 100 K	20 - 35	−65 to −60	0.4	>24
PGA	~140 K	<70	35 - 40	~7	6 - 12
85/15 PLGA	~80 K	40 - 55	50 - 55	1.4 - 2.8	5 - 6
75/25 PLGA	~100 K	40 - 55	50 - 55	1.4 - 2.8	4 - 5
50/50 PLGA	~100 K	~36	45 - 50	1.4 - 2.8	1 - 2
75/25 PCLA	~100 K	~8	Amorphous	0.3 - 1.4	22
20/80 PCLA	~50 K	~5	Amorphous	0.3 - 1.4	16
PLLA/P4HB	-	~36	~34	1	<12
Poly Carbonate	~450 K	~230	~93	~3.1	>14

[a]Tensile or flexural modulus. [b]Time to complete resorption. PLGA: poly(D,L-lactic acid-co-glycolic acid), PCLA: poly(ε-caprolactone-*co*-D,L-lactic acid), PLLA: poly(L-lactic acid), PGA: poly(glycolic acid), PLLA/P4HB: poly(L-lactic acid)/poly(4-hydroxybutyrate), Poly carbonate: poly(trimethylene carbonate).

Having seen the variety in degradation rates obtained with different polymers, the next key factor to have in mind is the inflammatory response caused by these. Inflammation has not been observed in an aggressive manner as a result provided by the use of the polymers previously mentioned, but it is something that must be studied in new polymers assigned for drug release purposes [36]. In Chapter I, the importance of the inflammatory response due to polymeric coatings has been discussed and therefore its relevance is understood.

As discussed previously, VSMC proliferation is one of the most important indicators of restenosis after stent implantation in animal models as well as in humans. This observation has attracted researcher's interest along the years and has rendered numerous articles about molecular mechanisms which control the cell cycle during *in-vivo* and *in-vitro* experiments. In addition, preclinical studies have also contributed to clarify the effectiveness of antiproliferative strategies in order to limit neointimal development during a lesion when applying gene therapy and drug release treatments.

This chapter is focused on the development of new coating designs based on drug release strategies which are going to be tested in animal models to limit neointimal lesion development. Before undergoing *in-vivo* testing with humans, animal models are a key factor to achieve a better understanding of the mechanical model of neointimal thickening produced after stent implantation or balloon angioplasty, to establish safety margins and to have some initial results related with efficacy and toxicity [37]–[39].

When planning an *in-vivo* on animal models, rats have been extensively studied specially for balloon angioplasty. Nevertheless, prior to a human *in-vivo*, porcine and rabbit models are nowadays considered standard for the evaluation of drug eluting stents [37]–[43] . Although animal *in-vivo* trials are useful and contribute with significant data, there are known differences on results obtained from animal trials when compared to human. These known variations limit their biological significance. Furthermore, drug eluting stent are usually implanted on atherosclerosis-free vessels when tested on animals, showing a cleaner scenario with a quicker recovery than expected. Additionally, neointimal response caused by stent implantation is exaggerated in pigs and rabbits, and the healing time is reduced (4-6 weeks in pigs and rabbits and 6-9 months in humans).

Rabbit models show an additional particularity as they do not offer the possibility of coronary stenting due to their small size, being the aorta or the iliac arteries the most suitable stenting locations for this purpose. Although this might seem a great drawback when using rabbits for this type of practices, its healing process is closer to humans than to pigs and therefore it's also widely used to study inflammatory, proliferative and thrombotic reactions [39].

Some main issues have already been presented such as: Which *in-vivo* should be used to test these new stents? Which polymer combinations should be targeted in this Chapter? How many layers should be targeted for final designs? Which drugs should be tested for initial designs? All these are main issues tackled in this chapter. As the previous work has constructed the bases which enable the production of different multilayered stents, Chapter III will be centered on achieving tailored drug release and producing novel stent designs. As described in Chapter I, the goal of this chapter is to achieve complete control of drug release in order to produce a target type of stent which will be designed to perform with a designed release profile. This stent will be tested in an *in-vivo* trial to check its efficacy.

3.2 Materials and methods

In-vitro drug release

HPLC system, extraction methodology and chromatogram configuration were used as described in chapter II for sirolimus analysis. On the other hand, PAP-1 was also used to pharmacologically load stents in this chapter. This drug was treated the same way as sirolimus when extracting and preparing it for the analytical process. Several methods were initially tried out to analyze PAP-1 content through HPLC [44]–[47], but in the end, the one which rendered best results was the same modified method used for sirolimus. Calibration curves were done in the working range to check linearity for PAP-1, enabling drug quantification.

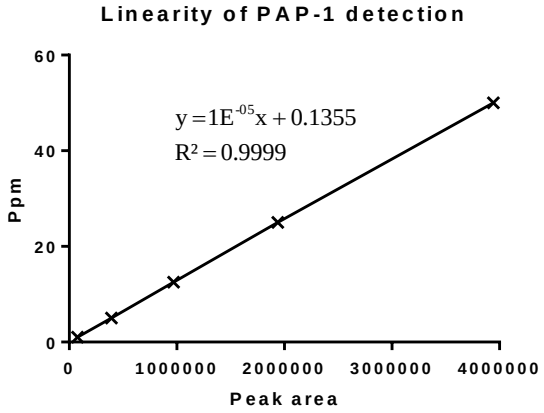

Figure 2: Calibration curve of PAP-1 elaborated with samples ranging from 0.2 to 50 ppm. A trend line with its associated equation and quadratic error is shown on the graph. These graphs were elaborated before a release analysis was performed in order to have a quantification method available.

As done in the previous chapter with sirolimus, PAP-1 spraying mixes had to be optimized by preparing different solutions and checking the coating quality obtained through SEM imaging. This drug was sprayed in acetone when mixing it with PLA or PLGA, but the solution varied when using pHPMA. This last polymer is soluble in ethanol, but PAP-1 shows a very low solubility in this solvent. To create the spraying mix, a proportion of 33% of ethanol with 66% of acetone showed best results.

Spraying in an industrial environment

Throughout this chapter, practically all stents were sprayed with the same machine elaborated during chapter II. Only the last type of stent, shown at the last part of this chapter, is prepared on an industrial spraying machine provided by Iberhospitex SA. This change was proposed to try the scalability of the process and to obtain the best quality results possible. An image showing this industrial sprayer can be seen next in Figure 3. Basic parameters had to be optimized in order to obtain repeatable results. Pump flow for example, was slowly increased until a steady and constant solvent spraying cone was obtained. In the case of PLGA mixes, the flow was finally set to 0.035 ml/min while pHPMA mixes were set to 0.08 ml/min.

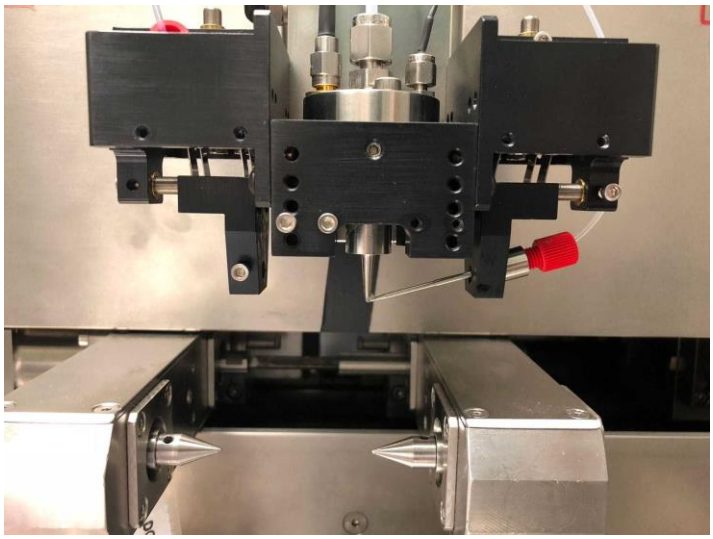

Figure 3: Stent sprayer provided by Iberhospitex SA. At the center of the image a sonicating tip and a spraying mix output are shown. At the bottom part, two metallic cones were used to hold and rotate the stent strut throughout the spraying process. While the cones spin and rotate the stent strut, the sprayer moves horizontally over the stent from left to right and later, from right to left completing a whole cycle.

Another modification had to be done to the solvent composition of the mixes to achieve a constant flow in the industrial sprayer due to the volatility of the solvents. PLGA was dissolved in dioxane instead of acetone, while pHPMA required a mix of 20% ethanol and 80% dioxane instead of only using ethanol. Air pressure was set to 0.95-1 bar for all spraying mixes used with this machine and finally, calibration curves were done with polymers which were going to be used to check linearity in the working range. This was useful to ascertain how many times the nozzle had to pass over the stent to achieve a desired quantity of polymer on the strut.

On the case of PLGA mixes, a correct nozzle speed was found to be 230 mm/s, while pHPMA was set to 300 mm/s. This speed was fixed after checking the mass increase deposited on the strut after each iteration. If the mass added was constant and similar to the one obtained with the lab sprayer, the speed was acceptable. Results were checked through SEM imaging to validate the coating quality. Calibration curves obtained with both polymers at the working range are seen in Figure 4. After adjusting all parameters, these graphs verified that the number of layers sprayed on the struts increased lineally with the number of times the sprayer's nozzle passed over the strut. When the mixes are prepared with a 50/50 polymer/drug weight ratio, the weight of the coatings include polymer and drug. When preparing stents for *in-vivo* testing, the struts are charged with 153.1 +- 0.8 µg of PAP-1.

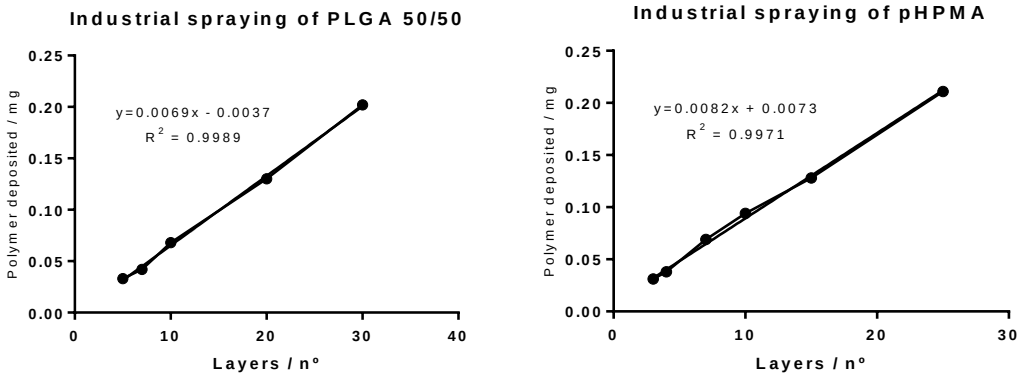

Figure 4: Calibration of industrial sprayer with PLGA 50/50 (left) and pHPMA (right). Both show linear results which are suitable to validate a given set of parameters as capable of producing repeatable results. Stent struts were sprayed a given number of layers and then weighted. The same strut underwent the process again to accumulate a different number of layers and its weight was checked again. This process was repeated until verification lines were complete.

In vitro evaluation through scratch test in pharmacological liberation medium

Stents designed in this chapter which presented an interesting pharmacological liberation were studied in an *in-vitro* scratch test. To achieve this, a modified version of the scratch wound essay [48]–[50] was done in order to have information on the toxicity of stent liberations or effectiveness of the pharmacological load present in the medium. Throughout this experimentation, a cos-7 cell line was used to obtain a quick and easy procedure which would be useful as a check test to control the effect of drug concentration released into the medium. To prepare this experiment, cells were seeded in 12 well plates (0.3×10^6 cells per well) and incubated in supplemented Dulbecco's modified Eagle's medium until a cell monolayer was achieved. Next, a wound was scratched at the center of the well using a 200 µl pipette tip in a flowing movement to give a clean straight edge. Each well was washed with PBS to remove scratched cells. Control wells were then treated with normal growth medium while the rest were treated with medium which contained PAP-1, as these other wells corresponded to different elution time points obtained from pharmacologically loaded stents.

Bright field images were acquired from each well after producing a scratch at the initial time point and next, images were obtained at the same spots 28 hours later. Wound closure was evaluated by calculating the area repopulated by cells using a cell tracking software (ImageJ, free to download from https://imagej.nih.gov/ij/download.html). Later, images from time points t=0 and t=28h were paired and used to evaluate the percentage area closed of each wound.

Porcine Model of Coronary in-Stent-Restenosis for in-vivo trial.

Thirteen Large-White x Landrace pigs (30.2±1.7 kg) underwent a percutaneous coronary intervention to stent each one of the main coronary arteries. Twenty-four hours before coronary catheterization, animals received loading dose of aspirin (200 mg) and clopidogrel (300 mg) (PO). Fasting animals were anesthetized and ventilated. Under aseptic conditions, a 6 Fr introducer was percutaneously placed into the femoral artery for coronary access. During the procedure, an appropriate anticoagulant treatment was maintained with an initial bolus of 9000 UI of heparin followed by boluses of 1500 UI of heparin every 30 min, if needed, in order to maintain an adequate anticoagulation range.

Using standard over-the-wire techniques, the three main coronary arteries were engaged with a 5-Fr guiding catheter. Radiopaque contrast (Iomeprol 350 mg/ml, Iomeron 350, Bracco, Wycombe, UK) was administered to obtain coronary angiographies, which were used to screen for appropriate vessel segments for stent implantation on the basis of anatomy and the diameter (between 2.3 and 3.0 mm) measured in situ on a fluoroscope console (Arcadis Avantic, Siemens AG, Germany). Polymer-coated, with or without PAP-1, stents of 3 mm in diameter and 23 mm of length were then implanted in the selected coronary segments. For stent deployment, angiographic contrast was used to inflate balloon at 7 to 15 atmospheres (2.97-3.37 mm) for 10 seconds to achieve a stent-to-artery ratio (SAR) of 1.1-1.3.

Only stents with the same treatment (with or without PAP-1) were implanted in each animal (control group, n=6; PAP-1 group, n=7) and only coronary arteries with a diameter suitable for the aimed SAR were stented. Two left anterior descending coronary arteries from PAP-1 animals resulted too small for the desired SAR. Thus, one more animal was included in the PAP-1 group, in which the left anterior descending and circumflex coronary arteries were stented. After angiographic confirmation of correct stent deployment, animals were awakened and weaned from mechanical ventilation. Dual anti-platelet therapy was continued with 200 mg aspirin and 75 mg clopidogrel daily during the 28 days follow-up.

3.3 Results and Discussion

3.3.1 Analyzing elution of different polymers in quick release medium

Following the design and fabrication procedures described in the previous chapter, some polymers were selected with the intention of elaborating coatings for DES and acquiring more information about their release profiles. To achieve this, three interesting DES designs were elaborated and left in an accelerated medium to be subsequently analyzed by HPLC. These stent coatings were composed of five layers of PLA, PLGA, or pHPMA with a 2% drug load of sirolimus each. A small drug load was added with the intention of limiting its possible effect on the general release as well as to reduce the amount of drug used during the first experiments. Another factor which also modified initial liberations was the use of accelerated medium. During the liberation process on an accelerated medium the small percentage of isopropanol mixed in the saline medium increased the drug release over time, but most important, it also reduced the degradation of sirolimus present on the medium. As releases were obtained faster, liberation curves had to be compared to others obtained using the same medium, but most important, this led to a reduced degradation which enabled the obtention of the most accurate HPLC results possible.

When the release profiles were obtained, they were plotted as seen in Figure 5. This graph showed a slow liberation curve which reached an 80% elution after one hundred and seventy hours from a five PLA layered stent in accelerated medium. In the other hand, over this curve, a liberation from a blend composed of 50% glycolic acid showed a coherent quicker release which pushed the elution curve upwards in the graph. Finally, over the PLGA curve, a pHPMA matrix liberation showed an extremely fast elution when compared with the other two polymers, achieving an 80% release during the first hour. All three different stents were elaborated by triplicate with the purpose of having information about the repeatability of the fabrication methods developed for this purpose.

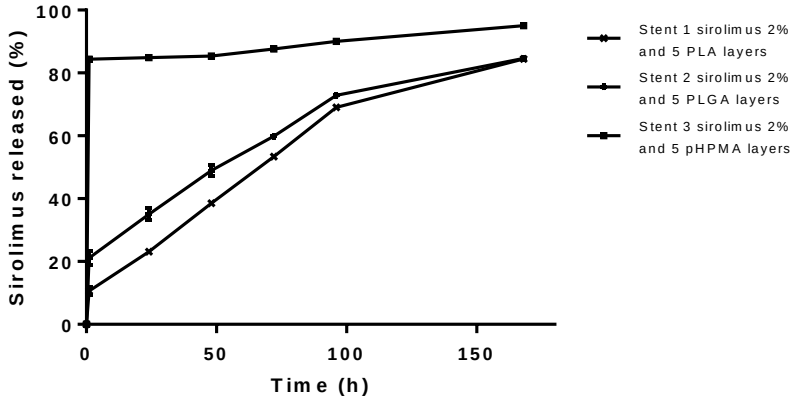

Figure 5: Sirolimus release from DES composed of five layers of different polymeric matrices charged with a 2% drug load in an accelerated medium. Total release was plotted as % released from the strut vs time (h). A slow elution was obtained with a PLA matrix, an intermediate release was achieved with a PLGA matrix and a fast release was observed from a pHPMA matrix.

After obtaining this data, the release achieved by the coatings made of PLGA, PLA and pHPMA were repeatable and showed promising results in order to start designing multilayered stents with different elution profiles. The quick elution obtained from a pHPMA matrix led to the idea of using this polymer to create a burst effect in a multilayered stent at a desired time point. This could be used to have a better control of the drug elution in a DES, but before creating specifically tailored layers successfully, a better understanding of the effect of drug and polymer concentrations had to be achieved.

3.3.2 Study of the effect of drug and polymer concentrations on pharmacological elution through release analysis in quick release medium

Driven by the need to acquire more information on the influence of the hydrophobic drug concentration and the thickness of the polymer layer, three different multilayered stent designs were prepared. These three types of stents were composed of ten, twenty and thirty layers of pHPMA charged with a 20% of sirolimus. This increase in drug load, compared with the previous stents discussed in Figure 5, was due to the idea of using higher drug loads which would resemble more the actual market standards. These stents were left in accelerated medium for one week and the results obtained were graphed as seen in Figure 6.

During this first timepoint, a reduction of drug release was appreciated when the amount of polymer was increased. As the concentration of sirolimus was constant throughout all the layers, results showed that outer layers eluted quicker than interior ones (which were attached directly to the stent strut). As the pHPMA layers eluted very fast, thicker coatings also showed that the bigger outer layers which dissolve in the medium also drag bigger quantities of the inner layers. Smaller coatings had thinner layers which eluted in a less turbulent way. After obtaining this information about pHPMA layers, burst coatings could start to be designed for DES in a coherent way and could be used to boost an initial release after implantation.

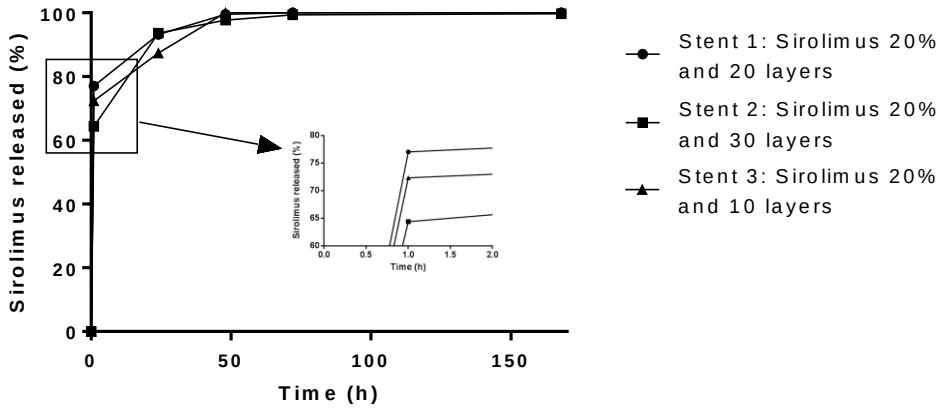

Figure 6: Sirolimus release of thirty, twenty and ten pHPMA layered stents with 20% drug load in an accelerated medium. Total release was plotted as % released from the strut vs time (h). This graph shows three different behaviors during the first 100 hours and provides a zoomed highlight of the first hour to check the initial tendencies. Quick releases were observed from pHPMA matrices which had a more controlled liberation with a higher drug load (20% instead of the previous 2%). Dragging effects are observed at thirty-hour time points which suggested keeping the layer amount of pHPMA not much higher than twenty. An increase in the layer thickness also showed a reduction in the initial liberation.

This dragging effect previously seen with thick layers of pHPMA can be a problem if the objective is to design thick layers of this polymer to use as a carrier matrix. To solve this issue, a new design was conceived which consisted in the addition of a small pHPMA coating on top of a stable and slower eluting polymer while also keeping pHPMA layers under twenty. To accomplish this, two different types of DES were developed. One had an interior coating of eighteen layers of pHPMA, three layers of PLGA on top and three exterior layers of pHPMA. All these layers contained a 20% drug charge which would be eluted on the medium. The other type of stent was elaborated the same way but with a thinner coating of eight layers of pHPMA in its interior. Both stents were provided with three final outer layers of pHPMA, as this polymer had proven in previous studies a good adhesion to the artery wall and could also provide a good grip in future designs during implantation.

As the previous release points obtained in accelerated medium indicated that most of the pHPMA was eluted during the first hour, the next experiment provided five elution points during the first sixty minutes. Results obtained were plotted as seen on Figure 7, which showed a combined and modulated release of PLGA and pHPMA layers avoiding the violent dragging phenomenon. In addition, the layer thickness phenomenon described previously and seen in Figure 6, is also seen in Figure 7.

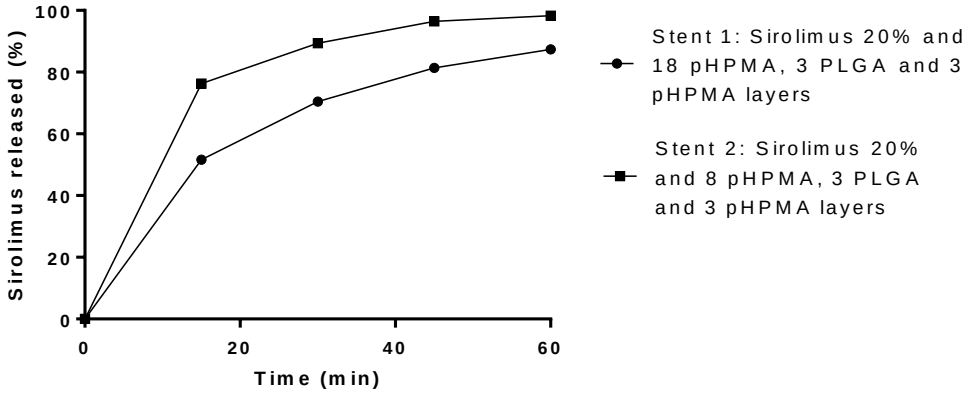

Figure 7: Sirolimus release in accelerated medium of different pHPMA and PLGA layered stents with 20% drug load for one hour. Total release was plotted as % released from the strut vs time (min). This graph shows two detailed release curves during an initial liberation period of one hour. PLGA intermediate coatings were applied to modulate liberation, resulting in a general reduction which evidences concentration phenomena. No dragging effects were observed.

Now that the influence of the polymer layer thickness had been studied, the impact of the drug load in the polymer matrix had to be tested. Aiming to obtain more information on this matter two more types of stents were elaborated, and their elution subsequently analyzed. Following the multilayered composition of eighteen layers of pHPMA with three of PLGA and three of pHPMA, one stent was elaborated with a 20% drug load and the other one with a 50%. This second ratio (50%) was chosen as it was one of the most common seen in DES nowadays in the market. Results were plotted as seen in Figure 8, concluding that a higher hydrophobic drug load showed a reduction in the pharmacological elution over time. Having studied both factors, drug load and polymeric thickness with pHPMA and PLGA, and understanding how they affected their pharmacological liberation, new DES could be designed with controlled and tailored release profiles.

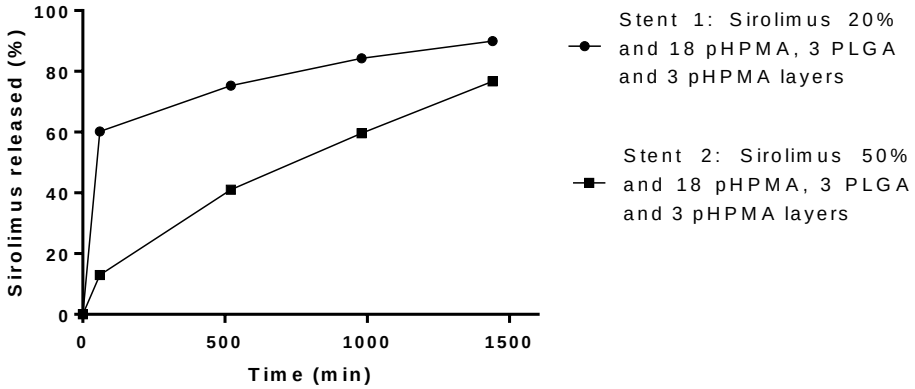

Figure 8: Sirolimus release of 20% and 50% charged pHPMA and PLGA stents in accelerated medium. Total release was plotted as % released from the strut vs time (min). A first stent design was produced by spraying eighteen layers of pHPMA, followed by three layers of PLGA and finished with another three layers of pHPMA. All these layers were sprayed with a 20% sirolimus load. A second stent design was produced the same way as the first stent but with a 50% sirolimus load. As concluded from this graph, higher hydrophobic drug load resulted in a reduction in the pharmacological elution over time.

After analyzing data obtain from these experiments, the importance of polymer thickness and drug load had been noticed. Next, five new designed stents were prepared. These were made like "stent 2" from Figure 8 but with two major changes. First, these stents were produced with a varying number of initial layers of pHPMA instead of the original eighteen. Second, only the first pHPMA coating contained a pharmacological load while the two other coatings had no drug load. PLGA was used to retain and elute in a gentle way the pHPMA loaded base lying underneath, as seen before, and the pHPMA as an exterior coating barrier with good adhesion. In order to quantify the amount of polymer and drug deposited on different stents, drug loads were expressed in mg of sirolimus/mm^2 of strut. All stents were loaded with a 50/50 drug/polymer ratio).

Results obtained after analyzing each release were plotted as shown in Figure 9. A release reduction was observed while the amount of coating sprayed on the strut was increased using PLGA and pHPMA barriers. Data plotted in graph A showed how stent labelled as "1" had slightly more drug load than stent "3", while stent "2" had almost as twice as the other two. This graph represents the addition of the release obtained at the different time points plus the final quantity extracted from the stent at the end of the experiment. Following, graph B shows how, after one hour, the quickest eluting stent was number "3" due to the lack of barrier layers. Stent "1" eluted slower than stent "3" as it contained exterior layers acting as barriers, followed by stent "2" being the slowest elution. This second stent eluted proportionally lower than stent "1" due to its higher drug concentration. Twenty-four hours after the first time point (graph C), the differences were not so drastic as in the previous graph (B). Stent "3" still showed the fasted elution, followed by numbers "1" and "2" with a smaller difference than before (graph B). This was related to the degradation of the barriers over time which allowed the drug to escape to the medium reducing their effect gradually.

Through this figure a clear relation was established between lower drug elutions due to higher sirolimus loads and polymeric barriers with no drug load. These results broaden the knowledge obtained to tailor desired drug releases in stents using pHPMA and PLGA.

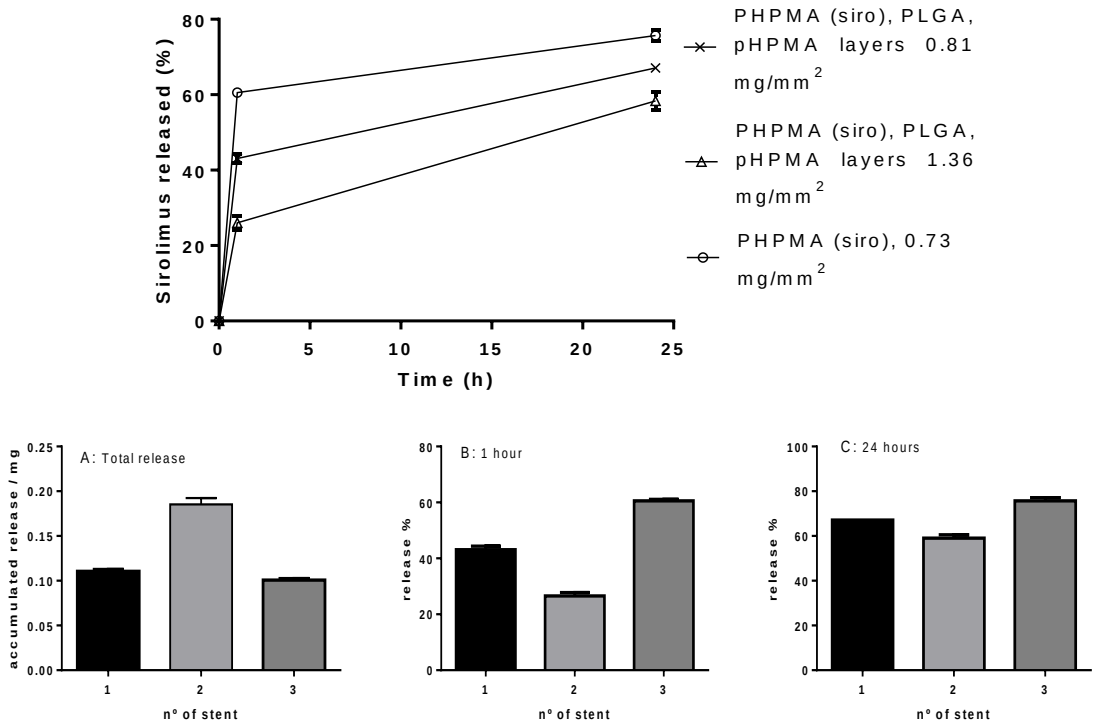

Figure 9: Sirolimus release of different pHPMA and PLGA layered stents with a 50% drug charge. Total release was plotted as % released from the strut vs time (h). Graph A: Total liberation obtained from each type of stent, including drug released in the medium plus pharmacological load remaining on the strut. Graph B: Release obtained after one hour from each type of stent. Graph C: Release after twenty-four hours from each type of stent. On graphs A-C the columns from left to right represent the following stent composition. Starting with the strut's interior layer to its most exterior layer: PHPMA (sirolimus, 0.81 mg/mm2), three layers of PLGA and three layers of pHPMA (stent 1). PHPMA (sirolimus, 1.36mg /mm2), three layers of PLGA and three layers of pHPMA (stent 2). PHPMA (sirolimus, 0.73 mg /mm2) (stent 3). Slower elutions were observed on stent designs which contained polymer barriers (stents 1 and 2), being the stent with more drug concentration (stent 2) the one to exhibit a slower release.

These results showed how barriers and drug concentration could affect drug elution, but in order to have more detailed information on how to effectively apply these concepts to PLGA and pHPMA multilayers further research had to be done. How would pHPMA barriers differ from PLGA barriers and how would a different drug affect pharmacological release? Seeking an answer to this question, a varied range of stents was prepared and analyzed as shown next.

3.3.3 Elution study of tailored DES with barriers, bursts and different drug/polymer combinations in quick release medium.

On Figure 2, stent composition for following experimentations is detailed. Half of the stents were created with an interior layer of pHPMA loaded with sirolimus or PAP-1, while the other half were composed of PLGA loaded with sirolimus. These stents were either designed with thick or light barriers composed of PLGA or pHPMA, or with no barriers at all.

Figure 10 shows the total release obtained from all these stents plotted on a same graph to present an overall image of their behavior.

Table 2: Composition of different stents for the study of barrier, burst and drug concentration effects. Starting from left to right, the first column shows an identification label for each type of stent starting with "S" and followed by a number. In the case a label contains a "/", this indicates the alternative label given to that stent if the drug is changed from sirolimus to PAP-1. The second column shows the composition of the interior coating located next to the metallic strut. Some stent designs show the possibility of having sirolimus or PAP-1 in their composition, to clarify this, their label will change in the previous column depending on the drug they carry (' or '' indicates a PAP-1 load). The third column shows the composition of the exterior layers coated on top of the interior layers shown at the previous column. In the composition description of this third column some layers may be described with more than one polymer, from left to right (S3'') being the one in the left the most interior layer and the one at the right the most exterior layer. The last column shows the drug load of each stent in µg/mm². This table was designed as a quick composition reference for the next experiments.

Stent	Composition and nº of Interior layers	Composition and nº of exterior layers	µg/mm²
S1/S1'	10 pHPMA (Sirolimus/PAP-1)	10 pHPMA	0.53±0.097
S2	10 pHPMA (Sirolimus)	-	
S3/S3'	10 pHPMA (Sirolimus /PAP-1)	10 PLGA	
S3''	10 pHPMA (PAP-1)	3 PLGA + 3 pHPMA	0.52±0.092
S4	10 pHPMA (Sirolimus)	10 PLGA (Sirolimus)	0.68
S5	10 PLGA (Sirolimus)	-	0.45±0.103
S6	10 PLGA (Sirolimus)	10 PLGA	
S7	10 PLGA (Sirolimus)	10 pHPMA	
S8	10 PLGA (Sirolimus)	10 pHPMA (Sirolimus)	0.92

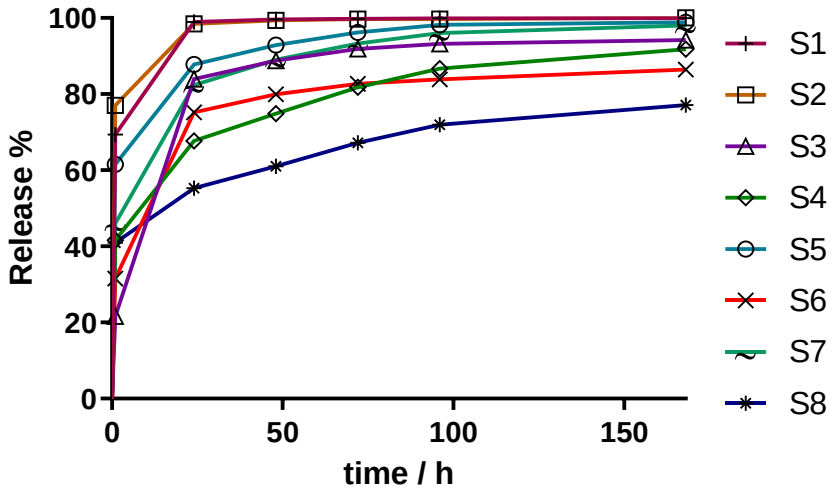

Figure 10: Sirolimus release from a wide variety of stents composed of pHPMA and PLGA coatings for the study of burst and barrier effects with sirolimus and PAP-1. Total release was plotted as % released from the strut vs time (h). Composition of all stents is described in Table 1. Results obtained through thorough analysis of this data led to the verification of barrier and burst effects with different combinations of PLGA and pHPMA coatings.

Figure *10* is broken down into 10 separate graphs which make the discussion of the phenomena observed easier and enables a fluid discussion of the results. With the intention of comparing the effects of PLGA and pHPMA barriers, two different graphs were elaborated (Figure 11) using data from Figure 10. Both graphs are followed by a small sketch located under them, which clarifies the layer composition of each stent.

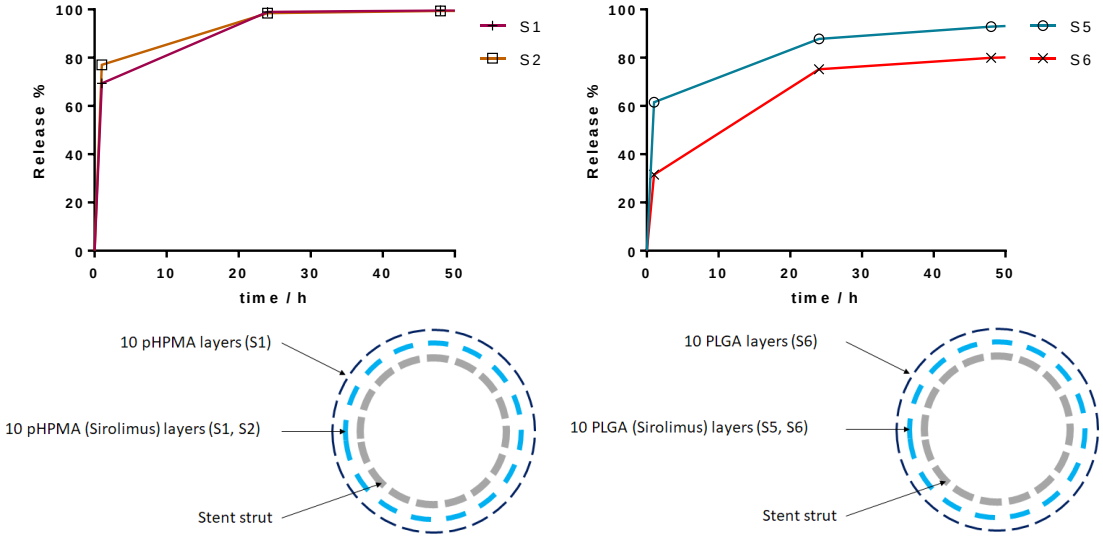

Figure 11: Comparative release study with PLGA and pHPMA barriers in stents of polymeric homogenous composition. The top left graph shows elution from stents composed of pHPMA layers loaded with sirolimus (S1 and S2) with pHPMA barriers (S1) followed by a layer diagram located under it. The top right graph shows elution from stents composed of PLGA layers loaded with sirolimus (S5 and S6) with PLGA barriers (S6) also followed by a layer diagram. Results showed how PLGA improved barrier effectiveness over PLGA matrices when compared with pHPMA barriers over pHPMA matrices.

On the left graph on Figure 11 two releases are compared. S1 showed a lower initial liberation than S2, as the first one contained a pHPMA exterior barrier which hold back the sirolimus elution. As the pHPMA barriers degraded, sirolimus started to leak into the media crossing through small pores and diffusing through its polymeric matrix. On the right graph, a similar experiment was performed. These stents were similar to S1 and S2, but in this case, coatings were elaborated with PLGA instead of pHPMA. S6 showed a high sirolimus retention, as it had an exterior barrier of PLGA which S5 did not have. PLGA degraded slower than pHPMA, this behavior was clearly seen on the elution profile. When comparing both graphs, PLGA barriers acted in a more aggressive manner than pHPMA barriers, which were subtler. This phenomenon was interesting as it can be used to elaborate small reductions on the release profiles, as well as it may be used to create a thin exterior layer which can be used to enhance adhesion between the polymeric matrix and the artery wall without practically affecting the overall release.

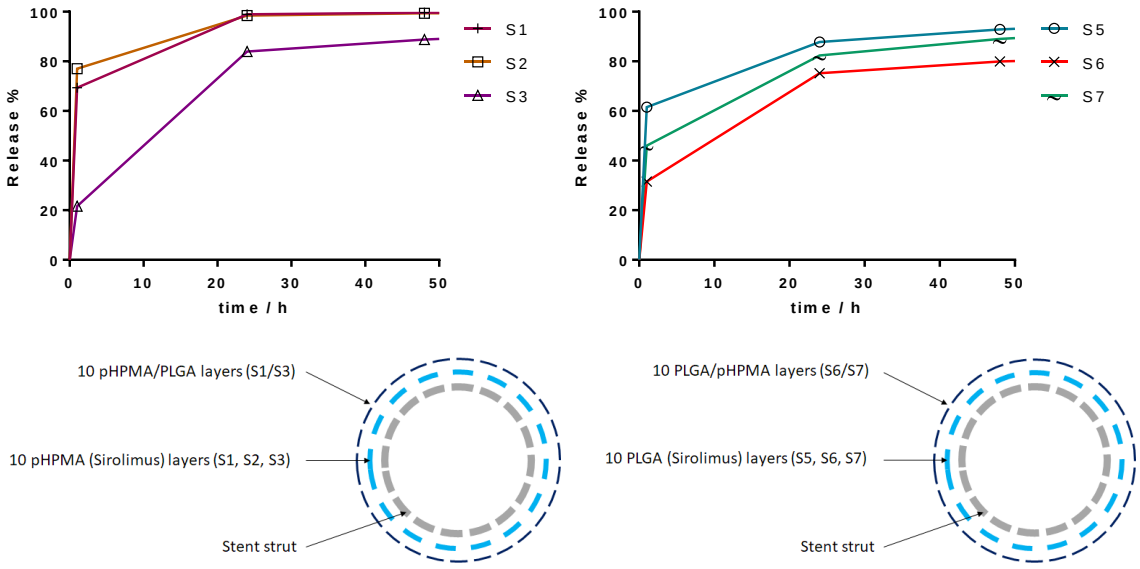

Figure 12: Comparative release study with PLGA and pHPMA barriers in stents of polymeric homogenous and heterogeneous composition. Top left graph shows elution from stents composed of pHPMA layers loaded with sirolimus (S1, S2 and S3) and in some cases coated with pHPMA (S1) or PLGA (S3) barriers, followed by a layer diagram located under it. Top right graph shows elution from stents composed of PLGA layers loaded with sirolimus (S5, S6 and S7) and in some cases coated with PLGA (S6) or pHPMA (S7) barriers, also followed by a layer diagram. Results show different behaviors obtained from pHPMA and PLGA barriers over PLGA or pHPMA matrices.

On Figure 12, an extra release profile from Figure 11 was added to both graphs with the aim of studying the barrier effects seen before while combining different polymeric matrices. On the left graph, a release profile was added belonging to a stent with the same interior sirolimus loaded pHPMA coating but with a PLGA exterior barrier. Although on normal circumstances pHPMA eluted very quickly, this PLGA exterior barrier showed a controlled and slower release which did not result in an aggressive pealing or detachment of the interior layers. The behavior described is crucial, as if this was not the case, the combination of polymers described would not be suitable for the elaboration of multi-layered stents. On the right graph, a release profile was added belonging to a stent with an interior sirolimus loaded PLGA coating, but with a pHPMA external barrier. As expected, the release profile of this stent laid in between of the ones obtained from S5 and S7. Its barrier was presumed to reduce elution under S5's profile, but not lower than the curve obtained from S6. Both combinations seen on Figure 12 showed a controlled release with a good behavior and no signs of peeling. There was one more effect which was of interest in this set of experiments and which is presented in Figure 13.

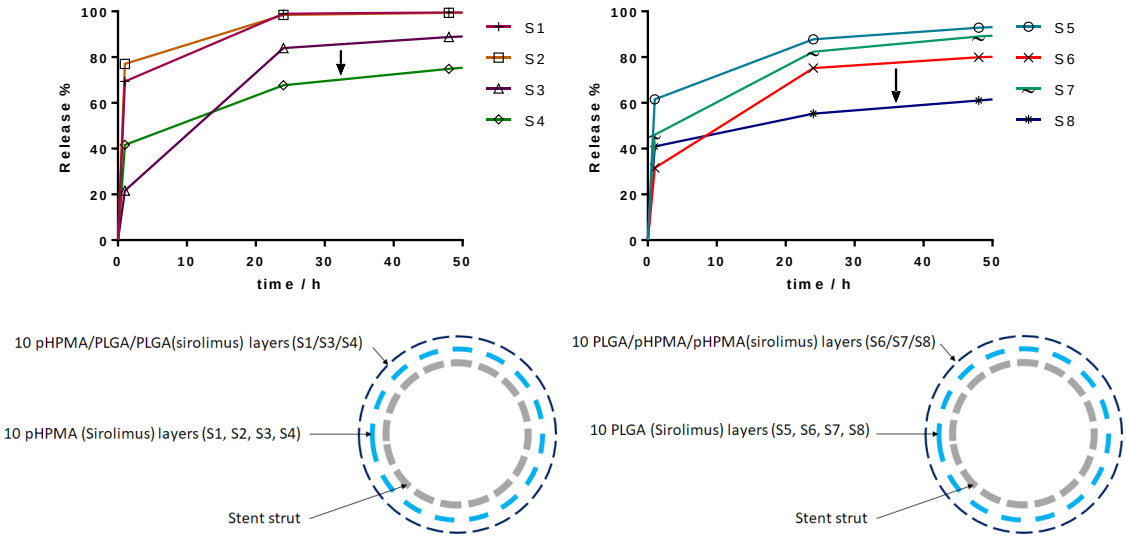

Figure 13: Release profiles used to study drug ratio and hydrophobicity effect on designed stents. These graph, based on the ones depicted in Figure 12, show the addition of S4 (on the left) and S8 (on the right) in order to study how their composition varied their release profile. Each graph is followed by a diagram which describes the composition of the stents used. Results show how drug concentration effects can have a greater impact on drug release profiled than barriers.

This graph shows the change in elution obtained when the barrier layers were filled with a pharmacological load. Through this experimentation the new coatings performed differently, producing interesting results. These new profiles were added to the ones shown in Figure 12 to make the discussion easier to follow, leading to Figure 13. On the left graph, a release profile was added belonging to a stent with an interior sirolimus loaded pHPMA coating, with a sirolimus loaded PLGA external layer. When the new profile was graphed, its initial release showed a slower elution when compared to S1 and S2, but quicker than S3. In the case of S4, its external PLGA layer was loaded with sirolimus. This led to an initial liberation higher than the one observed with S3, but as the coating started to fade and erode, the release from the PLGA matrix produced once again a slower elution than the one obtained from the pHPMA matrix of S3.

Most important, this showed that the influence of pharmacological load described previously, where a higher drug load rendered a reduction in the release profile, was having a greater impact in these stent elution profiles than the barriers. On the right graph, this phenomenon was very clear as the drug load present on stent S8 was twice than the rest. After analyzing these results, effective barriers could now be designed with PLGA and other reductive effects could be achieved at the expense an increase in the pharmacological load.

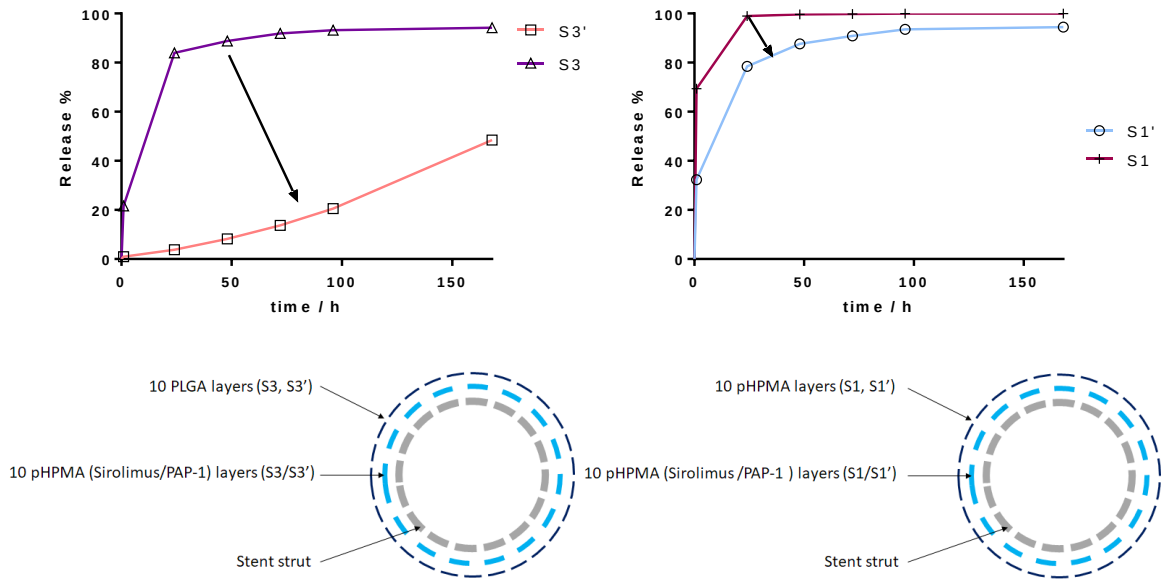

Figure 14: Effect of PLGA and pHPMA barriers over PAP-1 or sirolimus loaded matrices. Each graph is followed by a layer diagram placed under it. The graph at the left shows elution from a bilayered stents with an interior pHPMA coating loaded with sirolimus (S3) or PAP-1 (S3') and an exterior barrier of PLGA (S3 and S3'). At the right, a graph shows elution from a bilayered stents with an interior pHPMA coating loaded with sirolimus (S1) or PAP-1 (S1') and an exterior barrier of pHPMA (S1 and S1'). Elution profiles show differences due to hydrophobicity of the drug loaded in the polymeric matrices as well as the type of barriers used.

After observing the effect of sirolimus concentration on the release profile, Figure 14 shows the addition of two new profiles which come from the substitution of sirolimus by a more hydrophobic drug (PAP-1) in S1 and S3 stents. On the left graph, substituting sirolimus by PAP-1 in the interior layer and adding a strong PLGA barrier caused the release to drop drastically. On the other hand, in the graph located at the left, substitution of sirolimus with PAP-1 rendered a slower elution due to its increased hydrophobicity. It was also noticed that the pHPMA barrier causes a very subtle blocking effect with this drug. Once results from these experiments had been studied, the next step led to the tailoring of PAP-1 elutions in different stent configurations. Releases obtained from some initial designs are shown in Figure 15.

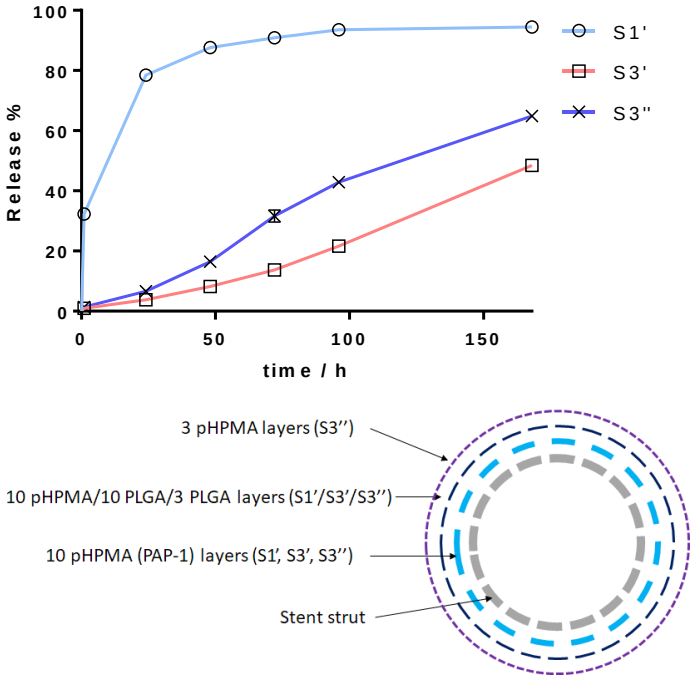

Figure 15: Tailoring PAP-1 elution through the study of various releases form different stent formulations. This graph is followed by a layer diagram placed under it Three different stent designs were studied with the objective of obtaining a suitable release which could last over 1 month for a future in-vivo model. Different burst, barrier and sustained release behaviors were observed.

Stent designs studied in Figure 15 showed tailored compositions and elutions which were elaborated to produce results which could be applied in an *in-vivo* trial. These stents were designed with a small exterior layer of pHPMA to enhance arterial adhesion. S1' displayed a rapid elution achieved from the ten interior layers of pHPMA loaded with PAP-1 slightly contained by the next ten layers of pHPMA. This profile showed an excessive burst effect lasting up to fifty hours, which would not be suitable for a 1 month *in-vivo*. S3' was designed substituting the 10 pHPMA layers of S1' with ten layers of PLGA.

This long-lasting profile was able to supply sustained elution over 1 month. S3 was elaborated by substituting the ten layers of PLGA from S3' with three layers of PLGA in order to produce a smaller barrier. This stent showed a burst effect ranging from twenty-five to seventy-five hours, with a continued long-lasting sustained release. Among these three types of stents, S3'' showed the most interesting results for *in*-vivo testing.

All these modifications showed that it was possible to tailor the PAP-1 release profile in a multi-layered stent elaborated with different combinations of PLGA and pHPMA in order to achieve bursts, barriers and sustained releases with a good control throughout all its profile. With the aim of checking the morphological structure of the most suited stent for *in-vivo* testing, SEM images were obtained as shown in Figure 16. These images showed a correct abluminal coating for the S3'' stent. This target stent design is studied in detail along the next section.

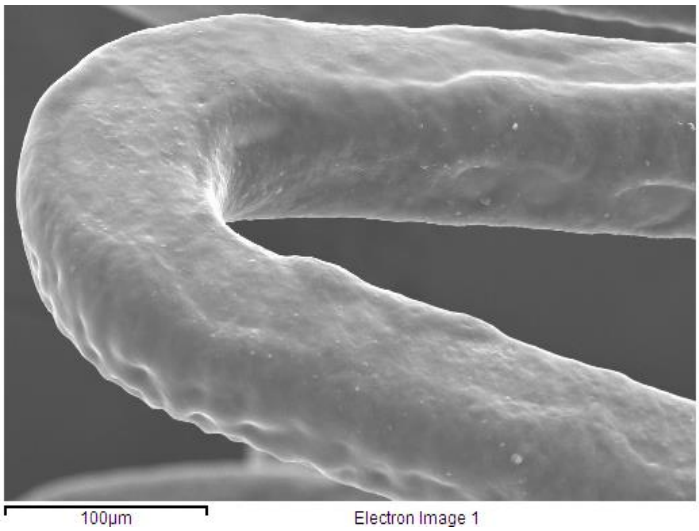

Figure 16: Morphology of S3'' stent obtained by SEM imaging. S3'' was composed of ten layers of pHPMA loaded with PAP-1, three layers of PLGA and three exterior layers of pHPMA. This image shows the abluminal coating at the front in focus, while the luminal side remains at the back. A correct abluminal coating is achieved from this multilayered stent design.

3.3.4 In-vitro testing through scratch test for PAP-1 release in target DES in supplemented medium.

Up to this point, all liberations were performed in modified quick medium to slightly increase the stability of the drug and to accelerate the elution. Stent designs discussed from now on were tested in full supplemented medium to achieve a more realistic elution environment as well as to observe elution times which could better match the ones seen in an *in-vivo* model. Stents with a full coating of pHPMA and others with external barriers of PLGA and pHPMA were tested as seen in Figure 17 to obtain equivalence between elutions in quick medium and supplemented medium.

Slight modifications were made in the extraction of the drug to preserve its stability, such as evaporation through N_2 currents or CO_2 freezing of water content during DCM extraction in order to avoid room temperature baths. An approximation of complete elution times was obtained through data analysis and extrapolation, showing that the pHPMA stents loaded with PAP-1 would maintain their release up to two weeks. In the case of the pHPMA stents loaded with PAP-1 and with PLGA and pHPMA barriers, these would maintain elution up to one and a half months. This last stent was found interesting to try in *in-vitro* and *in-vivo* experiments due to its controlled liberation and its coating material design. Following, a guiding *in-vitro* experiment was carried out.

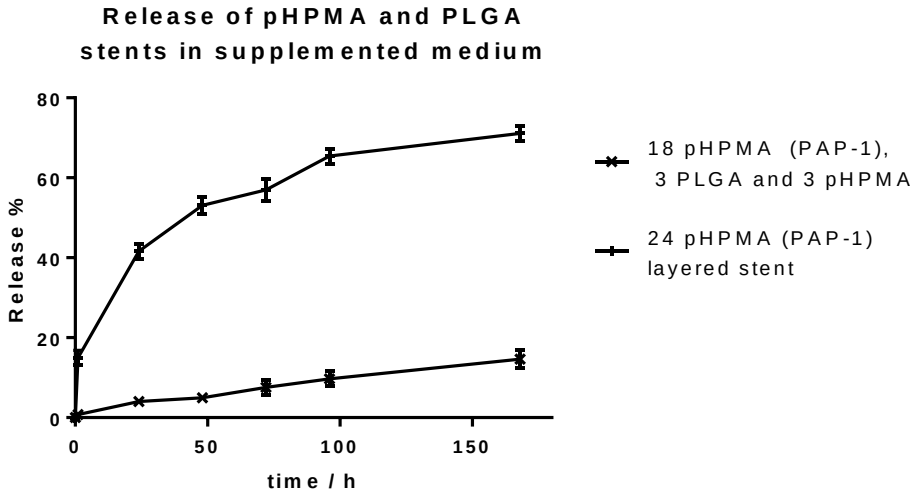

Figure 17: Evaluation of release from different stents in supplemented medium. Elution profiles obtained in supplemented medium can be compared with the ones obtained in quick elution medium. Total release was plotted as % released from the strut vs time (h). A fast elution was registered from stents designed with twenty-four pHPMA layers loaded with PAP-1. A slow elution was observed from stent designs composed of eighteen interior layers of pHPMA loaded with PAP-1, three PLGA layers and three exterior pHPMA layers. Slightly slower elutions are observed in supplemented medium when compared with results obtained in quick elution medium.

Now that results had led to a viable stent design which had an interesting elution and an adequate material selection, an *in-vitro* test was done to check that the drug load selected would not produce anomalous results. The following test was done to evaluate if the amount released would be toxic or if it was enough to produce a change in proliferation. To assess this, a scratch test was performed as described at the beginning of this chapter, comparing results of a control culture vs one treated with the obtained releases from a target stent. Results are shown next in Figure 18 and Table 3.

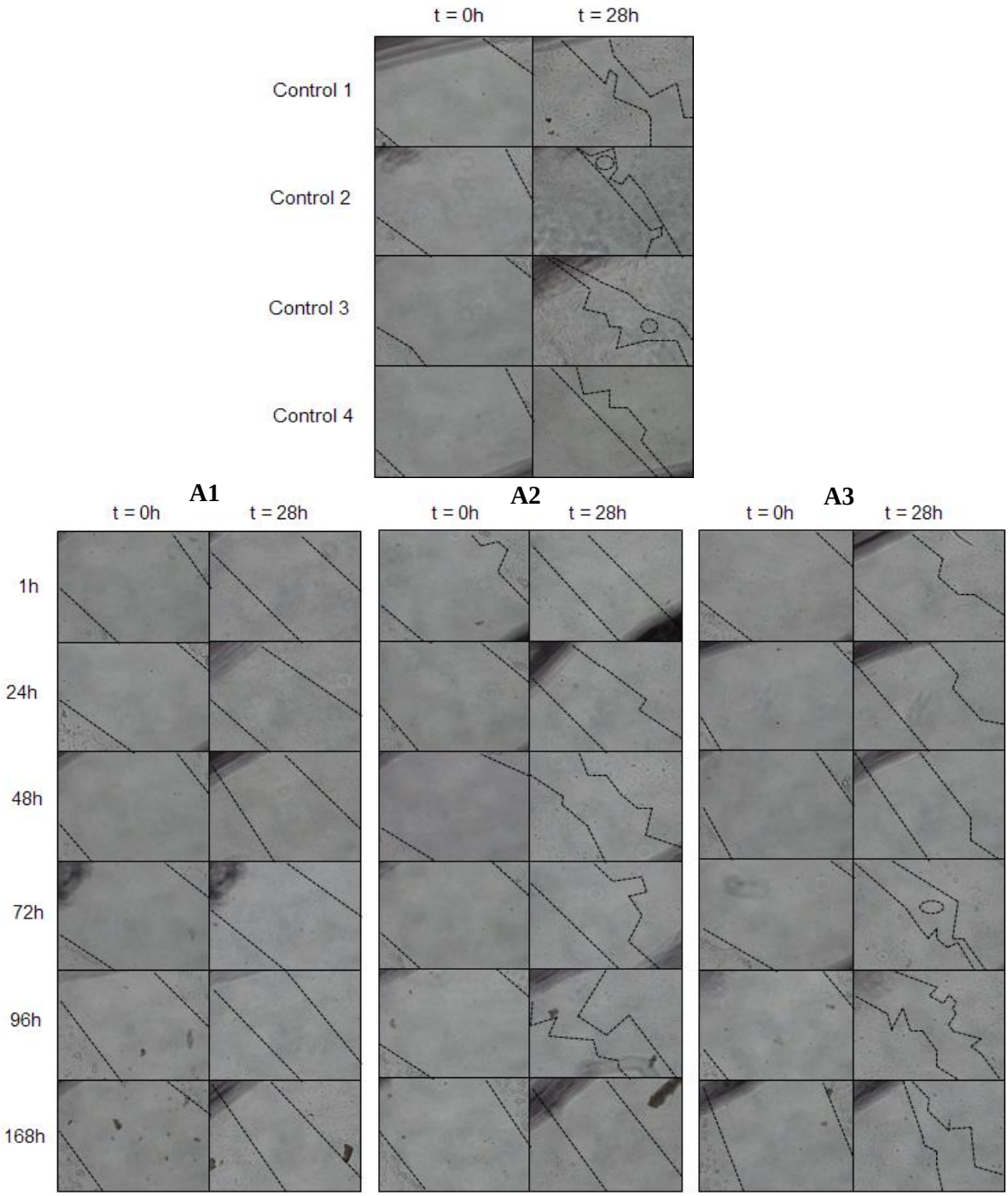

Figure 18: In-vitro scratch test adding PAP-1 release to cos-7 cell line from stents composed of eighteen interior layers of pHPMA loaded with PAP-1, three PLGA layers and three exterior pHPMA layers (S3''). The top group of brightfield images are obtained from the control group. First column corresponds to images taken at the initial point right after producing the standardized scratch and the second column to images taken at twenty-eight hours at the same spot. Rows correspond to different controls labelled 1-4 descending vertically. Controls are treated with culture medium without any PAP-1. Under the controls, there are three groups of images corresponding to triplicates of S3''. In this case, each row corresponds to different culture medium used in the experiment. First row (1h) corresponds to samples which were treated with culture medium containing release from the first hour of an S3'' stent. Second row corresponds to samples treated with culture medium containing the release obtained starting from the first hour up to twenty-four hours. This tendency continues descending vertically until the last row, which contains the release obtained during the period between ninety-six to one hundred and sixty-eight hours from a S3'' stent. This experiment was performed in triplicate, labelling each iteration as A1, A2 and A3. No toxicity is observed as well as a reduction in proliferation.

Table 3: Wound healing evaluation from in-vitro scratch test performed to cos-7 cultures exposed to liberations obtained from stents composed of eighteen interior layers of pHPMA loaded with PAP-1, three PLGA layers and three exterior pHPMA layers. Results obtained from Figure 18 expressed in % area of closed wound. The top table corresponds to the bottom group of images from the previous figure (A1-A3). First column shows the time lapse from which the release medium was used. Second to fourth columns show % area of closed wound of stents A1-A3. Last column shows the average % area of closed wound from each specific time lapse (A1-A3). Bottom table shows the results obtained from the top group of images of the same figure (Controls). First to fourth columns show % area of closed wound of control stents C1-C4. Last column shows the average % area of closed wound from all the controls.

Release from time lapse / h	**A1: Cut closed during 28h / %**	**A2: Cut closed during 28h / %**	**A3: Cut closed during 28h / %**	**Average S1-S3 / %**
0-1	23.5	40.6	28.2	*30.8*
1-24	20.5	38.2	41.4	*33.4*
24-48	32.0	49.2	49.2	*43.5*
48-72	15.5	48.6	73.5	*45.9*
72-96	30.5	58.3	58.4	*49.1*
96-168	43.3	32.6	66.5	*47.5*

C1: Cut closed during 28h / %	**C2: Cut closed during 28h / %**	**C3: Cut closed during 28h / %**	**C4: Cut closed during 28h / %**	**Average C1-C4 / %**
75.0	87.1	76.0	82.5	*80.2*

These results showed how the control samples had almost completely closed the wound after twenty-eight hours, while the samples which contained PAP-1 from the DES had not. This slower wound healing rate was associated to the antiproliferative action of the drug. These samples had been incubated in supplemented medium containing PAP-1 obtained at different time points during a drug release study, showing that the amount of drug released was enough to affect proliferation on an *in-vitro* test. Although *in-vivo* results may broadly vary from the ones obtained *in-vitro*, this was a useful and quick test used to check if the quantity of drug released could affect cells in direct contact with the stent. It also showed its antiproliferative action in live cells without any unexpected adverse effects, which was a positive indicator sought before moving on to an in-vivo trial.

3.3.5 Analysis of tailored PAP-1 loaded DES in supplemented medium. Redesigning to find an optimal release.

After obtaining these results, the slowest eluting stent from Figure 17 showed an interesting profile which was later tried out in a small in-vivo with 3 pigs. Each pig had three stents deployed, each loaded with 75 +- 1.2 µg of PAP-1, to be studied for one month before data was collected. Although results obtained showed healing and low restenosis, PAP-1 content in blood stream ceased to appear after two weeks. As seen in the results, a thick initial pHPMA layer may not be stable enough to hold the whole coating structure laid over it and may partially start peeling off when placed in an artery. To avoid this, the stent was redesigned to present a more consistent behavior. The initial thick coating which provided the sustained release was elaborated with eighteen layers of PLGA loaded with PAP-1. Over this polymer matrix a smaller pHPMA coating was added to provide a burst effect, leaving the PLGA matrix under it to sustain the structure. A last thin PLGA layer was added in order to protect the pHPMA layer and to act as a barrier.

More studies were carried out with these layer combinations as seen in Figure 19. Three stents with this interior PLGA layers and different exterior coatings were prepared as described previously to study their different eluting profiles. The aim of this study was to achieve a similar type of release than the previous stent design but with a PLGA interior. These profiles were analyzed as presented in this figure, showing a burst effect that lasted seventy-five hours. After this time point, the burst phenomenon was not appreciated and the effect of the remaining elution from the pHPMA layers on the stent was not identified. Another interesting observation was provided by the thicker initial PLGA coatings in supplemented medium. The layer combination selected enabled more efficient burst effects, leaving the “reduction of release per increase of concentration” effect, observed previously in this chapter, to appear much later. In this case, the burst effect of the eight layers of pHPMA over the PLGA matrix in supplemented medium was too big if left unprotected, therefore, making the option with the PLGA external barrier more interesting.

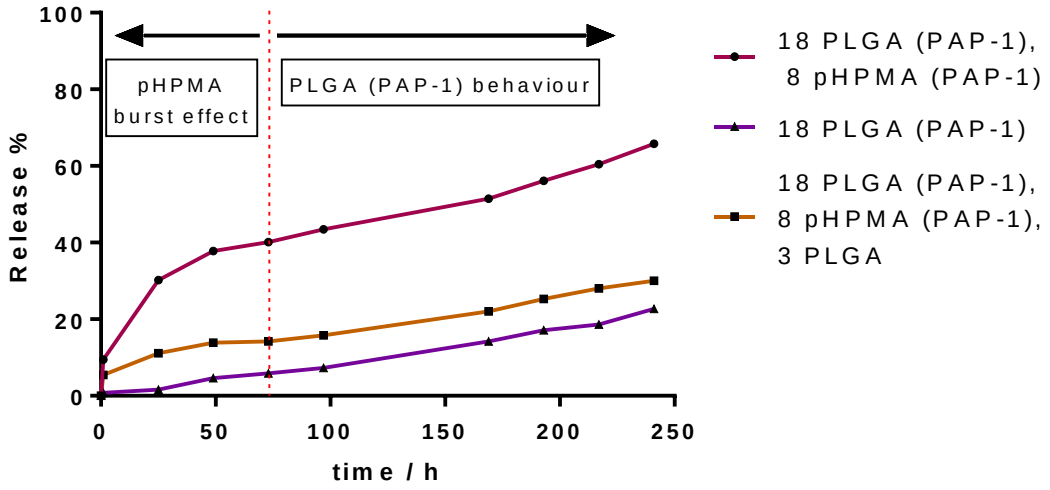

Figure 19: Release profiles obtained from three different stent combinations with PAP-1 drug loads, left in supplemented medium for two hundred and fifty hours. Total release was plotted as % released from the strut vs time (h). Elution were observed from stent designs composed of the following layers: A first stent was composed of eighteen interior layers of PLGA loaded with PAP-1 and eight pHPMA layers also loaded with PAP-1. A second type of stent composed of eighteen interior layers of PLGA loaded with PAP-1. A third type of stent composed of eighteen interior layers of PLGA loaded with PAP-1, eight pHPMA layers also loaded with PAP-1 and three exterior PLGA layers. Burst effects can be observed at the left of the red dotted line. To the right of the red dotted line, the PLGA sustained release behavior is predominant.

Discarding the unprotected eight layered pHPMA burst stent, the other two were left for twenty days in total as seen in Figure 20. As the burst effect faded off on further time points, the stent with a higher drug load ended up crossing the other stent's release profile. As mentioned earlier, this phenomenon had been observed when using thicker initial coatings of PLGA in full supplemented medium. This study was performed up to a six-hundred-hour time point.

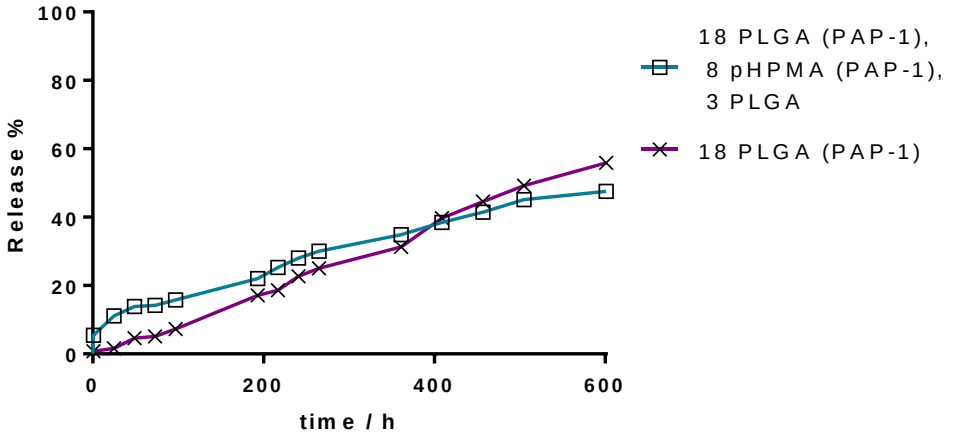

Figure 20: Release profiles obtained from PAP-1 loaded stents in supplemented medium during six hundred hours. Total release was plotted as % released from the strut vs time (h). Elution were observed from stent designs composed of the following layers: A first stent was composed of eighteen interior layers of PLGA loaded with PAP-1, eight pHPMA layers also loaded with PAP-1 and three exterior layers of PLGA. A second type of stent composed of eighteen interior layers of PLGA loaded with PAP-1. Burst and sustained release are achieved with a combination of PLGA and pHPMA. The phenomenon of elution reduction due to an increase in concentration is clearly seen at the four-hundred-hour time point, while the burst effect can be observed through the initial one hundred hours.

Data obtained from these experiments suggested that an initial PLGA matrix loaded with PAP-1 and a small protected burst layer of pHPMA can present a suitable release for *in-vivo* testing ranging one to three months. Although the stent which presented a burst effect could be used for future *in-vivo* testing, this quick initial release was preferred to be subtler. As presented next, one last type of stents was prepared with a tailored composition which best suited the release profile and characteristics sought, slightly reducing the initial burst effect.

3.3.6 Elution study of a final tailored design for multilayered PAP-1 DES.

As to obtain a secure, long-lasting stent with a controlled burst effect, a final design was prepared. This one was composed of eighteen layers of PLGA with PAP-1 adhered to the strut, three layers of pHPMA with PAP-1 to produce a small initial burst effect and three final pHPMA layers to enhance adhesion with the artery wall. These stents were prepared with an industrial sprayer as described in the beginning of this chapter. Each stent was weighted after each polymeric coating was finished to ensure that the polymer and drug quantities were correct. After finishing the coatings and letting them dry for twenty-four hours, three stents were crimped and expanded to check their release profile comparing it to uncrimped and unexpanded stents. Release profiles were finished after one month and analyzed after, producing the graph seen in Figure 21.

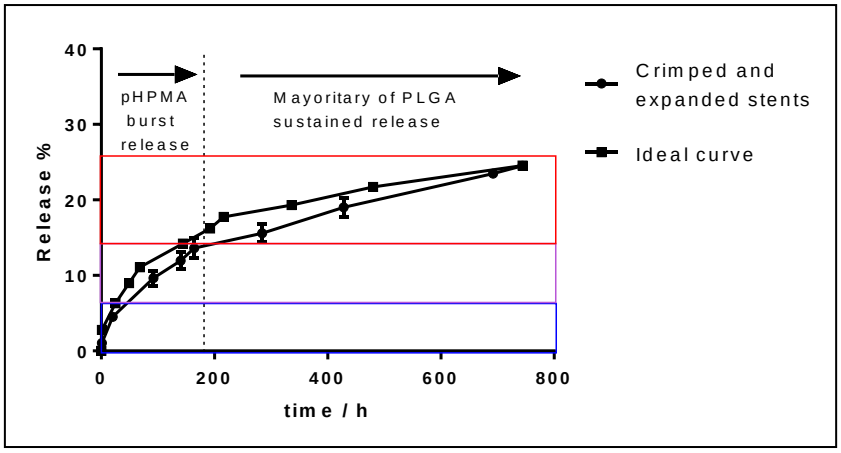

Figure 21: Release profiles obtained from crimped and expanded stents as well as from and uncrimped multilayered PAP-1 loaded stents in supplemented medium during eight hundred hours. Crimped and expanded stents elutions are compared to the ones obtained from others elaborated the same way, but which had not undergone these mechanical processes. The curves can be divided into three different areas colored in blue, purple and red corresponding to different elution speeds observed. This separation was due to the burst effect obtained from the PAP-1 in a pHPMA matrix which faded off gradually.

Stents that underwent a crimping and expansion process showed a slight reduction in their elution. This was attributed to the action of the crimper which compressed and compacted the stents coating as well as possibly removing a very small part of the external pHPMA layers which could stick to the crimper during the process. Although this phenomenon is very common, it could affect the release profile of the designed stent making the study of the possible elution deviation interesting. In this case, the reduction observed was quite small and practically did not change from the uncrimped stents. As the figure shows, there was a clear area where the pHPMA burst could be appreciated, lasting up to two hundred hours. After that, the effect of the pHPMA could not be considered a burst effect and the elution was PLGA matrix predominant.

Three different regions were defined when examining the changes in the slopes throughout the elution time. In Table 4, the different slope ranges are listed for the different stents studied in Figure 21. Starting from the top, the blue row represents the fastest burst effect of the outer layers of pHPMA shown during the first twenty-five hours. After that, a purple area shows a smaller slope corresponding to the rest of the burst effect and the interior layers of pHPMA which started to be mixed with the PLGA matrix. On the last area colored as red, some pHPMA still remained but only mixed with the most exterior layers of PLGA. This small quantity of PAP-1 slightly increased the expected release from a PLGA matrix. This residual elution is caused by three different phenomena. First, an interface between two layers can contain a mix of both, showing a small content of a drug eluting when its layer has already completely eluted. A drug may also diffuse slightly into another layer, showing this remaining elution described previously. Something which should also be considered is that

degradation will not occur homogeneously thinning all the exterior layer at the same rate, thus producing this residual elution effect.

Table 4: Mean average slope calculated at highlighted zones for elution curves depicted in Figure 21. SA corresponds to an uncrimped and unexpanded stent model, while the other three stents have been crimped and expanded. The last column of the table shows the slope range of each zone.

SA (ideal)	SB	SC	SD	Range
0.206	0.169	0.170	0.121	0.12-0.21
0.069	0.061	0.058	0.049	0.049-0.069
0.018	0.020	0.019	0.014	0.014-0.020

The morphology of these stents was also studied through SEM imaging, showing a good abluminal coating while the luminal protected part was kept clean. An example of the images obtained is shown next on Figure 22.

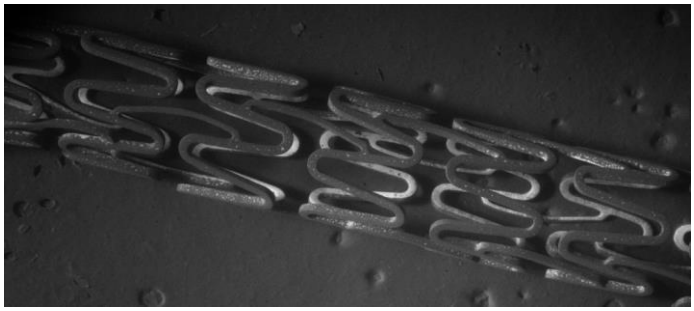

Figure 22: Sem image of a tailored DES produced in an industrial sprayer. Composition of these stents was the following: Eighteen layers of PLGA (loaded with PAP-1), three layers of pHPMA (loaded with PAP-1) and three layers of pHPMA. Layers are listed in interior to exterior order. Correct abluminal coating was observed while luminal protected area remained clean.

This final version, tailored and thoroughly studied, is tested in an *in-vivo* trial.

.

3.3.7 In-vivo study of PAP-1 loaded stents.

As result from the collaboration with Dr. Mercè Roqué and IDIBAPS (Hospital Clínic de Barcelona), a porcine in-vivo trial was possible. Data shown next, as well as the methodology described for *in-vivo* trials on porcine models (materials and methods) is part of their work using our last stent model and is presented as found in the submitted article titled “Kv1.3 blockade Inhibits Proliferation of Vascular Smooth Muscle Cells In Vitro and Intimal Hyperplasia In Vivo”, currently undergoing revision in the journal “Revista Española de Cardiología”. The porcine model used in this in-vivo trial is described in the materials and methods section of this chapter. Stents used in this trial are loaded with 153.1 +- 0.8 µg of PAP-1 and results obtained are shown next on Figure 23 and Table 5.

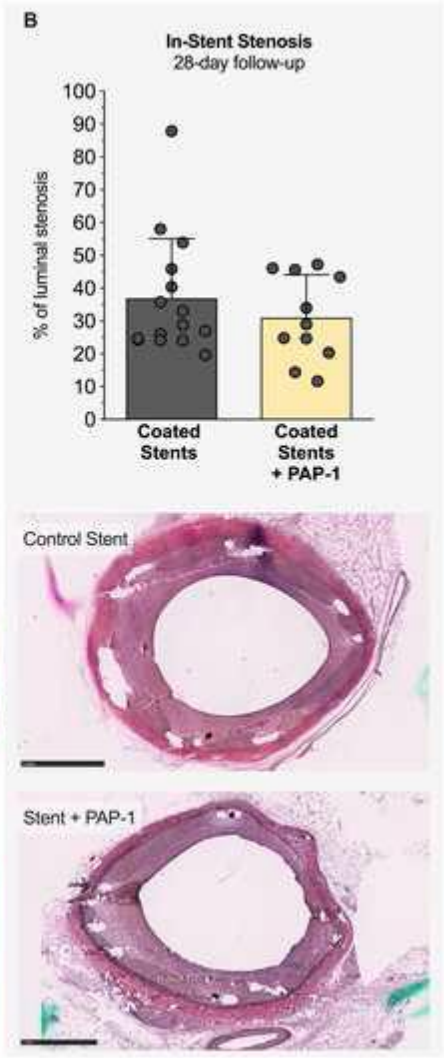

Figure 23: Effect of Kv1.3 inhibition with PAP-1 on Porcine Models of Coronary In-Stent Restenosis. Superior: Bar graph representing mean ± SEM of percentage of luminal stenosis of control (n=15) and PAP-1-eluting coronary stents (n=12). Inferior: Representative photomicrographs of stented coronary segments cross-sections at 28-day follow-up. Verhoeff Van Gieson stain. Original magnification: 10x.

Table 5: Morphometric Analysis of the Coronary Stented Arteries. Morphometric data of stented coronary arteries are summarized in this table. A mild tendency towards a decreased intimal proliferation was observed.

	Control (n=15)	PAP-1 (n=12)	P value
Neointimal area (mm^2)	1.75±1.16	1.50±0.56	0.499
Area of media	1.66±1.20	1.43±0.37	0.546
Intima-media thickness	3.41±2.05	2.92±0.78	0.458
Area of stenosis (%)	36.90±18.23	31.01±13.08	0.372
Endothelial area (%)	99.47±1.13	99.55±1.51	0.879
Endothelization >95%	100% (15/15)	100% (12/12)	-
Injury score of Schwartz	0.79±0.43	0.68±0.53	0.560
Injury score of Schwartz ≥1	20% (3/15)	27.27% (3/12)	0.678
Inflammation score	1.11±0.70	1.07±0.71	0.904
Inflammation score ≥1	53.33% (8/15)	45.45% (5/12)	0.705
Fibrin score	0.29±0.38	0.21±0.34	0.598
Fibrin score ≥1	13.33% (2/15)	9.09% (1/12)	0.750

P values from *t* test.

Although a tendency towards a lesser intimal area in the PAP-1 treatment group can be observed, no significant differences in the morphometric parameters analyzed have been demonstrated. Several facts may be considered to explain these results. *In-vivo* release conditions may have been different than those estimated in vitro, and the drug may not have been properly released. Supporting this point of view, we have analyzed the remaining PAP-1 concentration in the stented segments, which is approximately 40-50% of the initial concentration, therefore implying the release was not complete, as expected by the preliminary experiments of release profile analysis. Another possible explanation for the lack of effect is the limitation of PAP-1 concentration which could be incorporated into the polymer. In our in vitro assays, a maximum concentration of 1.5 $\mu g/mm^2$ was achieved, preserving an adequate electron microscopy structure of the coated stent. It is possible that higher concentrations of the study drug would have produced a more effective reduction in intimal proliferation. In summary, implantation of PAP-1-eluting stents did not result in a statistically significant decrease of intimal proliferation in the coronary arteries, compared to polymer alone coated stents, although a mild tendency towards a decreased intimal proliferation was observed.

To note, it is debated whether late vascular response (i.e., neointimal formation after 28 days) after DES implantation in swine models may or may not correlate with clinical restenosis or increased target legion revascularization (TLR) in clinical trials out to 4 years long-term. In addition, it has been suggested that long-term time points in pig models should be used for safety and biocompatibility assessment as they remain insufficiently validated for efficacy endpoints. The polymer used in our stent has shown to have no side-effects, like excessive inflammation or fibrin deposition. Also, there was no evidence of occlusive or residual thrombosis in any of the stented coronary segments analyzed. Reendothelialization was also analyzed, which was complete, with 100% of endothelial lining recovered at 28 days after stent implantation, in PAP-1 and control treatment groups.

3.4 Concluding Remarks

Throughout this chapter, the elution of sirolimus and PAP-1 from pHPMA and PLGA matrices with multilayered stents has been studied. The knowledge provided by the results of these experiments have enabled the creation of burst layers, barriers and different sustained release profiles which can be used to modify sirolimus and PAP-1 elution from medical devices. pHPMA matrices have shown very quick releases which are useful for burst effects but have shown to be unreliable for thick interior layers as they may peel off. PLGA matrices have shown sustained releases with PAP-1 and sirolimus which have been studied in different mediums and with different drug loads. Stents loaded with these drugs have shown slower elutions with PAP-1 than with sirolimus due to difference in hydrophobicity.

A reduction in the drug release has been observed during the experiments, associated to an increase of pharmacological load. This phenomenon has been studied in a variety of cases with sirolimus and PAP-1 in different polymeric matrices and has proven to produce a greater effect than barriers but at the expense of a greater drug concentration. This behavior has been observed in long duration releases in supplemented medium, appearing later than burst effects in exterior layers. The combination of these two phenomena can be tailored to appear at a same liberation curve, becoming helpful tools used to modulate releases.

All the knowledge provided by this experimentation has enabled the elaboration of multilayered stent designs which can tailor drug liberation to be suited for different applications. These outcomes have generated interesting stent designs which have been tested *in-vitro* and *in-vivo* with promising results. A multilayered stent used for a last *in-vivo* trial has been elaborated in an industrial environment to prove the scalability of the process. The images and release profiles obtained from the stents created have shown the viability of its industrial production. Although restenosis reduction was achieved when compared with control stents in a porcine model *in-vivo* trial, future animal testing is suggested to achieve multilayered combinations and PAP-1 concentrations which can reduce restenosis in a more efficient manner. Furthermore, the polymer used in our stents has shown to have no side-effects, like excessive inflammation or fibrin deposition. Also, there was no evidence of occlusive or residual thrombosis in any of the stented coronary segments analyzed.

3.5 References

[1] M. Sabate *et al.*, “Everolimus-eluting stent versus bare-metal stent in ST-segment elevation myocardial infarction (EXAMINATION): 1 year results of a randomised controlled trial,” *Lancet*, vol. 380, no. 9852, pp. 1482–1490, 2012.

[2] T. Kimura *et al.*, “Comparison of everolimus-eluting and sirolimus-eluting coronary stents: 1-year outcomes from the randomized evaluation of sirolimus-eluting versus everolimus-eluting stent trial (RESET),” *Circulation*, vol. 126, no. 10, pp. 1225–1236, 2012.

[3] J. Aoki *et al.*, “Three-Year Clinical Outcomes of Everolimus-Eluting Stents From the Post-Marketing Surveillance Study of Cobalt-Chromium Everolimus-Eluting Stent (XIENCE V/PROMUS) in Japan,” *Circ. J.*, vol. 80, no. 4, pp. 906–912, 2016.

[4] T. Palmerini *et al.*, “Stent thrombosis with drug-eluting and bare-metal stents: Evidence from a comprehensive network meta-analysis,” *Lancet*, vol. 379, no. 9824, pp. 1393–1402, 2012.

[5] K. Miura *et al.*, “Stent Fracture and Peri-Stent Contrast Staining After Everolimus-Eluting Stent Implantation — 5-Year Outcomes —,” *Circ. J.*, vol. 81, no. 10, pp. 1514–1521, 2017.

[6] J. M. de la Torre Hernandez *et al.*, “Procedural resources utilization and clinical outcomes with bioresorbable everolimus-eluting scaffolds and Pt-Cr everolimus-eluting stent with resorbable abluminal polymer in clinical practice. A randomized trial,” *Catheter. Cardiovasc. Interv.*, vol. 90, no. 2, pp. E25–E30, 2017.

[7] S. Saito *et al.*, “A randomized, prospective, intercontinental evaluation of a bioresorbable polymer sirolimus-eluting coronary stent system: The CENTURY II (Clinical Evaluation of New Terumo Drug-Eluting Coronary Stent System in the Treatment of Patients with Coronary Arte,” *Eur. Heart J.*, vol. 35, no. 30, pp. 2021–2031, 2014.

[8] D. A. K. Sharma, “Different coronary stent design.” 2020. [Online]. Available: https://www.slideshare.net/awakush/coronary-stent-design-ppt.

[9] F. Otsuka *et al.*, “Pathology of Second-Generation Everolimus-Eluting Stents versus First-Generation Sirolimus- and Paclitaxel-Eluting Stents in Humans,” *Circulation*, vol. 129, no. 2, pp. 211–223, 2014.

[10] G. A. A. Ferns and T. Y. Avades, “The mechanisms of coronary restenosis: Insights from experimental models,” *Int. J. Exp. Pathol.*, vol. 81, no. 2, pp. 63–88, 2000.

[11] A. Cheong *et al.*, “Potent suppression of vascular smooth muscle cell migration and human neointimal hyperplasia by KV1.3 channel blockers,” *Cardiovasc. Res.*, vol. 89, no. 2, pp. 282–289, 2011.

[12] L. A. Pardo *et al.*, “Voltage-Gated Potassium Channels in Cell Proliferation Voltage-Gated Potassium Channels in Cell,” pp. 285–292, 2015.

[13] H. Wulff, N. A. Castle, and L. A. Pardo, “Voltage-gated potassium channels as therapeutic targets,” *Nat. Rev. Drug Discov.*, vol. 8, no. 12, pp. 982–1001, 2009.

[14] A. Erdogan *et al.*, “Margatoxin inhibits VEGF-induced hyperpolarization, proliferation and nitric oxide production of human endothelial cells,” *J. Vasc. Res.*, vol. 42, no. 5, pp. 368–376, 2005.

[15] M. D. Cahalan and K. G. Chandy, “The functional network of ion channels in T lymphocytes,” *Immunol Rev*, vol. 231, no. 1, pp. 59–87, 2009.

[16] N. Villalonga *et al.*, “Immunomodulation of voltage-dependent K^+ channels in macrophages: molecular and biophysical consequences,” *J. Gen. Physiol.*, vol. 135, no. 2, pp. 135–147, 2010.

[17] M. Roqué *et al.*, “role oF kv1.3 Channel in vasCular smooth musCle Cells ProliFeration in a PorCine model oF restenosis,” *J. Am. Coll. Cardiol.*, vol. 65, no. 10, p. A1578, 2015.

[18] G. Colmenares *et al.*, “Evolution of coronary drug-eluting stents, from the first to the fourth generation,” *CES Med.*, vol. 31, no. 2, pp. 163–171, 2017.

[19] X. Gu *et al.*, “Biodegradable, elastomeric coatings with controlled anti-proliferative agent release for magnesium-based cardiovascular stents,” *Colloids Surfaces B Biointerfaces*, vol. 144, pp. 170–179, 2016.

[20] Elsawy, M. A., Kim, K. H., Park, J. W., & Deep, A. (2017). Hydrolytic degradation of polylactic acid (PLA) and its composites. Renewable and Sustainable Energy Reviews, 79, 1346-1352.

[21] La Mantia, F. P., Morreale, M., Botta, L., Mistretta, M. C., Ceraulo, M., & Scaffaro, R. (2017). Degradation of polymer blends: A brief review. Polymer Degradation and Stability, 145, 79-92.

[22] Rescignano, N., Tarpani, L., Romani, A., Bicchi, I., Mattioli, S., Emiliani, C., ... & Armentano, I. (2016). In-vitro degradation of PLGA nanoparticles in aqueous medium and in stem cell cultures by monitoring the cargo fluorescence spectrum. Polymer Degradation and Stability, 134, 296-304.

[23] Nair, N. R., Sekhar, V. C., Nampoothiri, K. M., & Pandey, A. (2017). Biodegradation of biopolymers. In Current Developments in Biotechnology and Bioengineering (pp. 739-755). Elsevier.

[24] S. Park *et al.*, “An Evaluation of Poly(L-Lactic Acid) Plate and Screw System for Fixation of Mandible Fracture in Rabbit Model,” *Tissue Eng. Regen. Med.*, vol. 8, no. 4, pp. 398–405, 2011.

[25] Bartnikowski, M., Dargaville, T. R., Ivanovski, S., & Hutmacher, D. W. (2019). Degradation mechanisms of polycaprolactone in the context of chemistry, geometry and environment. Progress in Polymer Science.

[26] Chen, Y., Hung, S. T., Chou, E., & Wu, H. S. (2018). Review of polyhydroxyalkanoates materials and other biopolymers for medical applications. Mini-Reviews in Organic Chemistry, 15(2), 105-121.

[27] Xu, Y., Kim, C. S., Saylor, D. M., & Koo, D. (2017). Polymer degradation and drug delivery in PLGA-based drug–polymer applications: A review of experiments and theories. Journal of Biomedical Materials Research Part B: Applied Biomaterials, 105(6), 1692-1716. [28] Z. Zhang, R. Kuijer, S. K. Bulstra, D. W. Grijpma, and J. Feijen, “The in vivo and in vitro degradation behavior of poly(trimethylene carbonate),” *Biomaterials*, vol. 27, no. 9, pp. 1741–1748, 2006.

[29] M. Zilberman and R. C. Eberhart, “Drug-Eluting Bioresorbable Stents for Various Applications,” *Annu. Rev. Biomed. Eng.*, vol. 8, no. 1, pp. 153–180, 2006.

[30] Ginjupalli, K., Shavi, G. V., Averineni, R. K., Bhat, M., Udupa, N., & Upadhya, P. N. (2017). Poly (α-hydroxy acid) based polymers: A review on material and degradation aspects. Polymer Degradation and Stability, 144, 520-535.

[31] S. Yang, K.-F. Leong, Z. Du, and C.-K. Chua, “The Design of Scaffolds for Use in Tissue Engineering. Part I. Traditional Factors,” *Tissue Eng.*, vol. 7, no. 6, pp. 679–689, 2001.

[32] H. Yasuda *et al.*, “Comparison of Sm complexes with Sn compounds for syntheses of copolymers composed of lactide and ε-caprolactone and their biodegradabilities,” *React. Funct. Polym.*, vol. 61, no. 2, pp. 277–292, 2004.

[33] C. K. S. Pillai and C. P. Sharma, “Review paper: Absorbable polymeric surgical sutures: Chemistry, production, properties, biodegradability, and performance,” *J. Biomater. Appl.*, vol. 25, no. 4, pp. 291–366, 2010.

[34] M. C. Serrano, E. J. Chung, and G. A. Ameer, “Advances and applications of biodegradable elastomers in regenerative medicine,” *Adv. Funct. Mater.*, vol. 20, no. 2, pp. 192–208, 2010.

[35] M. A. Woodruff and D. W. Hutmacher, “The return of a forgotten polymer - Polycaprolactone in the 21st century,” *Prog. Polym. Sci.*, vol. 35, no. 10, pp. 1217–1256, 2010.

[36] L. S. Nair and C. T. Laurencin, “Biodegradable polymers as biomaterials,” *Prog. Polym. Sci.*, vol. 32, no. 8–9, pp. 762–798, 2007.

[37] R. Virmani, “Drug eluting stents: are human and animal studies comparable?,” *Heart*, vol. 89, no. 2, pp. 133–138, 2003.

[38] R. S. Schwartz *et al.*, “Drug-eluting stents in preclinical studies recommended evaluation from a consensus group,” *Circulation*, vol. 106, no. 14, pp. 1867–1873, 2002.

[39] R. S. Schwartz, N. A. Chronos, and R. Virmani, “Preclinical restenosis models and drug-eluting stents: Still important, still much to learn,” *J. Am. Coll. Cardiol.*, vol. 44, no. 7, pp. 1373–1385, 2004.

[40] T. Suzuki *et al.*, “Stent-based delivery of sirolimus reduces neointimal formation in a porcine coronary model,” *Circulation*, vol. 104, no. 10, pp. 1188–1193, 2001.

[41] Y. Shi *et al.*, “In vitro and in vivo degradation of rapamycin-eluting Mg-Nd-Zn-Zr alloy stents in porcine coronary arteries,” *Mater. Sci. Eng. C*, vol. 80, pp. 1–6, 2017.

[42] A. E. Villa, L. A. Guzman, W. Chen, G. Golomb, R. J. Levy, and E. J. Topol, “Local delivery of dexamethasone for prevention of neointimal proliferation in a rat model of balloon angioplasty,” *J. Clin. Invest.*, vol. 93, no. 3, pp. 1243–1249, 1994.

[43] D. M. Whelan, “Biocompatibility of phosphorylcholine coated stents in normal porcine coronary arteries,” *Heart*, vol. 83, no. 3, pp. 338–345, 2000.

[44] P. Azam, A. Sankaranarayanan, D. Homerick, S. Griffey, and H. Wulff, “Targeting effector memory T cells with the small molecule Kv1.3 blocker PAP-1 suppresses allergic contact dermatitis,” *J. Invest. Dermatol.*, vol. 127, no. 6, pp. 1419–1429, 2007.

[45] L. E. Pereira, F. Villinger, H. Wulff, A. Sankaranarayanan, G. Raman, and A. A. Ansari, “Pharmacokinetics, Toxicity, and Functional Studies of the Selective Kv1.3 Channel Blocker 5-(4-Phenoxybutoxy)Psoralen in Rhesus Macaques,” *Exp. Biol. Med.*, vol. 232, no. 10, pp. 1338–1354, 2007.

[46] A. Manuscript and T. Structures, “NIH Public Access,” vol. 6, no. 3, pp. 247–253, 2009.

[47] A. Schmitz and A. Sankaranarayanan, “Design of PAP-1, a selective small molecule Kv1. 3 blocker, for the suppression of effector memory T cells in autoimmune diseases,” *Mol. Pharmacol.*, vol. 68, no. 5, pp. 1254–1270, 2005.

[48] C. C. Liang, A. Y. Park, and J. L. Guan, “In vitro scratch assay: A convenient and inexpensive method for analysis of cell migration in vitro,” *Nat. Protoc.*, vol. 2, no. 2, pp. 329–333, 2007.

[49] Y. Chen, “Scratch Wound Healing Assay,” vol. 2, no. 5, pp. 1–3, 2012.

[50] J. M. Walker, *Cell Migration: Developmental Methods and Protocols.*, 2nd ed. Humana Press.

[51] D. Y. Kwon *et al.*, “Biodegradable stent,” *J. Biomed. Sci. Eng.*, vol. 5, no. April, pp. 208–216, 2012.

Chapter IV.

Drug liberation based on plasma-enhanced adhesion of biodegradable nanoparticles

Originally published as:

Ponce, A., Ramos-Pérez, V., & Borrós, S. (2019). Controlled Release on Cardiovascular Stents Using Plasma-Enhanced Adhesion of Biodegradable Nanoparticles. Med One, 4(4).

This page intentionally left blank

4.1 Introduction

Throughout the previous chapters, CAD treatment has been approached through DES tailoring. The main reason for this was DES being the most common solutions for CAD treatment, with overall good results [1]–[6]. Another issue addressed was that although there are a variety of DES present in the market, none presents an optimal model which solves all the derived consequences of stent implantation. Due to the lack of a unique solution, a variety of different methods based on drug delivery systems and gene therapy systems have been tested out. Results from these drug eluting stents have been obtained by elution analysis of pharmacological release and in vitro or in vivo testing [7]–[14].

A second approach, gene therapy, is a technique that uses nucleic acids to treat or prevent diseases by acting on the genetic roots of the illness [15][16]. The goal of gene therapy is to modify a gene, or genetic pathway, to prevent or treat a disease. Although gene therapy can be applied with DES treatment, it would render better results if eluted with a carrier that ensured a controlled delivery. There have been different techniques developed to treat inflammatory responses through gene modification, but these efforts have not been directed to achieve restenosis reduction through controlled release with DES. One of the most promising carriers used which enables safe and efficient delivery systems are nanoparticles [9][17]–[20].

When applying nanoparticles locally, they can penetrate the vessel wall and form a depot which will allow a sustained release of drugs into the arterial wall. This method allows a focused treatment which targets affected cells [21]. Nanocarriers can be tailored to have specific sizes, shapes, densities or functionalities. Customization makes nanoparticles ideal as drug delivery vehicles when used to encapsulate desired drugs or gene vectors. It is of vital importance to ensure the non-toxicity of the nanoparticles used for drug delivery, as they are going to be used to penetrate the targeted cells [22]. As mentioned before, nanoparticles can be excellent carriers and can prove useful when developing a therapeutic strategy for DES. Achieving a controlled release of encapsulated contents is possible as long as adhesion of nanoparticles to a stent surface is guaranteed. A good range of biodegradable and biocompatible materials have been tried out to fulfil this task, showing there is no unique solution to this question. Up to date, DES have been made of different polymers, but some of the most used ones are poly(lactic acid) and poly(lactic-co-glycolic acid) [23]–[28].

In this study, a promising approach has been implemented to fulfil therapeutic delivery of DES through the adhesion of poly(β-amino ester) (pBAE) nanoparticles to the stent strut. If this system brings positive results, on one hand, it will be useful to deliver antiproliferative drugs. On the other hand, it will also be useful to ensure controlled and localized release of a large number of microRNA (miRNA). These endogenous, noncoding, single-stranded RNAs have been demonstrated to reduce proliferation of smooth muscle cells, which is a key factor for stent treatment. miRNAs are novel regulatory RNAs for neointimal lesion formation, making them a useful tool for the treatment of proliferative vascular diseases such as atherosclerosis, postangioplasty restenosis, transplantation arteriopathy, and stroke [29]. Our approach can also enhance the therapeutic treatment, as it provides a regulated release of small interfering RNA (siRNA), which have an important role on regulating the inflammatory process [30]. This tailored release is able to span over an initial burst, producing a better controlled pharmacological liberation.

pBAEs used in this study have previously shown high transfection efficiencies, biodegradability and biocompatibility. Furthermore, nanoparticles made from these polymers can be tailored in a cell-specific manner by changing their composition [31]. Recently, pBAEs have been used in different therapeutic applications and proven successful. Multiple applications have been described in stem cell modification or osteodifferentation, showing great promise to deliver interfering RNA (RNAi) in a safe way [32][33]. Since different backbone structures can be easily designed for pBAEs, there is a great variety of polymers to choose from [34][35].

In previous studies, results show that polymer structure has a direct influence on RNAi binding and delivery efficiency, concluding that the polymer structures C6 and C32 outperformed most of the rest [36]. These polymers show a high flexibility and can be easily tuned to fulfil specific purposes [33][37]–[39]. Due to this flexibility, different strategies have been tried out in order to produce nanoparticles with pBAEs. Positive results have been achieved, demonstrating that they can act as functional nanocarriers with a low toxicity [40].

Research in this area has led to an approach which focuses on creating pBAE based nanoparticles for drug delivery/gene therapy systems designed to prevent in-stent restenosis. Controlled delivery mechanisms using pBAEs are achieved in this study through the chemical bonding of nanoparticles to an initial polymer layer adhered to the stent strut. This first layer is composed of a tailored pentafluorophenyl methacrylate (PFM) coating which enables the chemical adhesion of nanoparticles, avoiding the instantaneous total release of the carriers when in contact with the medium. Nanoparticles will bond to the PFM layer; therefore, it is of great importance to produce a coating which maintains the highest number of aromatic groups as possible to enhance adhesion. While polymerization is carried out on a stent strut, the luminal part remains protected to ensure the polymer will only be deposited on the abluminal side. Chemical adhesion of the nanoparticles and their usefulness in gene therapy are also tested.

As discussed, although there have been several advancements in the understanding and treatment of atherosclerosis, there is still much more to be done. Our proposal hopes to open a pathway for pharmacological and/or gene delivery systems based on the plasma-enhanced adhesion of pBAE nanoparticles on PFM layers for stent implantation. Once a PFM layer is adhered to the substrate, pBAE nanoparticles will bond to the polymer due to its chemical nature. In this case, the carbonyl group from the esters of the PFM chains react with the amine group from the nanoparticles through a nucleophilic substitution reaction with pentafluorophenol acting as the leaving group [41]. This process is illustrated on Figure 1.

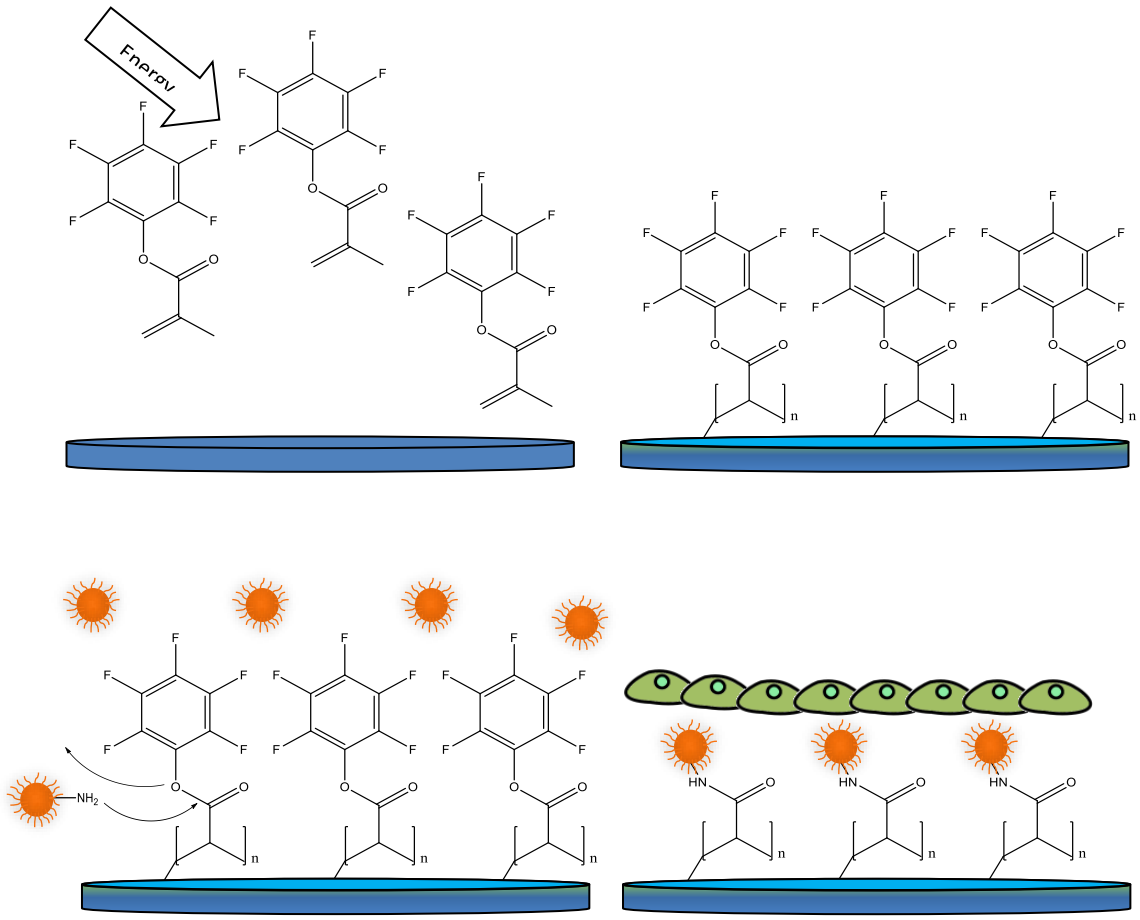

Figure 1. Schematic representation of the coating process with pentafluorophenyl methacrylate (PFM) and nanoparticles on a stent strut. Image at the top left shows PFM monomer being activated in a plasma reactor. Top right image shows PFM bonded to the sample surface after the activation process. Bottom left image shows how nanoparticles bond to the PFM and image at the bottom right shows how, after being treated with bovine serum albumin (BSA), the samples are seeded with cells.

We believe that through the bonding of carriers to a polymeric layer attached to a stent, a controlled and localized treatment can be achieved. This method will ensure the persistence of loaded nanoparticles on the stent, avoiding the carriers to be completely removed through the blood stream at first contact. When a stent is expanded at the affected area, nanoparticles will stay on the polymer matrix and mostly penetrate the target adjacent cells on to which they are pressed. This approach can render a higher nanocarrier efficiency due solely to the tailored release method. This leads to the main objective of this chapter, described previously in chapter I:

- Develop a strategy to coat stents with nanocarriers which can show a good adhesion and avoid the washing away of the nanoparticles when deployed.

4.2 Materials and methods

Materials

Tween-20 detergent and Bovine Serum Albumin (BSA) were obtained from Sigma-Aldrich (St. Louis, United States). Pentafluoro phenyl methacrylate (PFM) was obtained from Manchester Organics Ltd. (London, England). Dulbecco's Modified Eagle Medium was provided by Lonza (Basel, Switzerland) and fetal bovine serum by Cultek (Madrid, Spain). Glutamine and penicillin/streptomycin were obtained from Labclinics (Barcelona, Spain). Petri dishes and well plates were provided by SPL Life Sciences (Naechon-myeon, South Korea) while eppendorfs by Thermofisher (Waltham, United States). Trypsine was obtained from Gibco Life Technologies (New York, United States). Chromium Cobalt Alloy CrCo stent struts and electropolished CrCo discs (20 × 1 mm) were made from alloy L605 and provided by IberHospiTex (Barcelona, Spain). Glass wafers were provided by Labbox (Barcelona, Spain). Medical silicon used to develop the silicon wafers was obtained from Nusil Technologie Europe (Mougins, France) and COS-7 cells (CRL-1651TM) were provided by ATCC (Manassas, United States).

Oligopeptide-ended pBAE were synthetized in-house through a method previously described by our research group [31][42]. Briefly, poly(β-amino ester)s were synthesized following a two-step procedure. First, an acrylate-terminated polymer was synthesized by addition reaction of primary amines with diacrylates (at 1:1.2 molar ratio of amine:diacrylate). Then, pBAEs were obtained by end-capping modification of the resulting acrylate-terminated polymer with different kind of amine- and thiol- bearing moieties. In general, oligopeptide-modified pBAEs were obtained by end-modification of acrylate-terminated polymer C32 with thiol-terminated oligopeptide at 1:2.1 molar ratio in dimethyl sulfoxide. The mixture was stirred overnight at room temperature and the resulting polymer was obtained by precipitation in a mixture of diethyl ether and acetone (1:1).

For this paper, tri-arginine end-modified pBAE polymer, C32-CR3 was chosen to be used as the polymer for nanoparticle formation: A solution of C32 (0.15 g, 0.075 mmol) dissolved in dimethyl sulfoxide (2 mL) and a solution of Cys-Arg-Arg-Arg-CONH2·4HCl (CR3, 0.11 g, 0.15 mmol) in dimethyl sulfoxide (1 mL) were mixed and stirred overnight at room temperature. End-modified polymer CR3-C32-CR3 was obtained by precipitation in a mixture of diethyl ether:acetone (1:1).

Nanoparticle Synthesis

pBAE nanoparticles loaded with green fluorescent plasmid (GFP) were synthetized using the method we have previously described [40][42][43]. Briefly, pBAE stock solutions in dimethyl sulfoxide (100 mg/mL) were diluted with acetate buffer (25 mM acetate buffer pH 5.0) at appropriate concentrations to obtain the desired Polymer–DNA ratios (w/w). An appropriately diluted pBAE (100 µL) was added to a solution of green fluorescent protein vector (pGFP) (100 µL at 60 µg/mL in acetate buffer 25 mM pH 5.0), mixed with vortex vigorously for a few seconds and incubated at 37 °C for 30 min. These nanoparticles were finally diluted in ultrapure water to achieve the desired working volume containing 1 µg/well of pGFP.

Morphology

Scanning electron microscopy (SEM, Jeol JSM-5310, Tokio, Japan) equipped with a microanalysis Oxford Instrument Link-Isis software (Abingdon, England) for data analysis, a profilometer (Veeco Instruments, DEKTAK 6M, New York, United States), an atomic force microscopy (AFM, Park Systems XE 100 Series, Suwon, South Korea) and an infrared (IR) spectrophotometer (Thermo Scientific, iS10, Waltham, United States) with a complementary Attenuated Total Reflection (ATR) accessory (Thermo Scientific, Smart ATR, Waltham, United States) were employed to characterize shape, thickness, rugosity and quality of the surfaces produced. To obtain SEM images, samples required a gold coating which was obtained with a mini sputter Coater (Quorum, SC7620, Lewes, UK). AFM was used with a non-contact mode. Samples were placed over a sample carrier disc and fixed with double-sided adhesive tape at room temperature in a vibration-free environment.

In Vitro Transfection Assay

COS-7 cells were cultured in Dulbecco's modified Eagle medium (DMEM) with 10% fetal bovine serum (FBS), 1% penicillin/streptomycin and 1% glutamine. These cells were grown in Petri dishes up to 90% confluence in their culture medium at 37 °C under 5% CO2. The cells were harvested by trypsination, collected by centrifugation (5 min at 130× g), resuspended and counted in a Neubauer chamber (Thermofisher, Waltham, United States).

After completing the synthesis of nanoparticles, which encapsulate pGFP, the glass samples with PFM were taken out of the reactor and placed in a 24 well plate. All samples were covered with a nanocarrier solution and left for two hours to ensure the chemical binding. Later, all wells were aspirated and either washed with BSA, or left unwashed. BSA was left for one hour on the selected wells before being aspirated. Cells were seeded at a density of 50,000 cells per well in 24 well plates for the glass disc samples. CrCo disc samples required seeding 100,000 cells per well in 12 well plates. Cells were left incubating in supplemented medium for 24 hours (h) before checking transfection for the first time, and later checked again at 48 h.

When reproducing this process with metallic stents, small variations had to be done. In this case, 6 well plates were seeded with 150,000 cells per well in 3 mL of supplemented medium each and left incubating for 2 days. Once accomplished, stents were coated with PFM and left for 2 h in a 1.5 mL eppendorf with the nanoparticle solution. Later, all eppendorfs were aspirated, washed with BSA and left for 1 h in this solution. After completing this process, stents were ready for in vitro testing. Following, stents were added to the wells to start the transfection assay. Images were taken 24 and 48 h after.

Plasma Polymerization Reactor

A plasma deposition apparatus which consists of a stainless-steel discharge vessel (diameter: 26 cm, length: 24 cm) parallel plate reactor was used throughout the whole experimentation. In this model the ground electrode is the reactor chamber itself, and the radiofrequency (RF) electrode is a stainless-steel plate. All the samples were treated on the central part of this plate. The RF electrode was connected to a RF pulse generator (13.56 MHz) via a matching network. The O2 used to clean the reactor was added through a flux controller while the monomer was supplied via a standard manifold which was able to adjust gas flux using needle valves.

System pressure was determined by a Pirani type vacuum meter, located between the reactor and a cold trap which was fed with dry ice. The two-stage mechanical pump (RV12 903, Edwards, GB, Bolton, England) is located after the cold trap, and evacuates the vessel to a reactor chamber at pressure of 0.1 mbar. All polymerizations were performed on silicon wafers, glass wafers, CrCo discs and CrCo stent struts. These samples were treated under pulsed plasma with a pulsed RF power ranging from 12 to 52 W, duty cycles (DC) of 10/20, 2/12, 2/22 and 2/52 with deposition times from 5 to 65 min. Before starting the polymerization, the monomer (PFM) and the entry lines were preheated with heating jackets up to 75 °C. After preheating, monomer (PFM) flow was stabilized and fixed to achieve an internal reactor pressure of 0.35 mbar. A diagram of the reactor used can be seen in Figure 2.

4.3 Results and Discussion

4.3.1 PFM coatings through plasma polymerization

Due to the unique geometry of this reactor and the variety of surfaces which were coated (glass, CrCo disks and stents), plasma polymerization conditions had to be optimized. Finding the ideal parameters for this reactor was crucial in order to ensure the maximum number of functional groups on the PFM coatings. This allowed an increase in the number of nanoparticles attached to the surface, thus accomplishing the highest therapeutic activity possible. To ensure the maximization of functional groups on PFM layers for each sample, different parameters were tested to optimize the process in our reactor, as shown in Table 1.

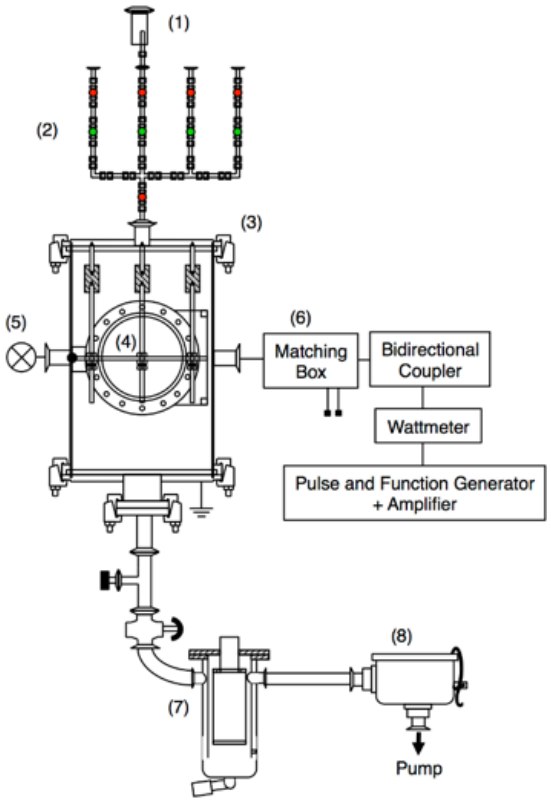

Figure 2. Schematic diagram of stainless steel vertical plasma reactor and its electrical components:
(1) monomer feed, (2) gases feed, (3) cylindrical chamber, (4) holder sample, (5) pirani gauge, (6) matching box and electrical system, (7) cold trap, and (8) chemical trap.

Table 1. Three different plasma processes are defined with a ton = 2 ms for the exception of the first one (ton = 10 ms). As this first process is the one commonly used in our laboratory it was used as a reference to compare results. In this experiment tprocess refers to the time it takes to complete a polymerization, starting when plasma is generated inside the reactor and finishing when the reactor is turned off. As expected in plasma polymerization, $C = \frac{t_{on}}{t_{on} + t_{off}}$*, ton shows the time the plasma pulse is active and toff indicates the time the plasma pulse is shut down. Ppeak is the input power given to the system and Peq is the equivalent power applied taking in account the time that the plasma pulse is active.*

DC	$t_{process}/min$	P_{eq}/W	P_{peak}/W
10/20	5	7.5	15
2/12	15	1.9	12
2/22	30	1.9	20
2/52	65	1.9	52

Samples obtained must be reproducible and show a good stability of the PFM deposited on their surface. Time of reaction is also taken into account, but as a secondary objective which should be minimized. After the polymerization, each sample was stored in argon atmosphere and an infrared (IR) spectrum (Thermo Scientific, iS10, Waltham, United States) was obtained in less than 24 h. Spectrums studied were used to obtain a ratio between the signal from the ester and the aromatic group. This ratio indicates the stability of the PFM, showing a lower value in the samples which maintain their aromatic group. Degradation of PFM results in a reduction of aromatic group signaling, causing the ratio (Carbonyl group/aromatic group) to increase its value. Figure 3 shows the results obtained after applying the procedure to glass and CrCo disks.

On the two graphs, the same tendencies can be observed for both substrates. Plotted results were separated in three different groups labelled as A, B and C. Group A shows the highest ratio and therefore, the poorest quality PFM obtained. Although the reaction time is very short, quality of the PFM coating remains a primary target. Groups B and C obtained a very low ratio (Carbonyl group/aromatic group), although group C presented a longer reaction time. Group B shows low ratios with low and intermediate reaction times, presenting the best results out of the three groups. Among the two DC tested in group B, 2/12 is chosen as the most suitable due to its low ratio and short time of reaction.

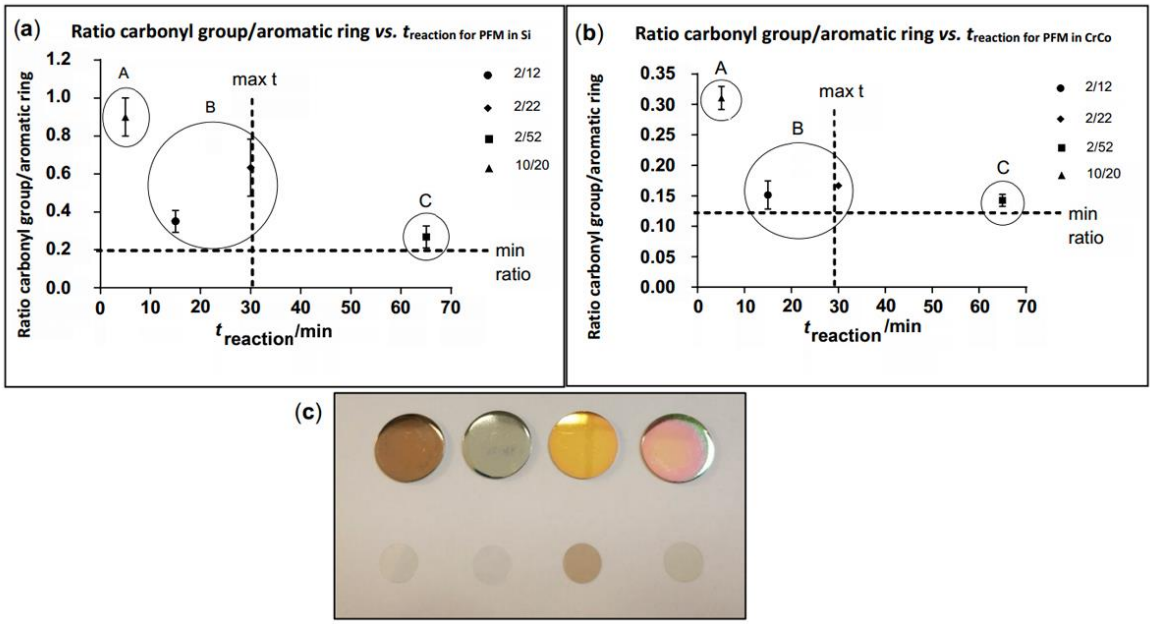

Figure 3. Ratio carbonyl/Aromatic group vs treaction and images of Si samples. Graph labelled (a) located at the top left, shows ratio carbonyl/Aromatic group vs treaction for Si samples. At the top right, graph (b) shows ratio carbonyl/Aromatic group vs treaction for CrCo samples. These graphs show the results obtained through an optimization process elaborated to acquire an optimum coating process. A low carbonyl/Aromatic group ratio is desirable as it results in a good quality PFM coating, considering a low reaction time as a secondary target. At the bottom of the figure, image labeled (c) shows samples with PFM obtained after polymerization. First row of samples displays coated CrCo discs, while second row displays coated glass discs. Starting from left to right, the following DCs have been used: 10/20, 2/12, 2/22 and 2/52. Among all DC and reaction times tested, 2/12 is selected as optimum due to the quality of the coatings produced and the low reaction time achieved.

4.3.2 Characterization of optimized PFM surfaces on CrCo surfaces

Once a DC of 2/12 is chosen as the most appropriate, the polymerized PFM surfaces obtained on CrCo discs was characterized through SEM imaging, profilometry and AFM. Film growth rate and thickness were obtained by coating different CrCo discs at different time intervals. Profilometry was used to determine the step on these different samples. A film growth rate of 3.4 nm/min and a final thickness of 79.8 ± 4.6 nm were obtained after a 15 min reaction. In order to obtain some more information about the morphology of this PFM coating, an AFM was needed. Not only the final thickness was relevant, but also its rugosity. This is an important factor to take in account, as an irregular surface may influence negatively in the inflammatory process [44]–[46]. Being so, maintaining this parameter to a minimum should be sought.

An AFM analysis was performed on the samples rendering flat, homogeneous surfaces which show the characteristic structures of PFM coatings. Roughness average (Ra) obtained is 0.550 nm, root mean square roughness (Rq) is 0.644 nm and maximum roughness (Rmax) is 2.093 nm, as shown in Figure 4. While Ra is the most common parameter used, Rq presents useful complementary information. Rq amplifies occasional high or low readings, while Ra simply averages them. Rmax shows the length of the highest peak obtained. Mean roughness depth (Rz) is the arithmetic mean value of the single roughness depths of consecutive sampling lengths. Elaboration of this surface morphology was achieved as a result of the experimentation with reactor geometry and the use of pulsed plasma conditions. This plasma methodology allows a controlled nucleation and film growth with a slow deposition rate, enabling the formation of films with such a low roughness.

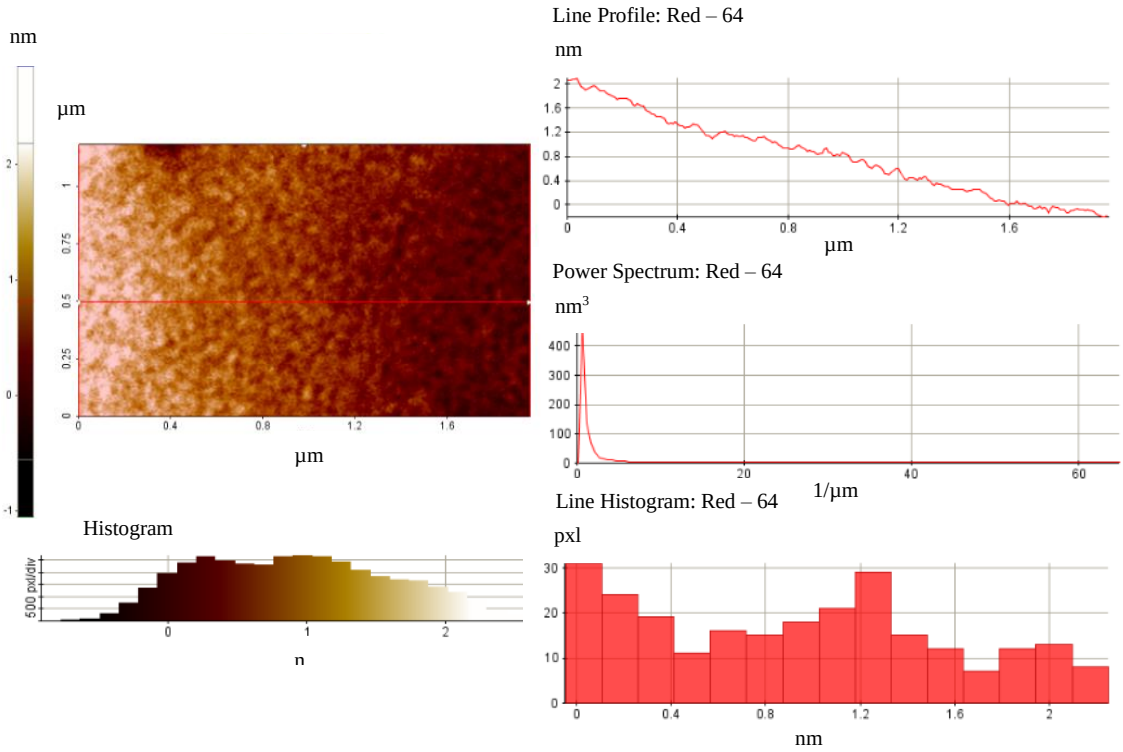

Line	Min(nm)	Max(nm)	Mid(nm)	Mean(nm)	Rpv(nm)	Rq(nm)	Ra(nm)	Rz(nm)	Rsk	Rku
Red	-0.202	2.093	0.945	0.782	2.296	0.644	0.550	2.023	-0.215	1.974

Figure 4. Data collected from AFM analysis on CrCo surfaces. Characteristic worm-like structure from PFM are shown at the top left image. Additional analysis data is presented through Histogram (bottom left), Line profile (top right), power spectrum (middle right) and line histogram (bottom right) graphs. Attached to the bottom part of the figure, a chart summarizes the roughness data obtained. Ra and Rz show values much lower than 1 µm. This reduced roughness values are of vital importance when producing an implantable surface which must reduce inflammatory response [44]–[46].

As shown in Figure 4, surfaces obtained show reduced values for average roughness. These results are desirable when producing a stent surface in order to avoid inflammatory response. AFM characterization of the PFM layers showed roughness results much lower than 1 µm (Ra = 0.550 nm, Rq = 0.644 nm and Rz = 2.023 nm), producing optimum quality and smooth coatings. Once the surfaces obtained had been analyzed, the optimized process was ready to be used throughout the experimentation.

As a next step, a method to attach nanoparticles on to the plasma polymerized surfaces was necessary. This will be addressed in the next section.

4.3.3 Study of nanoparticle bonding on PFM coatings

This section describes several experiments carried out in order to test nanoparticle bonding to PFM surfaces with no associated toxicity. Initial experiments were carried out on glass discs to ensure cells could grow easily on a well-known substrate. Glass waffles were coated with PFM, later taken out of the reactor, and placed in a 24 well plate. All samples were prepared as described previously in the "In Vitro Transfection Assay" section. Nanoparticles were deposited over the PFM layers and incubated for 24 and 48 h, aiming to check for cell morphology and transfection.

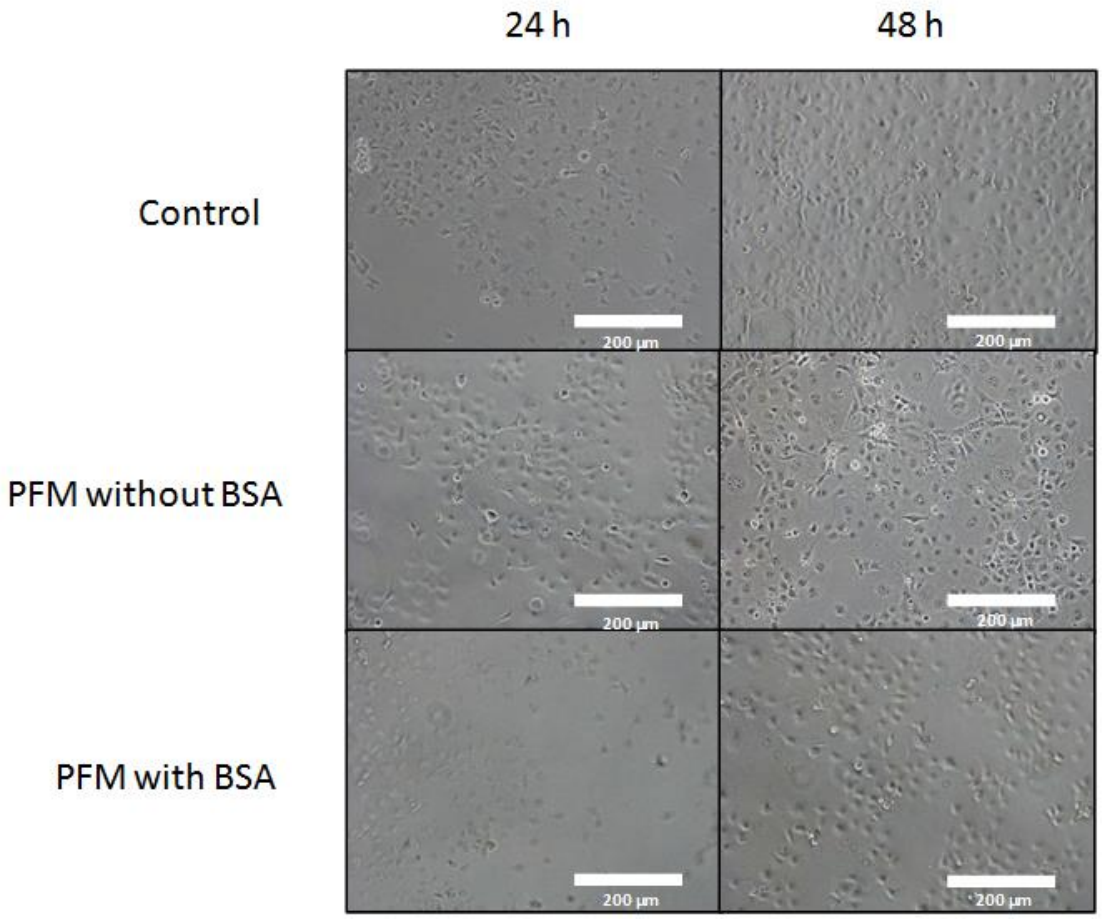

Figure 5. Bright field of various images obtained from COS-7 cells growing with PFM and with/without BSA treatment. All the pictures were taken under 10× magnification. The white bar indicates 200 µm. Sites chosen for each experiment may show slight variations on initial cell count, resulting on visual diffences in cell concentrations at 48 h. No change was appreciated in cell growth when the whole sample was inspected. Normal growth rates and typical morphologies for this cell line were observed after 24 and 48 h for controls and PFM with BSA samples. Slight shrinkage and blebbing of cells were observed in PFM without BSA samples.

First, toxicity of the PFM layer was tested in vitro using COS-7 cells (Figure 5). In this figure, images displayed in the first row have been obtained from the control group after 24 and 48 h. Cells have grown without any possible detrimental factor, showing an expected growth rate with a characteristic healthy morphology for this cell line. On the other hand, the second row shows cells growing directly on the PFM layer with signs of stressed morphologies (including shrinkage, blebbing of cells and initiation of apoptosis).

In a previous article from our group, PFM has proven to become cytotoxic six hours after its polymerization due to the elution of pentafluoro phenol [41]. Its release must be avoided, as this is a serious concern for an implantable device. For that reason, images shown in the third row of Figure 5 aim to solve this issue. This last row shows samples which have been treated to ensure there is no liberation of pentafluoro phenol from the PFM layer. Absence of pentafluoro phenol elution was achieved through the treatment of PFM layers with BSA for one hour, followed by a gentle rinse. Once this process was completed, the PFM surface was prepared to be exposed to the cells. Normal growth rates and typical morphologies for this cell line are observed after 24 and 48 h. Results obtained conclude that this treatment allows the elimination of pentafluoro phenyl groups, found in excess on the PFM surface, avoiding cytotoxicity. This procedure renders a suitable coating for cells to grow on.

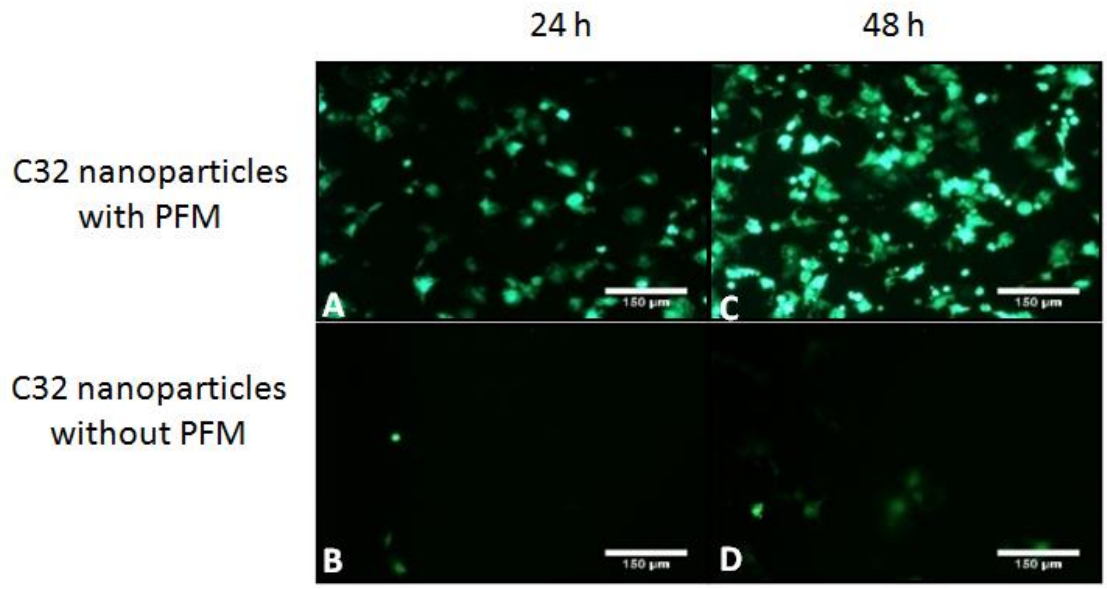

Figure 6. Dark field images of C32 NPs with and without PFM on COS-7 cells. Images in the left column are taken 24 h after cell seeding. At the right column, images are taken another 24 h later at the same area. Total time elapsed since cell seeding for images shown at the second column is 48 h. First row shows images from transfected cells deposited over a glass disc coated with PFM and C32 nanoparticles. Samples shown on this first row are coated with PFM and nanoparticles followed by a BSA treatment and a final rinse. Once this treatment is finished, cells are seeded over the samples. Second row shows transfection of cells seeded on glass discs which had C32 nanoparticles deposited on top for an hour and then rinsed with BSA. Controls of C32 nanoparticles with no plasmid, with and without PFM have also been performed showing black images due to absence of transfection. Results obtained show how nanoparticles which are not bonded to PFM are easilly washed away. First row shows how, after bonding, nanoparticles stay attached to the PFM coating and are able to transfect cells 24 and 48 h after. All the pictures were taken under 10× magnification. The white bar indicates 150 µm.

Once the samples were coated with PFM, glass discs were treated with C32 nanoparticles which encapsulated pGFP. Nanoparticle bonding was followed by a post treatment with BSA and a final BSA rinse. As depicted in Figure 6, samples treated with PFM, nanoparticles and BSA were able to transfect even after undergoing a previous rinse. This is due to the bonding process achieved, which enabled the adhesion of the nanocarriers to the surface for future release of the encapsulated pGFP. On the second row (no PFM coating applied), practically all the nanoparticles had been removed after the washing process and very low transfection was identified after 24 and 48 h since cell seeding. This clearly shows that without PFM, nanoparticles don't adhere to the surface and are practically completely washed away. These experiments were repeated on CrCo discs, rendering the same results. Results obtained with disc samples led to the repetition of experimentation with cardiovascular stents.

4.3.4 Elaboration of PFM coated stents with bonded nanoparticles

To reproduce a common stent model which could allow a selective coating, stents were masked to protect their lumen. Figure 7 presents an image of the device designed to place the stents in the reactor, while the interior area remains masked.

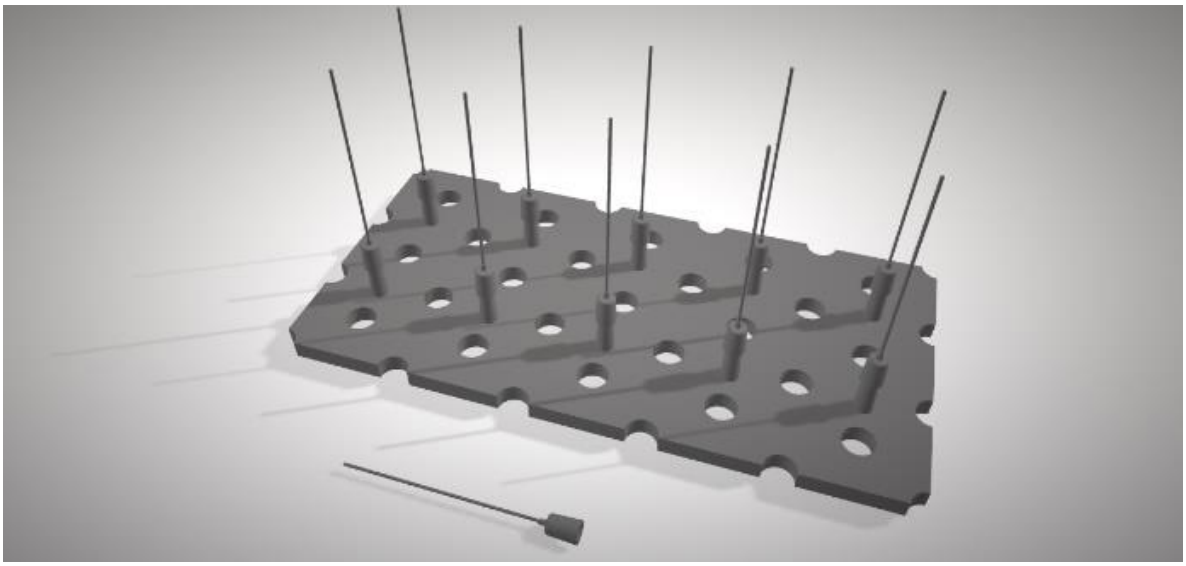

Figure 7. Image of the structure used to mount the needles which hold the stents in position inside the reactor. A small polytetrafluoroethylene plate (100 × 150 × 3 mm) was machined to obtain 10 small conic adapters which were used to place the needles. Holes were drilled into the base to match the ones in the reactor and, that way, avoid interfering with the monomer flow. Metallic needles were wrapped with polytetrafluoroethylene tape so stents could later be fitted tightly to protect their lumen.

CrCo stents were treated with PFM and then incubated with C32 nanoparticles and BSA (as described above). Part of these stents were analysed by SEM. PFM treated stents which did not undergo an immersion process with nanoparticles were used as controls. SEM pictures of both, CrCo discs and stents, are presented in Figure 8.

When CrCo disks samples were prepared, their surface was partially masked with a silicon wafer. As shown in Figure 8, when removing the wafer, a clear interface could be observed through SEM imaging. Both sides of each interface were studied through EDX analysis. Presence of polymeric coating was confirmed through the obtention of a clear carbon signal. This result was not obtained in areas which had been masked, as no carbon signal can appear over a clean CrCo surface. As shown by the SEM images, stent coatings displayed surface uniformity and smoothness throughout all the analysed samples. These results are coherent with the low average roughness of the samples obtained previously.

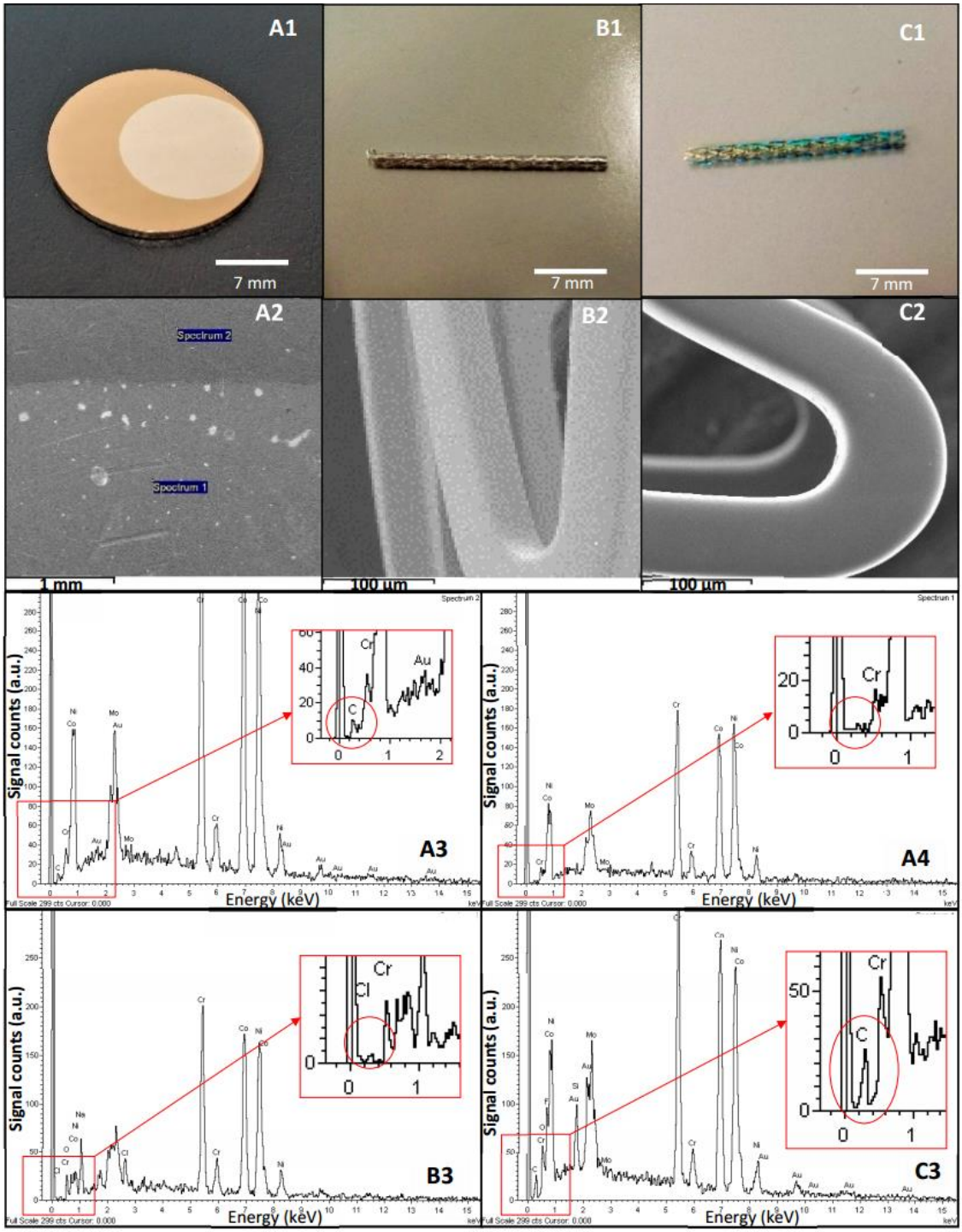

Figure 8. Analysis of CrCo surfaces coated with PFM. Images labelled as A (A1–A4) correspond to result obtained from a CrCo disc. Label B (B1–B3) corresponds to results obtained from a clean stent while label C (C1–C3) represents results acquired from a stent coated with PFM. Images A1, B1 and C1 have been taken under 1.75× magnification. Top left image shows CrCo disc with a PFM interface (A1). Image A2 is obtained by SEM, where a clear interface was seen. Two sites were selected for EDX analysis (spectrum 1 and spectrum 2). A3 and A4 images are the EDX spectra obtained from each site. Top right corner of A3 and A4 show their corresponding label which relates them to image A2, where analysis areas are tagged. Image B1 was obtained from a clean stent. Image B2 was obtained by SEM and image B3 is an EDX spectrum of this clean stent. C1 was taken from a stent coated with PFM. Image C2 shows an image obtained by SEM from this coated stent and image C3 shows its respective EDX analysis. Scale is shown at the bottom of each image (A1, A2, B1, B2, C1, and C2). Results show how the polymerization procedure rendered PFM coatings on CrCo discs and stents, which have been masked to protect specific areas.

4.3.5 In vitro transfection study of PFM coated stents with bonded nanoparticles

Following experiments required seeding COS-7 cells in 6 well plates which were left to incubate for 2 days. Once completed, cell medium was changed and stents with PFM and nanoparticles were placed on each well. This plate was left incubating for 24 h and images were taken in both light field and fluorescence mode.

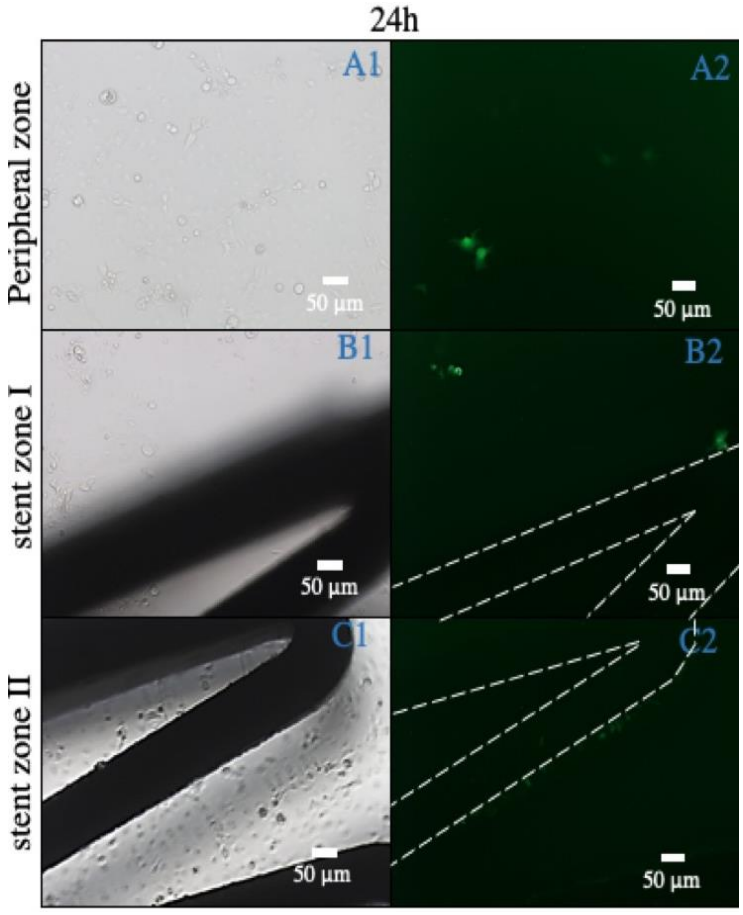

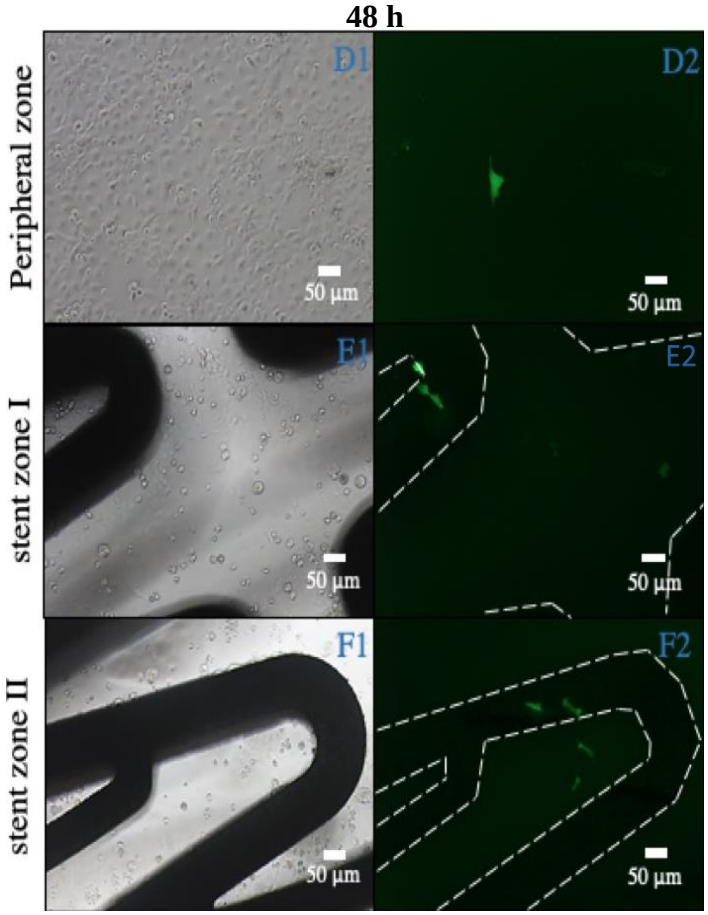

Figure 9. Transfection of COS-7 cells with NP coated stents. This figure is separated into two different blocks, showing results after 24 and 48 h since cell seeding. At the first block and starting from left to right, the first column shows three different light field sites. These three images (A1, B1 and C1) were obtained after leaving COS-7 cells in contact with stents, which had been coated with PFM and C32 nanoparticles, for 24 h. The second column (A2, B2 and C2) shows respective darkfield images of the first column (A1, B1 and C1). A third column shows three different light field sites. These images (D1, E1, and F1) were obtained after leaving COS-7 cells in contact with stents, which had been coated with PFM and C32 nanoparticles, for 48 h. Next, a fourth column (D2, E2 and F2) shows the respective darkfield images of the third column (D1, E1 and F1). Pictures where the stent strut is not seen have been taken from the surrounding area up to 5 mm apart from the stent (first row at each block). Images shown in the second and third row of each block have been taken from areas where the stent structure is visible. Negative controls with stents containing nanoparticles without plasmid were not visible due to absence of transfection. Green signal shows pGFP transfection.

Microscope observation was repeated 48 h after and results obtained are shown in Figure 9. 24 h after cell seeding, some transfected cells had started growing over the stent strut as well as other cells which were not in direct contact with the stent surface. These transfected cells were identified visually due to their fluorescence. Transfection in surrounding areas is explained through a small nanoparticle release from the stents surface.

As mentioned previously, nanoparticles were covalently bonded with the PFM chains during the preparation of the samples. During this process, even after bonding, nanoparticle aggregation may occur. Although rinsing the finished stents should eliminate most of the unreacted nanoparticles, their polymeric chains may entangle and adhere to others. When introducing one of these stents in a different medium, the liberation of aggregated nanoparticles which did not bond to PFM can transfect some adjacent cells (approximately a 10%). This initial release was then followed by transfection of adhered nanoparticles on the stent surface. More transfection was seen 48 h after cell seeding, and new cells start to grow over the stents.

4.4 Concluding Remarks

PFM has been polymerized with a high functional group retention using pulsed plasma deposition with optimum conditions in a maximum reaction time of 15 min. Glass and CrCo surfaces have been coated with PFM, which was used to attach pBAE nanoparticles through chemical bonding. The procedure described in this article has been applied to coat glass and CrCo discs as well as CrCo cardiovascular stents. Results obtained have shown the capability of this coating to transfect COS-7 cells successfully in an initial screening. This methodology is an interesting and viable way of attaching loaded pBAE nanoparticles to stent struts for controlled release. These tailored surfaces can be used to develop pharmacological and/or gene delivery systems based on the adhesion of pBAE nanoparticles on PFM layers for stent implantation.

A new DES design has been achieved through the development of an original way to adhere nanocarriers to produce a tailored release. A strategy has been developed which enables the coating of stents with nanocarriers which can show a good adhesion and avoid the washing away of the nanoparticles when deployed. These conclusions show how the last aim proposed in chapter I has also been accomplished, leading to the end of this thesis.

4.5 References

[1] Fernando A, Pérez-Vizcayno MJ, Cárdenas A, García del Blanco B, García-Touchard A, López-Minguéz JR, et al. A Prospective Randomized Trial of Drug-Eluting Balloons Versus Everolimus-Eluting Stents in Patients with In-Stent Restenosis of Drug-Eluting Stents the RIBS IV Randomized Clinical Trial. J Am Coll Cardiol. 2015;66(1):23-3.

[2] Sen H, Lam MK, Tandjung K, Löwik MM, Stoel MG, De Man FHAF, et al. Complex patients treated with zotarolimus-eluting resolute and everolimus-eluting Xience V stents in the randomized twente trial: Comparison of 2-year clinical outcome. Catheter Cardiovasc Interv. 2015;85(1):74–81.

[3] Kim, C. H., Park, K. W. K., Kang, J., Kang, S. H., Han, J. K., Yang, H. M., et al. TCT-753 Long-Term Comparison of Platinum Chromium Everolimus-Eluting and Cobalt Chromium Zotarolimus-Eluting Stents: Three-Year Outcome of the HOST-ASSURE Randomized Trial. J Am Coll Cardiol. 2017;70(18):B318–9.

[4] Iqbal J, Verheye S, Abizaid A, Ormiston J, De Vries T, Morrison L, et al. DESyne novolimus-eluting coronary stent is superior to Endeavor zotarolimus-eluting coronary stent at five-year follow-up: Final results of the multicentre EXCELLA II randomised controlled trial. EuroIntervention. 2016;12(11):e1336–42.

[5] Baan J, Claessen BE, Dijk KB van, Vendrik J, van der Schaaf RJ, Meuwissen M, et al. A Randomized Comparison of Paclitaxel-Eluting Balloon Versus Everolimus-Eluting Stent for the Treatment of Any In-Stent Restenosis: The DARE Trial. JACC Cardiovasc Interv. 2018;11(3):287–97.

[6] Lowik M, Van Der Heijden LC, Kok MM, Zocca P, Danse PW, Jessurun GAJ, et al. “Four-year clinical outcome following randomised use of zotarolimus-eluting stents versus everolimus-eluting stents in all-comers: insights from the DUTCH PEERS trial.” Eur Heart J. 2018;38: 620.

[7] Schofer J, Schlüter M, Gershlick AH, Wijns W, Garcia E, Schampaert E, et al. Sirolimus-eluting stents for treatment of patients with long atherosclerotic lesions in small coronary arteries: Double-blind, randomised controlled trial (E-SIRIUS). Lancet. 2003;362(9390):1093–9.

[8] Abou-chebl A, Bashir Q, Yadav JS. Drug-eluting stents for the treatment of intracranial atherosclerosis: initial experience and midterm angiographic follow-up. Stroke. 2005;36:e165-e168.

[9] Schampaert E, Cohen EA, Schlüter M, Reeves F, Traboulsi M, Title LM, et al. The Canadian study of the sirolimus-eluting stent in the treatment of patients with long de novo lesions in small native coronary arteries (C-SIRIUS). J Am Coll Cardiol. 2004;43(6):1110–5.

[10] Halkin A, Stone GW. Polymer-based paclitaxel-eluting stents in percutaneous coronary intervention: A review of the TAXUS trials. J Interv Cardiol. 2004;17(5):271–82.

[11] Holmes DR, Leon MB, Moses JW, Popma JJ, Cutlip D, Fitzgerald PJ, et al. Analysis of 1-Year Clinical Outcomes in the SIRIUS Trial: A Randomized Trial of a Sirolimus-Eluting Stent Versus a Standard Stent in Patients at High Risk for Coronary Restenosis. Circulation. 2004;109(5):634–40.

[12] Ylä-Herttuala S, Baker AH. Cardiovascular Gene Therapy: Past, Present, and Future. Mol Ther. 2017;25(5):1095–106.

[13] Nakano K, Egashira K, Masuda S, Funakoshi K, Zhao G, Kimura S, et al. "Formulation of Nanoparticle-Eluting Stents by a Cationic Electrodeposition Coating Technology. Efficient Nano-Drug Delivery via Bioabsorbable Polymeric Nanoparticle-Eluting Stents in Porcine Coronary Arteries." JACC Cardiovasc Interv. 2009;2(4): 277–83.

[14] Kozuma K. "Has the Development of Drug-Eluting Stents Ended With Limus-Eluting Stents?" Circ J. 2018;82(2): 330–31.

[15] Verma IM, Somia N. "Gene Therapy - Promises, Problems and Prospects." Nature. 1997;389(6648): 239–42.

[16] Somia N, Verma IM. "Gene Therapy: Trials and Tribulations." Nat Rev Genet. 2000;1(November):91–9.

[17] Jin Sook Kwon, Gwangju (KR); Young Keun Ahn, Gwangju (KR); Myung Ho Jeong, Gwangju (KR); Sun Jung Song, Gwangju (KR); Dong Lyun Cho G (KR). Gene delivery stent using titanium oxide thin film coating and method for fabricating the same. 2018. p. 21.

[18] Fernández EF, Santos-Carballal B, de Santi C, Ramsey JM, MacLoughlin R, Cryan SA, et al. Biopolymer-based nanoparticles for cystic fibrosis lung gene therapy studies. Materials. 2018;11(1).

[19] Sanchez-Salcedo S, Vallet-Regí M, Shahin SA, Glackin CA, Zink JI. Mesoporous core-shell silica nanoparticles with anti-fouling properties for ovarian cancer therapy. Chem Eng J. 2018;340(January):114–24.

[20] Baghdan E, Pinnapireddy SR, Strehlow B, Engelhardt KH, Schäfer J, Bakowsky U. Lipid Coated Chitosan-DNA Nanoparticles for Enhanced Gene Delivery. Int J Pharm. 2018;535(1–2):473–9.

[21] Luderer F, Löbler M, Rohm HW, Gocke C, Kunna K, Köck K, et al. Biodegradable sirolimus-loaded poly(lactide) nanoparticles as drug delivery system for the prevention of in-stent restenosis in coronary stent application. J Biomater Appl. 2011;25(8):851–75.

[22] Kumar CS. Nanomaterials: toxicity, health and environmental issues. Vol. 5. St. Martin's Press; 2006.

[23] Garg S, Serruys PW. Coronary stents: Current status. J Am Coll Cardiol. 2010;56(10 SUPPL.): S1–42.

[24] Abizaid A, Costa JR. New Drug-Eluting Stents an Overview on Biodegradable and Polymer-Free next-Generation Stent Systems. Circ Cardiovasc Interv. 2010;3(4):384–93.

[25] Alexy RD, Levi DS. Materials and manufacturing technologies available for production of a pediatric bioabsorbable stent. Biomed Res Int. 2013;2013.

[26] Nogic J, McCormick LM, Francis R, Nerlekar N, Jaworski C, West NEJ, et al. Novel Bioabsorbable Polymer and Polymer-Free Metallic Drug-Eluting Stents. J Cardiol. 2018;71(5): 435–43.

[27] Song L, Li J, Guan C, Jing Q, Lu S, Yang L, et al. Randomized comparison of novel biodegradable polymer and durable polymer-coated cobalt-chromium sirolimus-eluting stents: Three-Year Outcomes of the I-LOVE-IT 2 Trial. Catheter Cardiovasc Interv. 2018;91(November 2017):608–16.

[28] Xu W, Yagoshi K, Koga Y, Sasaki M, Niidome T. Optimized polymer coating for magnesium alloy-based bioresorbable scaffolds for long-lasting drug release and corrosion resistance. Colloids Surfaces B Biointerfaces. 2018;163:100–6.

[29] O'Connell, R. M., Rao, D. S., & Baltimore, D. MicroRNA regulation of inflammatory responses. Annu. Rev. Immunol. 2012. 30:295–312.

[30] Cuneo AA, Herrick D, Autieri M V. Journal of Molecular and Cellular Cardiology Il-19 reduces VSMC activation by regulation of mRNA regulatory factor HuR and reduction of mRNA stability. J Mol Cell Cardiol. 2010;49(4):647–54.

[31] Dosta P, Segovia N, Cascante A, Ramos V, Borrós S. Surface charge tunability as a powerful strategy to control electrostatic interaction for high efficiency silencing, using tailored oligopeptide-modified poly(beta-amino ester)s (PBAEs). Acta Biomater. 2015;20:82–93.

[32] Yang F, Cho S-W, Son SM, Bogatyrev SR, Singh D, Green JJ, et al. Genetic engineering of human stem cells for enhanced angiogenesis using biodegradable polymeric nanoparticles. Proc Natl Acad Sci. 2010;107(8):3317–22.

[33] Tzeng SY, Hung BP, Grayson WL, Green JJ. Cystamine-terminated poly(beta-amino ester)s for siRNA delivery to human mesenchymal stem cells and enhancement of osteogenic differentiation. Biomaterials. 2012;33(32):8142–51.

[34] Anderson DG, Akinc A, Hossain N, Langer R. Structure/property studies of polymeric gene delivery using a library of poly(β-amino esters). Mol Ther. 2005;11(3):426–34.

[35] Akinc A, Lynn DM, Anderson DG, Langer R. Parallel synthesis and biophysical characterization of a degradable polymer library for gene delivery. J Am Chem Soc. 2003;125(18):5316–23.

[36] Green JJ, Langer R, Anderson DG. Yields Insight into Nonviral Gene Delivery. Acc Chem Res. 2008;41(6):749–59.

[37] Jones CH, Chen M, Ravikrishnan A, Reddinger R, Zhang G, Hakansson AP, et al. Mannosylated poly(beta-amino esters) for targeted antigen presenting cell immune modulation. Biomaterials. 2015;37:333–44.

[38] Tzeng SY, Wilson DR, Hansen SK, Quiñones-Hinojosa A, Green JJ. Polymeric nanoparticle-based delivery of TRAIL DNA for cancer-specific killing. Bioeng Transl Med. 2016;1(2):149–59.

[39] R. Núñez-Toldrà, P. Dosta, S. Montori, V. Ramos, M. Atari SB. Improvement of osteogenesis in dental pulp pluripotent-like stem cells by oligopeptide-modified poly(β-amino ester)s. Acta Biomater. 2017;(53):152–64.

[40] Borrós S, Ramos V, Segovia N, Dosta P, inventors; IQS, assignee. Modified Poly (Beta-Amino Ester) s for Drug Delivery. United States patent US 0250410 A1. 2018. Sep 6.

[41] Francesch L, Borros S, Knoll W, Förch R. Surface reactivity of pulsed-plasma polymerized pentafluorophenyl methacrylate (PFM) toward amines and proteins in solution. Langmuir. 2007;23(7):3927–31.

[42] Segovia N, Dosta P, Cascante A, Ramos V, Borrós S. Oligopeptide-terminated poly(β-amino ester)s for highly efficient gene delivery and intracellular localization. Acta Biomater. 2014;10(5):2147–58.

[43] Dosta P, Ramos-Perez V, Borros S. Stable and efficient generation of poly([small beta]-amino ester)s for RNAi delivery. Mol Syst Des Eng [Internet]. 2018; Available from: http://dx.doi.org/10.1039/C8ME00006A

[44] Kathuria YP. The potential of biocompatible metallic stents and preventing restenosis. Mater Sci Eng. 2006;417:40–8.

[45] Mcclean DR, Eigler NL. Stent design: implications for restenosis. Rev cardiovasc Med. 2002;3, S16-S22.

[46] Scott NA, Robinson KA, Nunes GL, Thomas CN, Viel K, Iii BK, et al. Comparison of the thrombogenicity of stainless steel and tantalum coronary stents. Am Heart J. 1995;129(5), 866-872.

Chapter V.

Conclusions

This page intentionally left blank

Conclusions

Through the elavoration of this thesis, an in-lab procedure has been developed to analyze, characterize and elaborate multi-layered stents. These methods have enabled a good understanding of the composition and elaboration approaches used to produce the market golden standards. At the same time, these have been used to guide the initial designs of the stents elaborated in chapter II. After evaluating different techniques which allowed the activation and coating of DES, plasma activation and spray coating have proven to give best result in a laboratory environment when producing multilayered stents. After initial attempts are performed to achieve good quality coatings on metallic stent struts, various combinations of PLA, PLGA and pHPMA are successfully sprayed while good morphology can be observed through SEM.

These achievements have permited the elaboration of a broad design variety for chapter III, which is focused on the study of the release profiles obtained through the different polymer and drug combinations tested. Elution of sirolimus and PAP-1 have been studied from different polymeric matrices, leading to elution tailoring obtained through burst layers, barriers and different sustained release profiles which can be applied to medical devices. The use of pHPMA has shown very quick releases which are useful for burst effects, while PLGA matrices were used for sustained releases. These polymer combinations have been studied in different mediums and with different drug loads to study concentration, solubility and hydrophobicity effects on the elution. Increase in drug load has shown to cause a reduction on DES release and has proven to have a greater effect than barriers at the expense of having to add more drug quantity. This phenomenon has been detected in long duration releases in supplemented medium and appears later than burst effects created in outer layers, making these two phenomena appear at a same liberation curve and becoming helpful tools used to modulate releases.

Through the elaboration of chapter III, the production of multilayered stents with tailored release profiles when loading PLGA and pHPMA matrices with sirolimus or PAP-1 has been made possible. These outcomes have generated interesting stent designs which have been tested *in vitro* and *in vivo* with promising results. A multilayered stent used for a last *in vivo* trial has been elaborated in an industrial environment to try the scalability of the process. The data collected from the resulting stents have shown the viability of its industrial production.

Experimentation discussed in chapter IV has shown that PFM can be polymerized through pulsed plasma over CrCo with a high functional group retention to attach PBAE nanoparticles on its surface. This technology has been oriented to produce DES coated with PFM and PBAE NPs and an initial screening has been performed with cos-7 cells. Results obtained show an interesting and viable way of attaching these loaded PBAE nanoparticles to stent struts for controlled and tailored releases and opens a pathway for pharmacological and/or gen delivery systems based on this methodology.

This thesis has contributed with the optimization of different techniques and the elaboration of instrumental which allow the production of a laboratory setup for medical device experimentation. Results obtained have proven the viability to produce different multi-layered coating systems with tailored release profiles which can be applied on medical instrumentation such as DES. These methods have been scaled for industrial use and proven to render good results, opening a pathway for a new and complete drug release control for medical devices.

This page intentionally left blank